Maintenance of the Spindle Assembly Checkpoint by PLK1 and CDC7 kinases and characterisation of cell lines carrying mutations in the genes coding for the CDC7 kinase regulatory subunits

Aisling O'Connor (BSc)

Supervisor: Prof. Corrado Santocanale

Centre for Chromosome Biology,

National Centre for Biomedical Engineering,

School of Natural Sciences,

National University of Ireland Galway,

Ireland

A thesis submitted to the National University of Ireland, Galway

for the degree of Doctor of Philosophy

November 2016

Table of Contents

List of Figures

List of Tables

List of Abbreviations

Alphabetical order

APC/C	Anaphase promoting complex/cyclosome
5-Itu	5-Iodotubercidin
Amp	Ampicillin
ATM	Ataxia telangiectasia mutated
ATP	Adenosine triphosphate
ATR	ATM Rad-3 related
ATRIP	ATR interacting protein
BI	BI 6727
BUB	Budding uninhibited by benzimidazoles
CDC7	Cell division cycle 7
CDKs	Cyclin-dependent kinase
CDT1	Chromatin licencing and DNA replication factor 1
CENP	Centromere protein
CHK1	Checkpoint kinase 1
CPC	Chromosome passenger complex
CTF19	Chromosome transmission fidelity 19
DAPI	4’,6-diamidino-2-phenylindole
DBF4	Dumbbell forming protein 4
DDR	DNA damage repair pathway
DIC	Differential interference contrast
DMEM	Dulbecco’s modified Eagles medium
DMSO	Dimethyl sulfoxide
DNA	Deoxyribonucleic acid
dNTPs	Deoxyribonucleotides
Dox	Doxycycline
DRF1	DBF4 Related factor 1
DSB	Double strand breaks
EC	Error correction
EdU	5-Ethynyl-2’-deoxyuridine
ES	Embryonic Stem
Eto	Etoposide
EV	Empty vector
Fucci	Fluorescent ubiquitylation cell cycle-based interaction
G1	Gap1

G2	Gap2
GINS	Go-Ichi-Ni-San complex
GW	GW843682X
HEC1	Highly expressed in cancer protein 1
Hesp	Hesperadin
HU	Hydroxyurea
IMDM	Iscove's modified Dulbecco's medium
INCENP	Inner centromeric protein
kDa	Kilo dalton
k-mt	kinetochore-microtubule
KO	Knock out
KU	KU-55933
l	Litre
LB	Luria-Bertani
M	Mole
MAD	Mitotic arrest deficient
MAT1	ménage a trois 1
MCAK	mitotic centromere-associated kinesin
MCC	Mitotic checkpoint complex
MCM	Mini-chromosome maintenance
MG	MG132
min	Minutes
ml	Millilitre
mM	Millimole
MPM2	Mitotic protein monoclonal 2
MPS1	Mono-polar spindle protein 1
ms	Millisecond
MYT1	membrane associated tyrosine/threonine 1
Noco	Nocodazole
ORC	Origin recognition complex
PCNT	Pericentrin
PFA	Paraformaldehyde
PHA	PHA-767491
PIPES	Piperazine-N,N'-bis (ethanesulfonic acid)
PLK1	Polo-like kinase 1
PML	promyleocytic leukemia
PP	Protein phosphatase
pre-IC	Pre-initiation complex
pre-RC	Pre-replication complex

PTEMF	PIPES, Triton-X 100, Ethylene glycol tetaacetic acid, magnesium chloride, formaldehyde
Rev	Reversine
ROD	Rough deal
RPA	Replication Protein A
RPE-1	Retinal Pigmented Epithilial-1
rpm	Revolutions per minute
S	Synthesis
SAC	Spindle Assembly Checkpoint
Scc	Sister chromosome cohesion
SD	Standard deviation
SDS	Sodium dodecyl sulfate
SDS-PAGE	SDS-Polyacrylamide gel electrophoresis
SEM	Standard error of the mean
SPOC	Spindle positioning checkpoint
ssDNA	Single strand DNA
TCTP	Translationally controlled tumour protein
TEMED	Tetremethylethylenediamine
TOPII	Topoisomerase II
TPX2	Targeting protein for Xklp2
WT	Wild type
XL	XL413
ZW10	Zeste white 10
ZWNT-1	ZW10 interactor protein-1
µl	Microlitre
µM	Micromole

Declaration

I hereby declare that the work presented in this thesis, was carried out in accordance with the regulations of the National University of Ireland, Galway. The research is original and entirely my own work, unless otherwise stated. The thesis or any part thereof has not been submitted to the National University of Ireland, Galway, or any other institution in connection with any other academic award. Any views expressed herein are that of the author.

Quantification of foci in the experiment presented in Figure 3.1C and D and Figure 3.3C using the Operetta High-Throughput system was carried out with the assistance of Dr. David Gaboriau. The experiment presented in: Figure 4.4A was performed by Dr. Michael Rainey, Figure 4.4B by Gemma O'Brien and Dr. Michael Rainey and Figure 4.4C by Dr. Kevin Wu and Gemma O'Brien. The experiment presented in: Figure 4.5A and B were performed by Dr. Michael Rainey and Dr. Agnieszka Kaczmarcyk, Figure 4.5C by Dr. Agnieszka Kaczmarcyk and Figure 4.5D by Dr. Michael Rainey. The experiment and data analysis shown in Figure 4.7 was performed by Dr. Stefano Maffini at the beginning of a collaboration with Prof. Andrea Musacchio's laboratory. The experiment shown in Figure 4.9 was conducted with the assistance of Dr. Stefano Maffini. Generation of the HAP1 cell lines, which ectopically express DBF4, was carried out by Dr. Michael Rainey.

Signed: ……. Date: ……

Acknowledgements

First, I would like to sincerely thank my supervisor, Corrado or C-dawg, for your guidance, advice and support over the last 4 years, but most importantly for the sailing trips and pints. You have been a great supervisor and snap chat friend. Most of the time we did not understand each other but with the help of a translator we got through it. Maybe someday I will manage to Western successfully. I can finally say, that you never succeeded in making me cry during my PhD.

To all the Corrado kids, past and present, especially, Aga, Alex, David, Edel, Edel Mullen, Gemma a.k.a. Jimmy Jammers, Gosia, Guan-Nan, Huong, Jennifer, Kevin, Lorraine, Mike and Rachel. Thank you for all your help, advice, support and more importantly, for the tennis matches, the chats, laughs and giggles that made it a great lab to be part of. Many of you were not just work colleagues but friends. A special thank you to Mike for allowing me to annoy you every day over the last 4 years. I am sure that the list that you are keeping of all my stupid questions is very long at this stage! I would be carrying out experiments still if it was not for all your help and guidance. To Aga, my lab mother, thank you for teaching me to love mitosis and to see beyond my eyelashes when using a microscope. Gosia, thank you for the fantastic job that you did during your internship with us and for your contribution to Chapter 5. Edel, thank you for reading and translating my thesis into English. I would not have got this far, this quickly, if it was not for all your help and our spa trips.

To my collaborators in the MPI Dortmund, Andrea and Stefano, the experts in the SAC field, I learned a huge amount about the SAC during the 5 weeks that I was there. Thanks to everyone at the Institute who let me tag along for lunch, nights out and day trips.

To the friends that I made along the way outside of our lab, the PCI's, the Lahues, members of REMEDI, the NCBES, CCB and ARC. My life in Galway would not have been the same without all your friendships.

I would like to acknowledge Cancer Care West Hardiman for supporting my research, for introducing to some of the other Hardiman scholars and for the compulsory trips to the Burren.

To my former housemates, Edel, Marie and Steph, thank you for taking me in when I was homeless. There are a lot of good memories from the 2 and half years that I lived with you. You all became great friends and I think it is safe to say that we managed to remain friends even though we no longer live together. Thanks for letting me watch Home and Away, for introducing me to My Kitchen Rules, for all the nights out, birthdays, chats and laughs.

To my current housemates, the real ‘‘A team’’, Aisling, Ann Marie and Ann-Marie, I have only known you less than a year but it feels longer, in a good way. Thank you for all the ham and cheese toasties, shellac, for making sure other drivers do not crash into us on roundabouts and for all the fun nights out.

To all my friends, especially, Aisling, Amy, Brigita, Ciara (Pinky), Eimear (Reeny), Emma and Marie. We might only see each other a few times a year but when we do it is as though we only saw each other yesterday. Thank you for always being there, for making me smile, for the random texts, holidays and all the fun times.

Most importantly, thanks to my family, Mam, Dad, Karen and my Nanny. I will never be able to thank you enough for all your love, encouragement, help, support, advice, kindness, money, food and for just being there for me, always. I would have not got this far without all your love and support. Karen, my favourite sister, this will be you in 3 years.

ABSTRACT

The Spindle Assembly Checkpoint (SAC) ensures that accurate chromosome segregation occurs, by preventing progression into anaphase until all kinetochore-microtubule attachments are stable and bi-polar. During a mitotic arrest, induced by microtubule targeting drugs, the weakening of the SAC allows cells to progress through the cell cycle without chromosome segregation occurring. PLK1 plays a major role in mitosis and has recently emerged as a player in establishing and maintaining a robust SAC. However, mechanistically, the role of PLK1 in the SAC is not fully understood.

CDC7 kinase is essential for the initiation of DNA replication in eukaryotic organisms. In humans, it requires the binding of a regulatory subunit, either DBF4 or DRF1, for its activity, which persists from S-phase until anaphase.

To date, there is limited knowledge about the distinct functions of DBF4 and DRF1. Furthermore, the role for CDC7 kinase in mitosis in humans has not been established.

In this thesis, the role of PLK1 in SAC maintenance was assessed. PLK1 was found to be required for maintenance of Aurora B and its activity at the kinetochores. PLK1 and Aurora B cooperate to maintain a robust SAC but PLK1 does not cooperate with MPS1 or Haspin during checkpoint maintenance. It was found that CDC7 is an active kinase during mitosis where it cooperates with PLK1 in SAC maintenance.

Using genetically edited cell lines, this study has revealed that a deletion in *DBF4* causes an accumulation of cells in S-phase, and defective phosphorylation of the replicative DNA helicase subunit, MCM2.

These results indicate that PLK1 is directly involved in maintaining efficient SAC signalling and provide evidence for a novel role of CDC7 kinase in mitosis. Preliminary evidence suggests that DBF4 is the main CDC7 kinase regulatory subunit that is responsible for efficient S-phase progression and for phosphorylating MCM2.

CHAPTER 1:

INTRODUCTION

1.1 - The cell cycle

For a cell to replicate and divide, it must undergo a series of events in a precise and ordered manner. This is termed the cell cycle and it can be divided into four main phases, Gap 1 (G1), Synthesis (S), Gap 2 (G2) and M-phase which consists of mitosis and cytokinesis (Nurse, 2000).

G1-phase is the first and the longest phase of the cell cycle. Proteins required for genome duplication are synthesised during G1-phase and the cell size increases. It is during this phase that a cell must decide if it is ready to enter S-phase, where DNA replication occurs, discussed in more detail in Introduction section 1.2. In G2-phase, cells continue to grow and synthesise proteins needed for M-phase, where cell division occurs, discussed in more detail in Introduction section 1.4. Progression through the cell cycle is facilitated by a family of proteins called cyclins and their interacting partners, cyclin-dependent kinases (CDKs). There are several cyclins involved in the cell cycle and each of these oscillate during the various phases of the cell cycle, activating their respective CDK partner to allow transition between each phase (Malumbres and Barbacid, 2005). Failure to replicate the genome properly and to precisely distribute the genomic material to the daughter cell, can lead to genome instability, a hallmark of cancer (Shen, 2011). To help prevent this, cells possess numerous mechanisms, termed checkpoints, to preserve genome integrity which ensure the fidelity of cell division (Fragkos et al., 2015; Lara-Gonzalez et al., 2012).

1.2 - S-phase

DNA replication occurs during S-phase of the cell cycle. Accurate replication of DNA is required for proper transmission of genetic material from mother to daughter cell during M-phase. S-phase must occur in a timely and coordinated manner, to ensure that the genetic material is replicated only once per cell cycle (Sclafani and Holzen, 2007). Errors

in replication can lead to alterations in the genome over time, due to failure in duplicating the genome precisely, resulting in genome instability (Fragkos et al., 2015). DNA replication consists of three important events, initiation, elongation and termination. Replication begins with initiation which can be divided into two distinct stages, licencing and activation of DNA replication origins. There are multiple DNA replication origins present, which undergo temporal regulation (Mechali, 2010). Only a subset of origins in humans, 30,000-50,000, are activated during each cell cycle and these origins are activated at different times during replication (Mechali, 2010).

1.2.1 - Licensing of DNA replication origins

Origin licencing, the first stage of DNA replication initiation, occurs prior to S-phase, during G1-phase. This involves the sequential loading of proteins which make up the pre-replication complexes (pre-RC), onto the replication origin. First, the origin recognition complex (ORC), consisting of ORC subunit 1-6 (ORC1-6), is recruited to the origins (Li and Stillman, 2012). This is followed by recruitment of cell division cycle protein 6 (CDC6) and chromatin licencing and DNA replication factor 1 (CDT1) to the origins (Mendez and Stillman, 2000; Nishitani et al., 2001). The mini-chromosome maintenance complex 2-7 (MCM2-7) is then loaded. This completes the final step in the assembly of the pre-RC complex as shown in Figure 1.1 (Fragkos et al., 2015). It is important that each origin is only licenced once per cell cycle as re-activation of origins can lead to re-replication, which can cause DNA damage or genome instability (Blow and Dutta, 2005).

1.2.2 - Initiation of DNA replication origins

DNA replication initiation and origin activation occurs during the transition from G1- to S-phase and throughout S-phase. Cell division cycle 7 (CDC7) kinase and Cyclin dependent kinase 2 (CDK2), are recruited to the origins, which triggers the recruitment of additional proteins, to form the pre-initiation complex (pre-IC). Recruitment of CDC7, facilitates CDC45 association with the pre-IC but it is not clear how this occurs (Ballabeni et al., 2009; Masai et al., 2006). CDK2 phosphorylates Treslin which then binds to topoisomerase II binding protein 1 (TOPBP1); (Boos et al., 2011). This complex is

essential for the recruitment of additional factors, MCM10, DNA polymerase epsilon (Pol ε) and the Go-Ichi-Ni-San complex (GINS), to form the pre-IC (Boos et al., 2011) as shown in Figure 1.1. CDC7 kinase phosphorylates the MCM2-7 complex (Montagnoli et al., 2006), which leads to helicase activation and subsequent unwinding of the double stranded DNA (dsDNA) in a bi-directional manner, allowing progression into S-phase (Labib, 2010). The MCM2-7 double hexamer complex divides into two hexamers, once it is activated, which function at each replication fork arising from a single origin (Fragkos et al., 2015).

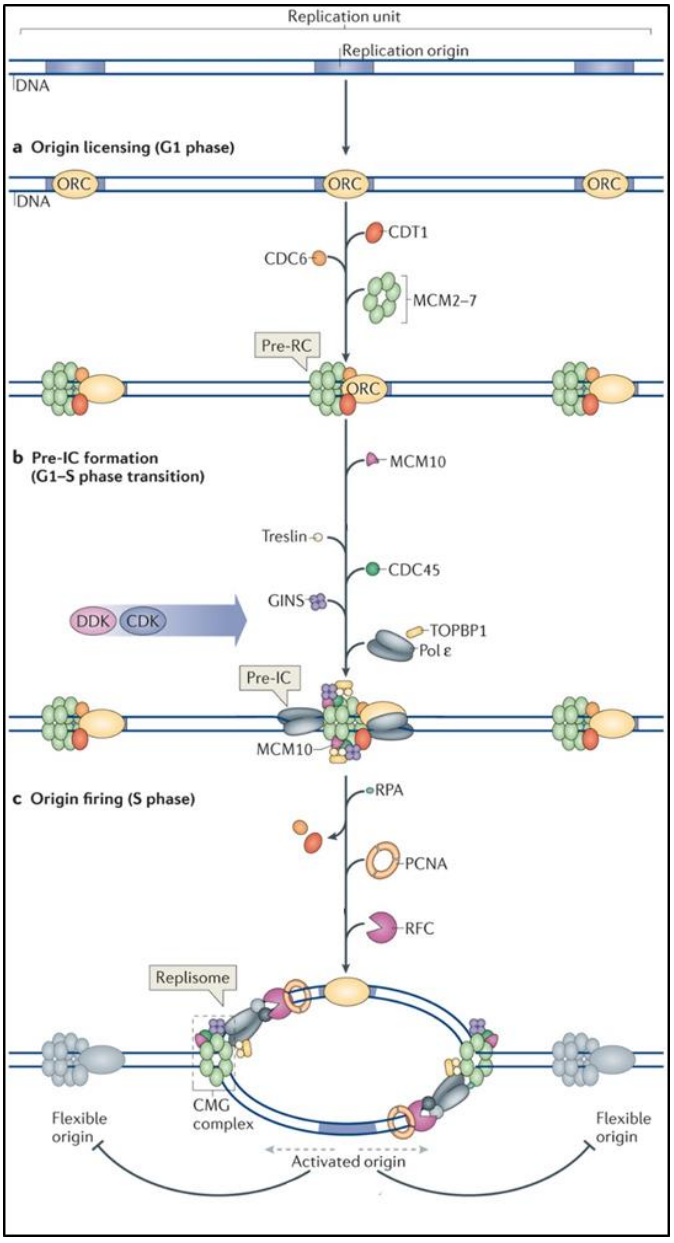

Figure 1.1 Major steps in initiation and elongation of DNA replication

a) Licencing of DNA replication origins and formation of the pre-RC complex. (b, c) Initiation of DNA replication origins which requires assembly of the pre-IC and activation of the MCM2-7 complex. Pre-IC assembly is triggered by CDK and CDC7 activity. The complex of CDC7 and its regulatory subunit is also known as DBF4 dependent kinase (DDK). CDK and DDK phosphorylation of residues within the MCM2-7 complex, results in activation of the MCM2-7 complex, unwinding of the DNA and subsequently elongation. The CMG complex, consists of CDC45, the MCM2-7 complex and the GINS complex. Figure adapted from Fragkos et al., 2015.

1.2.3 - Elongation and DNA synthesis

Unwinding of the dsDNA by the active helicase complex, produces two sister replication forks that continue to move apart from each other as the DNA unwinds. Activation of the helicase complex and the subsequent unwinding of the DNA, facilitates recruitment of additional replication factors, including Replication Protein A (RPA), DNA polymerase alpha-primase complex, epsilon and delta (Pol α-primase-complex, Pol ε and Pol δ), the processivity clamp proliferating cell nuclear antigen (PCNA) and the replication factor C complex (RFC) as shown in Figure 1.1 (Fragkos et al., 2015). RPA binds to the exposed single stranded DNA (ssDNA). The DNA polymerases, PCNA and RFC bind to the forks and contribute to progression of the replication fork (Branzei and Foiani, 2010). Replication of the leading strand occurs in a continuous manner in a 5' to 3' direction facilitated by Pol ε (Pursell et al., 2007). Simultaneously, the lagging strand is synthesised discontinuously in a 5' to 3' direction facilitated by Pol α and Pol δ to produce Okazaki fragments which are then joined together (Garg and Burgers, 2005). The function of Pol ε and Pol δ requires the Pol α-primase complex, which mediates the synthesis of RNA primers on DNA. To synthesise the lagging strand, repeated priming, clamp loading, Pol δ loading and polymerase release are required at each Okazaki fragment (Duderstadt et al., 2014).

1.2.4 - DNA Replication checkpoint

DNA replication is a closely monitored process, as accurate replication of DNA is essential for genome stability. To ensure that faithful duplication of DNA occurs, a surveillance mechanism, termed the replication stress checkpoint, part of the DNA damage response pathway (DDR), detects and corrects any errors in replication that occur due to either endogenous or exogenous sources of stress (Marechal and Zou, 2013). The response from the DDR pathway, promotes timely and accurate DNA repair, translesion synthesis, cell cycle arrest or apoptosis (Polo and Jackson, 2011).

Ataxia telangiectasia mutated (ATM) and ATM-related protein (ATR) are central players in the DDR pathway. They are preferentially activated depending on the type of damage

ensued. ATM is mainly activated in response to DNA double strand breaks (DSBs) while ATR is activated in response to replication stress (Polo and Jackson, 2011). Only the checkpoint response to replication stress will be discussed in the following section.

Replication stress can be caused by a variety of insults, with unrepaired DNA lesions being one of the most common sources of stress, resulting in stalled replication forks, which prevents accurate replication (Hoeijmakers, 2009). DNA lesions can arise via physiological processes, such as reactive oxygen species or by environmental factors, such as ultraviolet light (Helleday et al., 2014).

Lesions can cause nicks and gaps (Ayares et al., 1987) or the mis-incorporation of ribonucelotides (Potenski and Klein, 2014) by Pol ε and Pol δ, which are highly error prone, resulting in fork stalling. Replication fork stalling, due to obstructions on the DNA, can lead to uncoupling of the helicase complex and polymerase activities (Byun et al., 2005). This results in continued unwinding of the DNA by the helicase, leading to the generation of extended stretches of ssDNA. If the stress is not adequately dealt with, forks can collapse, resulting in the formation of DSBs, which can lead to genome instability, (Zeman and Cimprich, 2014).

Replication stress leads to checkpoint activation by checkpoint kinase 1 (CHK1)/ATR. The current model proposes that RPA binds to the exposed ssDNA, leading to the initiation of a signalling cascade that recruits a number of proteins to the stalled fork, the most important of which are ATR and ATR interacting protein (ATRIP); (Zou and Elledge, 2003). The effector kinase, CHK1 can then be phosphorylated by ATR (Liu et al., 2000), which in turn phosphorylates downstream substrates, causing a cell cycle delay, inhibition of origin activation and replication fork stabilisation, allowing recruitment of DNA repair proteins (Gonzalez Besteiro and Gottifredi, 2015; Smith et al., 2010). If the DNA damage is repaired, the checkpoint is inactivated to allow DNA replication to continue.

1.2.5 - Termination of replication

Eukaryotic DNA replication terminates when two replication forks merge. It involves unwinding of the last piece of DNA between the forks, filling in of any gaps and ligation of nascent strands, decatenation of daughter molecules and disassembly of the replisome (Dewar et al., 2015). The process of termination in higher eukaryotes has been difficult to study as it has been proposed that these events occur at random sites, making the events difficult to capture (Santamaria et al., 2000). A recent study in *Xenopus,* utilised a system in which converging forks were stalled using a reversible, site-specific barrier. By introducing tandem *lac* operators into a plasmid, a physical barrier to replication could be generated through the binding of *lac* repressors. The barrier could then be removed by the addition of Isopropyl β-D-1-thiogalactopyranoside (IPTG), allowing the termination events to be captured (Dewar et al., 2015). Results from this study indicated that upon removal of the barrier, DNA synthesis does not slow down during termination (Dewar et al., 2015). The 3' end of the leading strand was mapped to within a few nucleotides of the 5' end of the lagging strand suggesting that gaps between the two strands are filled in quickly (Dewar et al., 2015). In yeast, the MCM7 subunit of the helicase complex is ubiquitinylated by Dia2, a component of the Skp, Cullin, F-box containing (SCF) ubiquitin ligase complex, which, with Cdc48 segregase, promotes disassembly of the helicase during termination as shown in Figure 1.2 (Maric et al., 2014).

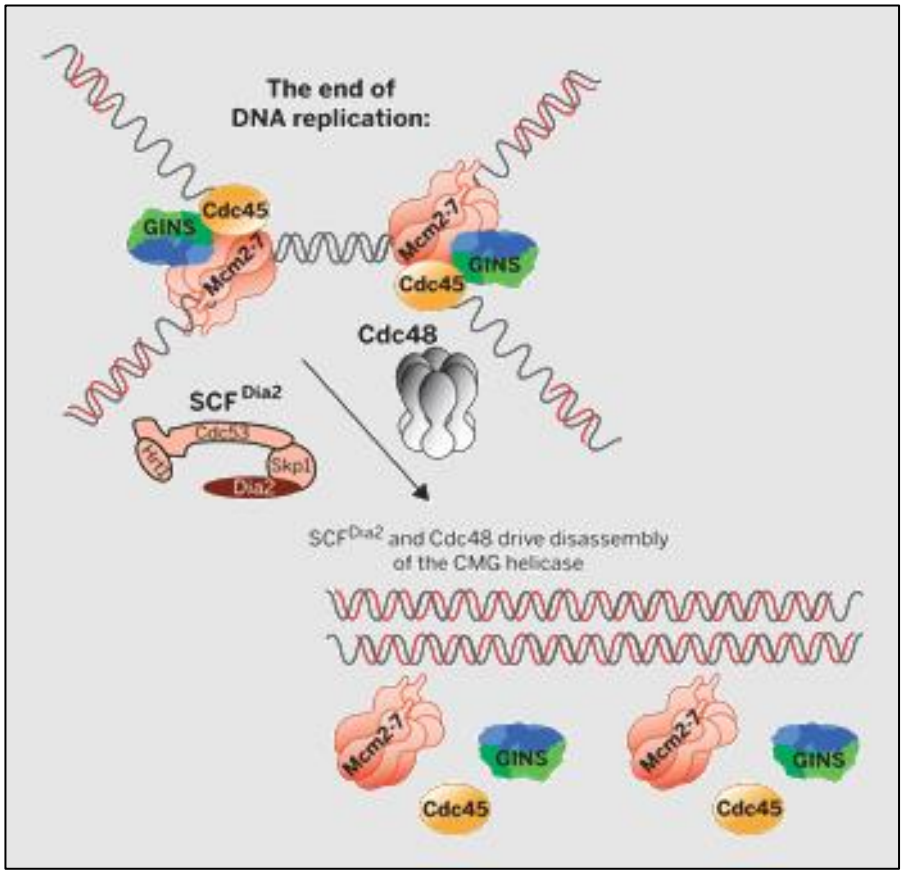

Figure 1.2 Process of helicase disassembly during termination

The helicase complex associates with replication forks until the end of termination. At this stage the helicase is ubiquitinylated by Dia2. Disassembly of the helicase complex is facilitated by the SCF complex and Cdc48 segregase. Figure taken from Maric et al. 2014.

1.2.6 - CDC7 kinase is essential for DNA replication initiation

Cdc7 was first identified in *S. cerevisiae* and characterised as a gene essential for DNA replication initiation (Hartwell, 1973), where its protein has been shown to phosphorylate the Mcm2-7p complex. Mutation of a single amino acid, proline to leucine, at position 83 of yeast *Mcm5*, bypasses the requirement for Cdc7p kinase function in replication initiation (Hardy et al., 1997; Jackson et al., 1993). Furthermore, the requirement for Cdc7p kinase activity is evaded when the N-terminal domain of Mcm4p is deleted. However, growth is impaired due to the inability of cells to activate the replication stress

checkpoint (Sheu and Stillman, 2010). Moreover, disruption of the interaction between Cdc7p and the Mcm2-7p complex, inhibits growth (Ramer et al., 2013).

CDC7 kinase is also important for DNA replication initiation in human cells. Microinjection of antibodies against CDC7 inhibits DNA replication in HeLa cells (Jiang et al., 1999). PHA-767491, a CDC7 kinase inhibitor blocks DNA synthesis and prevents origin firing in HeLa cells (Montagnoli et al., 2008). CDC7 kinase recruits CDC45 to the pre-IC during licensing of the replication origins and it also phosphorylates MCM4 (Ballabeni et al., 2009; Masai et al., 2006) as shown in Figure 1.1. Multiple residues on the N-terminus of MCM2, Ser40, Ser53, Ser108 and Ser139, have been shown to be phosphorylated by CDC7 kinase, *in vitro* and *in vivo* and are suggested to be important for replication initiation (Lei et al., 1997; Montagnoli et al., 2006; Tsuji et al., 2006). Phosphorylation of Ser40 by CDC7 kinase, requires prior phosphorylation of Ser41 by CDK2 (Montagnoli et al., 2006).

Altogether, this indicates that the MCM2-7 complex is the critical target of CDC7 during initiation of DNA replication.

1.2.7 - CDC7 kinase in the replication stress response

CDC7 has emerged as a player in the replication stress response. In yeast, Dbf4p the regulatory subunit of Cdc7p, is directly phosphorylated by Tel1/Mec1 (yeast homologs of ATM/ATR), in response to replication stress (Lee et al., 2012). This phosphorylation event inhibits origin firing and maintains Cdc7p/Dbf4p for the stabilisation of stalled forks (Lee et al., 2012; Yamada et al., 2013). CDC7 kinase has been shown to be stable and active upon the induction of replication stress, by hydroxyurea (HU) or etoposide (Tenca et al., 2007). Inhibition of CDC7 kinase in the presence of HU or etoposide increases cell death (Tenca et al., 2007). Furthermore, CDC7 kinase is known to phosphorylate Claspin (Kim et al., 2008), a mediator protein of the replication stress checkpoint response. Previous work from our lab, revealed that CDC7 kinase inhibition

decreases Claspin phosphorylation after treatment with HU. This delays CHK1 phosphorylation by ATR kinase, at stalled forks (Rainey et al., 2013).

CDC7 kinase has also been shown to participate in the process of Translesion Synthesis (TLS), facilitated by highly error prone TLS polymerases which maintain replication fork progression at damaged templates (Prakash et al., 2005). During this process, CDC7 kinase phosphorylates RAD18, which mediates binding of RAD18 to the chromatin and promotes RAD18 binding to DNA polymerase eta (Pol η); (Day et al., 2010; Yamada et al., 2013).

1.3 - CDC7 kinase and its regulatory subunits DBF4 and DRF1

CDC7 is a serine/threonine kinase, with yeast studies demonstrating that CDC7 protein levels remain constant throughout the cell cycle. However, its kinase activity fluctuates, increasing from late G1-M-phase (Jackson et al., 1993). In human cells, the levels of CDC7 protein were shown to increase in the presence of replication stress and its kinase activity has been demonstrated to fluctuate during the cell cycle, increasing during S-phase and in the presence of replication stress (Tenca et al., 2007; Yamada et al., 2002).

Two CDC7 kinase regulatory subunits have been identified to date. The first was identified in yeast and was named dumbbell forming factor 4 (DBF4) (Jackson et al., 1993; Johnston and Thomas, 1982). A second regulatory subunit, DBF4B was later discovered in higher eukaryotes (Montagnoli et al., 2002). DBF4B was first known as DBF4 related factor 1 (DRF1) and, for clarity, it will be referred to as DRF1 in this thesis. Although both DBF4 and DRF1 are capable of activating CDC7 kinase, they form mutually exclusive complexes with CDC7 (Montagnoli et al., 2002). The amino acid sequences of the two CDC7 kinase regulators are well conserved in three regions, called the N-, M- and C-motifs but there is limited amino acid sequence similarity outside of these regions. The C-terminus, in particular, is largely unconserved (Montagnoli et al., 2002; Yoshizawa-Sugata et al., 2005). Work in fission yeast has demonstrated that the Dbf4p, M- and C-motifs, bind to and activate Hsk1p (fission yeast homologue of human

CDC7) while the Dbf4p N-motif is required for tethering of the Hsk1p/Dbf4p complex to the replication machinery (Ogino et al., 2001). Determination of the crystal structure of human CDC7 and DBF4, revealed that the M- and C-motifs of DBF4 are required for interacting with the C- and N-lobes of CDC7, respectively, thus, stabilising and activating the kinase (Hughes et al., 2012). The C-motif of DBF4 is essential and minimally sufficient for CDC7 kinase activation (Hughes et al., 2012).

1.3.1 - DBF4

In budding yeast, Dbf4p, is the only Cdc7p kinase regulatory subunit. Its levels have been shown to fluctuate during the cell cycle, increasing from late G1-phase and decreasing during M-phase where it has been shown to be degraded during mitosis by the E3 ubiquitin ligase Anaphase promoting complex/cyclosome (APC/C) (Ferreira et al., 2000). In recent years, Dbf4p has been shown to be recruited to the centromere during telophase by the kinetochore protein chromosome transmission fidelity 19 (Ctf19p). Here, it recruits the replication initiation proteins, Sld3-Sld7, therefore playing a role in promoting early replication (Natsume et al., 2013). Dbf4p at the kinetochore, also facilitates recruitment of the cohesin loader, Scc2-Scc4 to centromeres in G1-phase which contributes to accurate pericentromeric cohesion loading during S-phase (Natsume et al., 2013).

In the replication stress checkpoint, yeast Dbf4p is phosphorylated by Mec1p (yeast homolog of ATM) and Tel1p (yeast homolog of ATR) proteins in response to replication stress and DNA damage (Lee et al., 2012). This phosphorylation event stabilises the Cdc7p-Dbf4p complex, protects stalled replication forks and prevents endo-replication caused by origin re-firing (Lee et al., 2012; Yamada et al., 2013). Rad53 (yeast homolog of CHK2) has also been shown to phosphorylate Dbf4p (Zegerman and Diffley, 2010).

In addition, Dbf4p has been shown to be a negative regulator of Cdc5p (*S. cerevisiae* ortholog of Polo-like kinase 1 (PLK1)), by binding to its Polo Box Domain (PBD). It has been shown to potentially be involved in the Spindle Positioning Checkpoint (SPOC), a checkpoint in budding yeast that prevents premature mitotic exit when the spindles fail to align (Chen and Weinreich, 2010; Miller et al., 2009).

In human cells, DBF4 has been described as a nuclear protein (Kumagai et al., 1999; Sato et al., 2003) that oscillates during the cell cycle (Jiang et al., 1999; Kumagai et al., 1999). Recent work from our lab has identified DBF4 at the centromere in S-phase. From this work, CDC7-DBF4 activity was shown to be required for the timely recruitment of Topoisomerase II (TOPII) to centromeres (Wu et al., 2016). TOPII is important for accurate chromosome segregation to occur (Gonzalez et al., 2011).

Depletion of DBF4 via antibody microinjection in human cells and conditional knockout experiments of DBF4 in mouse embryonic stem (ES) cells, have revealed that DBF4 is required for proper S-phase progression and cell viability (Kumagai et al., 1999; Yamashita et al., 2005). DBF4 overexpression has been shown to increase phosphorylation of MCM2 (Sato et al., 2003; Yamashita et al., 2005).

1.3.2 - DRF1

The second regulatory subunit, DRF1, was first identified in human cells, where it was described as a nuclear protein, that oscillates during the cell cycle, increasing from late G1-phase and decreasing during M-phase (Montagnoli et al., 2002). siRNA depletion of DRF1 has been shown to slow S-phase progression in HeLa cells (Yoshizawa-Sugata et al., 2005).

Subsequently, DRF1 was identified in *Xenopus*, where it is regulated during early development. It is expressed up until the mid-blastula stage and during this time it promotes the initiation of DNA replication (Silva et al., 2006). Following this, the levels of DBF4 rise, and it is present from the mid-blastula stage of development (Silva et al., 2006). CDC7 in complex with DRF1 was shown to interact with the cohesin loader complex, Scc2-Scc4, by immunoprecipitation experiments in *Xenopus* egg extracts (Takahashi et al., 2008).

Due to the lack of specific immunological regents for DRF1, it has been difficult to study the function of this protein. Thus, there is limited knowledge surrounding the function of DRF1. Additional experimental work is required to understand the overlapping or

functional difference of DBF4 and DRF1 enabling further understanding of the roles of CDC7 kinase.

1.3.3 - CDC7 in mitosis

To date, no known function of CDC7 kinase in M-phase has been reported in humans. Depletion of CDC7 in human cells has been shown to affect chromosome segregation but this could be an indirect effect as a result of a defect in replication (Montagnoli et al., 2004). Future work investigating a role of CDC7 kinase in mitosis is important to further understand the functions of CDC7 kinase.

1.3.4 - CDC7 in cancer and clinical applications

One of the hallmarks of cancer is the ability to sustain a proliferative signal, which can cause an elevation in protein levels (Hanahan and Weinberg, 2000). CDC7 is overexpressed in approximately 50% of the NCI-60 human cancer cell lines, while its expression in the corresponding normal cell lines is low. Furthermore, increased CDC7 expression correlated with an increase in DBF4 expression in these cancer cell lines (Bonte et al., 2008). In the same study, increased levels of CDC7 were also detected in primary breast, lung and colon tumours (Bonte et al., 2008).

Evading growth suppressors, such as tumour protein p53 (TP53), also known as the 'guardian of the genome', is another hallmark of cancer (Hanahan and Weinberg, 2011). Elevated levels of CDC7 has been shown to correlate with low levels of TP53 (Bonte et al., 2008). Another study revealed that CDC7 depletion increases apoptotic cell death in cancer cell lines, that were TP53 deficient, whereas, in normal fibroblasts, with TP53, G1 checkpoint activation is maintained, and cells do not undergo an abortive cell cycle (Montagnoli et al., 2004). Furthermore, depletion of CDC7 in TP53 deficient breast cancer cells causes cells to undergo apoptosis, whereas breast epithelial cells depleted of CDC7 do not (Rodriguez-Acebes et al., 2010). CDC7 depletion has been shown to induce apoptosis in a variety of other cancer cell lines including, ovarian carcinoma and pancreatic cancers (Huggett et al., 2016; Kulkarni et al., 2009).

A study demonstrated that when CDC7 is co-depleted with any of the DNA replication origin activation checkpoint proteins, FOXO3, p53, p15 or Dickkopf WNT Signalling Pathway Inhibitor 3 (DKK3), in normal fibroblasts, the G1 arrest is bypassed, resulting in a defective S-phase, followed by apoptosis (Tudzarova et al., 2010). This provides a mechanistic basis for the specific killing of cancer cells.

The preferential killing of cancer cells versus normal cells when CDC7 is depleted makes CDC7 an attractive target for cancer therapeutics. This has led to the development of several CDC7 kinase inhibitors (Koltun et al., 2012; Montagnoli et al., 2008; Swords et al., 2010). Several of these inhibitors have been shown to cause cell death in multiple cancer cell lines, including pancreatic cancer cell lines and multiple myeloma (Huggett et al., 2016; Natoni et al., 2013). Inhibitors have also been shown to have synergistic effects in combination with other chemotherapeutic agents (Ito et al., 2012; Natoni et al., 2013). Furthermore, CDC7 kinase inhibitors have shown tumour regression in xenograph and pre-clinical models (Koltun et al., 2012; Montagnoli et al., 2008). Furthermore, a CDC7 kinase inhibitor has shown a dramatic synergy with taxanes in eradicating carcinogen-induced breast carcinomas in rats (Montagnoli et al. 2010).

Therefore, further work into the functions of CDC7 kinase and its regulatory subunits is important, to help understand how CDC7 kinase inhibitors can be utilised as a therapeutic target for treatment of cancers.

1.4 - M-phase

1.4.1 - Mitosis and cytokinesis

Cell division occurs during M-phase of the cell cycle, which, as mentioned, consists of mitosis and cytokinesis. Mitosis is essential for the segregation of sister chromatids so that each daughter cell will inherit one copy of each chromosome. Accurate segregation depends on proper kinetochore-microtubule (k-mt) attachments and chromosome condensation (Nigg, 2001). The Spindle Assembly Checkpoint (SAC), monitors these

attachments and remains active until all kinetochores are properly attached to the microtubules of the mitotic spindle, discussed in Introduction section 1.5.

M-phase is the most dynamic phase of the cell cycle and it is divided into six phases, namely, prophase, prometaphase, metaphase, anaphase and telophase (Walczak et al., 2010), which are followed by cytokinesis, the final stage of M-phase, during which the cytoplasm of the mother cell divides to allow for the generation of two distinct daughter cells(Glotzer, 2001). These phases are outlined in Figure 1.3.

During prophase, chromosomes become defined as the chromatin begins to condense. The centrosomes separate from each other to form spindle poles from which the microtubules begin to nucleate from and the nuclear envelop starts to breakdown. Throughout prometaphase, the microtubules attach to the kinetochores, to form kinetochore-microtubule (k-mt) attachments (Walczak et al., 2010). These attachments are stable once the microtubule spindles from opposite poles attach to the sister kinetochores. Chromosomes then align along the equator, also known as the metaphase plate, during metaphase. Between metaphase and anaphase there is a checkpoint, called the SAC that prevents progression into anaphase until all k-mt attachments are stable and chromosomes are aligned. Chromosome are separated and pulled towards opposite poles during anaphase. Telophase, the last event that occurs during mitosis, results in the reformation of the nuclear envelop around the daughter nuclei and chromatin condensation occurs (Walczak et al., 2010). During cytokinesis cell cleavage occurs, allowing the formation of two new daughter cells that then enter into G1-phase, to begin a new cell cycle (Glotzer, 2001).

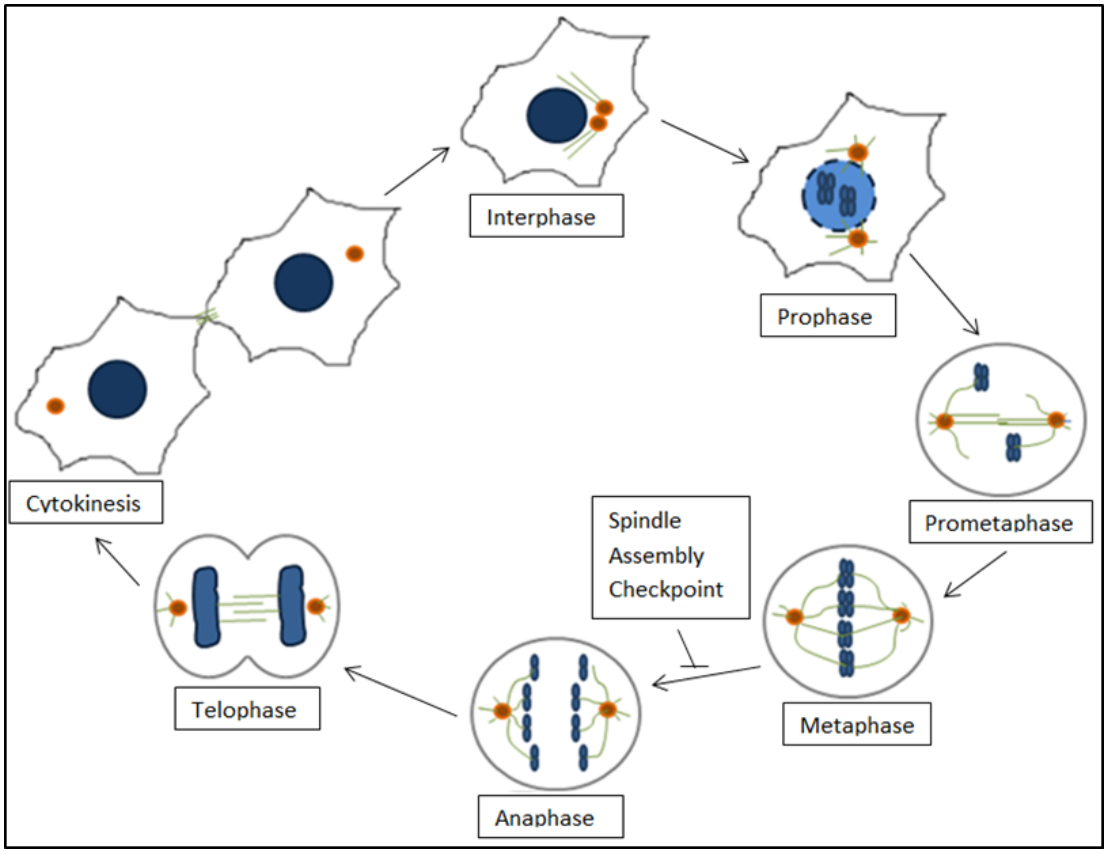

Figure 1.3 Stages of the M-phase of the cell cycle

During interphase (consisting of G1-, G2- and S-phases) the chromosomes are decondensed (dark blue circle). This is followed by the six stages of M-phase. Centrosome (orange), microtubules (green), nuclear envelope breakdown (dashed blue lines).

1.4.2 - Regulation of mitotic entry

The activation of two master regulators of mitosis, cyclin-dependent kinase 1 (CDK1) in complex with its binding partner Cyclin B, and PLK1, are required for mitotic entry (Lindqvist et al., 2009; Seki et al., 2008). These proteins are regulated by several other proteins to allow proper timing of entry into mitosis.

During S-phase and G2-phase, CDK1/Cyclin B form a complex but its activity is restricted due to phosphorylation of CDK1 at tyrosine 15 (Y15) and threonine 14 (T14) by Wee 1-like protein kinase (WEE1) and membrane associated tyrosine/threonine 1

(MYT1) kinase (Booher et al., 1997; Parker and Piwnica-Worms, 1992). For a cell to enter mitosis, CDK1/Cyclin B needs to become fully activated. PLK1, a second key kinase required for mitotic entry, is activated by Aurora A-Bora which activates the protein phosphatase cell division cyclin 25C (CDC25C) (Seki et al., 2008). CDK1 Y15 and T14 are then dephosphorylated by CDC25C, which allows further activation of the CDK1/Cyclin B complex (Lindqvist et al., 2009). Phosphorylation of WEE1 and MYT1, by PLK1, results in WEE1 degradation and inhibition of MYT1 kinase activity, which enhances CDK1/Cyclin B activity (Booher et al., 1997; Nakajima et al., 2003; Watanabe et al., 2004). The CAK complex, consisting of cyclin dependent kinase 7 (CDK7), Cyclin H and ménage a trois 1 (MAT1), is responsible for phosphorylating CDK1 on Thr 161 to allow for full activation of CDK1/Cyclin B and entry into mitosis (van Vugt and Medema, 2005).

1.4.2 - Regulation of mitotic exit

Inactivation of CDK1 and Securin degradation are required to promote mitotic exit. Preparation for exit from mitosis begins when the SAC is inactivated. This leads to APC/C degradation of Securin, an inhibitor of Separase, a protein required for the separation of sister chromatids (Uhlmann et al., 2000), resulting in a point of no return. The addition of inhibitory phosphorylation promotes the full inactivation of the CDK1/Cyclin B complex. Phosphorylation of Y15 on CDK1 is required to inhibit CDK1 activity and promote mitotic exit (D'Angiolella et al., 2007). Moreover, PP1 and PP2A have been shown to target CDK1 and contribute to CDK1 inactivation (Hegarat et al., 2016). The exit from mitosis also requires degradation of Cyclin B, by the APC/C (Glotzer et al., 1991), leading to inactivation of the CDK1/Cyclin B complex, after which cytokinesis ensues. PLK1 dependent phosphorylation of mitotic kinesin-like protein (MKlp) 2 is required for proper execution of cytokinesis to take place (Neef et al., 2003).

1.5 - The spindle assembly checkpoint (SAC)

1.5.1 - The role of SAC proteins in checkpoint establishment

The SAC, is a complex feedback control pathway that prevents metaphase to anaphase progression until all k-mt attachments are stable and bi-polar. Premature inactivation of the SAC can cause genome instability as a result of errors in chromosome segregation and aneuploidy(Weaver and Cleveland, 2005).

Signalling pathways, such as the SAC, usually consist of three phases: establishment, maintenance and silencing. The establishment of the SAC has been widely studied; many factors participate in and regulate SAC establishment at the kinetochore. This checkpoint consists of kinetochore proteins, which act as a platform for the recruitment of the checkpoint proteins and kinases, as well as the SAC proteins and kinases themselves (Table 1.1); (Chan et al., 2005; Musacchio and Salmon, 2007). Complete SAC function requires proper localisation and activation of all of the SAC proteins and kinases (Jia et al., 2013).

Table 1.1: List of the checkpoint proteins and their main function in the SAC

Protein name	Main function in the SAC	References
Aurora B	Recruitment of MPS1, inhibition of PP1 recruitment	(Emanuele et al., 2008; Saurin et al., 2011)
BUB1	Kinetochore recruitment of BUBR1	(Johnson et al., 2004)
BUB3	Component of the Mitotic Checkpoint Complex (MCC)	(Sudakin et al., 2001)
BUBR1	Component of the MCC, binds to CDC20 to prevent APC/C activation	(Sudakin et al., 2001)
CDC20	Component of the MCC, APC/C co-activator	(Sudakin et al., 2001; Visintin et al., 1997)

MAD1	Component of the MAD1:MAD2 complex	(Luo et al., 2002; Sironi et al., 2002)
MAD2	Component of the MAD1:MAD2 complex, component of the MCC	(Luo et al., 2002; Sironi et al., 2002; Sudakin et al., 2001)
MPS1	Phosphorylation of KNL1	(Yamagishi et al., 2012)
PLK1	Activation of Haspin	(Zhou et al., 2014)
Haspin	Activation of Histone H3 to allow recruitment of Aurora B	(Dai et al., 2005; Wang et al., 2010)
ROD	Component of the RZZ complex, recruitment of MAD1:MAD2	(Caldas et al., 2015; Scaerou et al., 2001)
ZW10	Component of the RZZ complex, recruitment of MAD1:MAD2	(Caldas et al., 2015; Scaerou et al., 2001)
Zwilch	Component of the RZZ complex	(Williams et al., 2003)
HEC1	Recruitment of MPS1	(Saurin et al., 2011)
PP1	SAC silencing, counteracts Aurora B	(Emanuele et al., 2008)
PP2A	SAC silencing, counteracts Aurora B	(Foley et al., 2011; Meppelink et al., 2015)

The kinetochore proteins, including those involved in the KMN network, are recruited to the kinetochore prior to or early in mitosis(Chan et al., 2005). The KMN network consists the kinetochore null protein 1 (KNL1), mis-segregation 12 (MIS12) and nuclear division cycle 80 (NDC80)/highly expressed in cancer protein 1 (HEC1) complexes. The KNL1 complex consists of KNL1 and ZWINT-1. The HEC1 complex consists of four proteins, HEC1, NUF1, SPC25 and SPC24. The MIS12 complex consists of four proteins, DSN1,

MIS12, NSL1 and NNF1. These act as a docking platform for the SAC proteins and kinases and serve as a site for microtubule attachments (Chan et al., 2005). Checkpoint kinases are then recruited to the kinetochore through a positive feedback loop (Figure 1.4). Several of these proteins form sub-complexes, such as, the chromosomal passenger complex (CPC), consisting of Aurora B, Survivin, Borealin and inner centromeric protein (INCENP), the mitotic checkpoint complex (MCC), composed of three SAC subunits and CDC20, and the RZZ complex, which consists of rough deal (ROD), Zeste white 10 (ZW10) and Zwilch (Table 1.1).

In the establishment phase of the SAC, PLK1, a kinase which has several well established roles in mitosis (Table 1.2) was recently implicated in the SAC, where it has recently been reported to phosphorylate and recruit Haspin to the kinetochores (Zhou et al., 2014).

Table 1.2: Localisations and functions of PLK1 during the G2/M-phase transition and throughout mitosis

Localisation	**Function**	**Reference**
Centrosome	Centrosome maturation and mitotic entry	(Eot-Houllier et al., 2010; Lindqvist et al., 2009; Watanabe et al., 2004; Zitouni et al., 2014)
Kinetochore	Kinetochore-microtubule attachment, APC/C activation, separation of chromatids and in the SAC	(Hansen et al., 2004; O'Connor et al., 2015; Raab et al., 2015; Sumara et al., 2004; von Schubert et al., 2015; Zhang et al., 2011)
Spindle midzone	Cleavage furrow formation	(Neef et al., 2003)
Midbody	Abscission	(Bastos and Barr, 2010)

This, in turn, promotes phosphorylation of Histone H3 on Threonine 3 (H3T3Ph) (Dai et al., 2005), facilitating recruitment of the CPC and activation of Aurora B at the

kinetochores (Wang et al., 2010; Wang et al., 2011) as shown in Figure 1.4. Aurora B then phosphorylates Haspin, triggering further phosphorylation on H3T3, through a positive-feedback loop (Wang et al., 2011). Furthermore, Aurora B activity at the kinetochore is regulated by PLK1, through a Survivin priming phosphorylation event (Chu et al., 2011). Aurora B phosphorylates HEC1 which allows the recruitment and activation of mono-polar spindle protein 1 (MPS1) (Saurin et al., 2011; Zhu et al., 2013). MPS1 has been shown to enhance the activation of Aurora B through phosphorylation of Borealin, a component of the CPC (Jelluma et al., 2008).

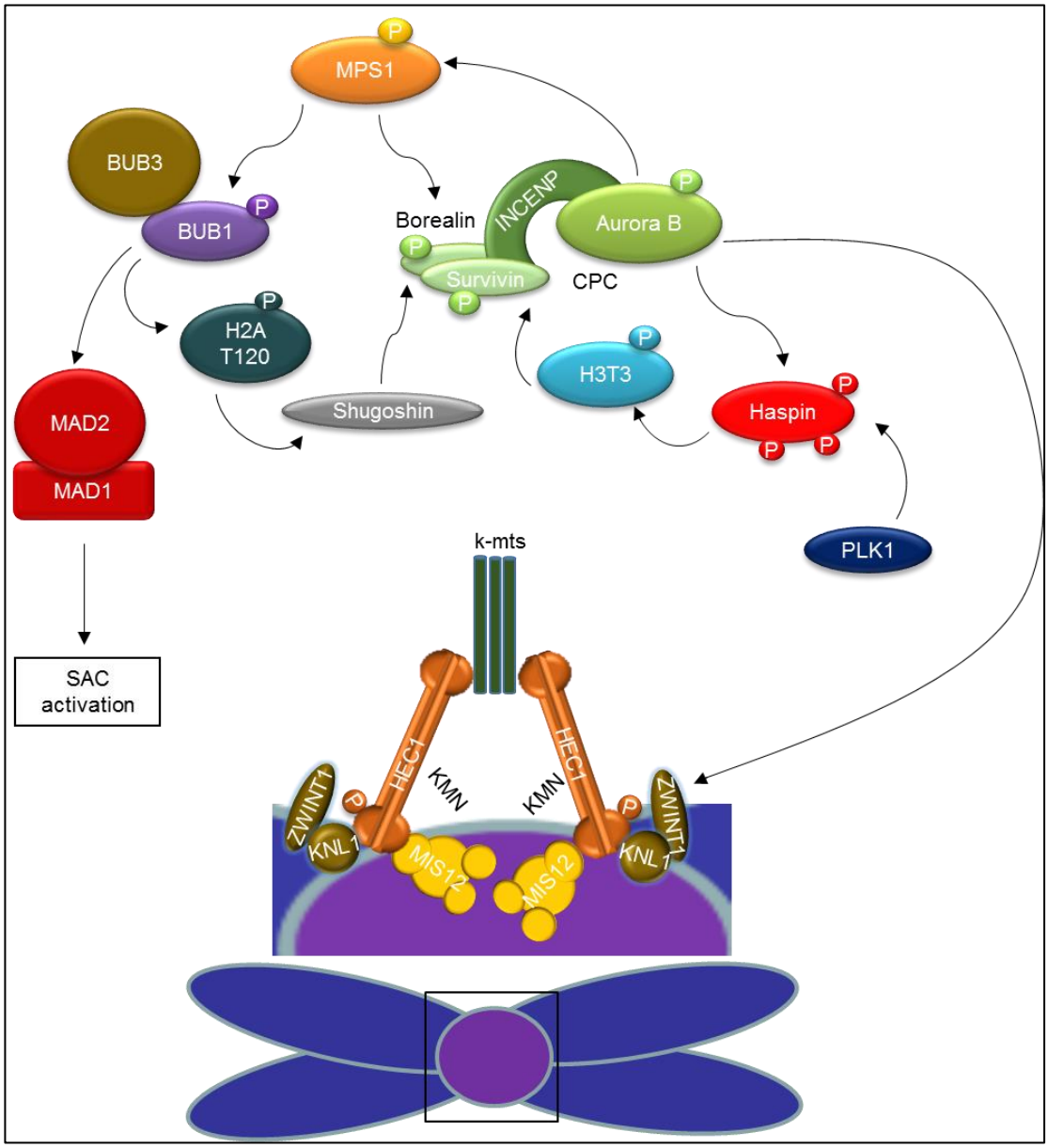

Figure 1.4 Model for kinetochore recruitment of the major SAC proteins

Assembly of the checkpoint occurs in a stepwise manner onto the kinetochore, facilitated by the KMN network. Haspin is activated by PLK1 which leads to the phosphorylation of Histone H3 on Thr3 and the recruitment of the CPC to the kinetochore. Aurora B kinase phosphorylates HEC1 which allows MPS1 to be recruited. This facilitates BUB1 recruitment to the kinetochore in complex with BUB3. Next the MAD1/MAD2 complex binds to the kinetochore which leads to SAC activation. Kinetochore (purple circle enclosed in the black box, sister chromatids (blue).

MPS1 phosphorylates MELT repeats of KNL1, to allow recruitment of the budding uninhibited by benzimidazole (BUB) proteins, BUB1 and BUBR1, and the mitotic arrested deficient (MAD) proteins, MAD1 and MAD2, to the kinetochores (Krenn et al., 2014; London and Biggins, 2014; Overlack et al., 2015). BUB1 then phosphorylates Histone H2A on Thr120 to recruit Shugoshin 1 (Sgo1) and Shugoshin 2 (Sgo2) (Kawashima et al., 2010). This in turn, enhances the activity of the CPC-Haspin-H3T3Ph feedback loop (Wang et al., 2011) as shown in Figure 1.4. Combined, these events lead to accurate checkpoint establishment.

There are four main types of attachments that can occur during mitosis (Figure 1.5). Monotelic attachments are recognised by the SAC and usually occur prior to amphitelic attachments, which lead to checkpoint silencing. Merotelic and syntelic attachments are recognised by the EC pathway (Gregan et al., 2011; Musacchio and Salmon, 2007). Amphitelic attachments occur when the sister kinetochores bind to microtubules that are nucleated from opposite poles to create stable and bi-polar attachments, generating tension and satisfying the checkpoint (Cimini and Degrassi, 2005; Uchida et al., 2009). Thus, leading to SAC silencing. Monotelic attachments, are those that occur when only one sister kinetochore is bound to microtubules which emanate from the spindle pole that it is facing. They normally occur prior to the formation of amphitelic attachments (Cimini and Degrassi, 2005). Syntelic attachments arise when both sister kinetochores attach to microtubules which nucleate from the same poles. Merotelic attachments occur when one or both sister kinetochores attach to microtubules that emanate from both spindle poles (Cimini and Degrassi, 2005). This latter form of attachment, cannot be sensed by the SAC as there are no unattached kinetochores and thus do not delay mitotic exit. Instead, they are corrected by the EC pathway, involving Aurora B (Gregan et al., 2011).

The EC pathway, specifically Aurora B, destabilises the erroneous attachments, by phosphorylation of key kinetochore proteins including components of the KMN network and mitotic centromere-associated kinesin (MCAK), to produce unattached kinetochores (Cheeseman et al., 2006; DeLuca et al., 2006; Lan et al., 2004; Zhang et al., 2007). These

unattached kinetochores are then recognised by the SAC and a ‘‘wait anaphase signal’’ is produced until k-mt attaches are corrected (Gregan et al., 2011).

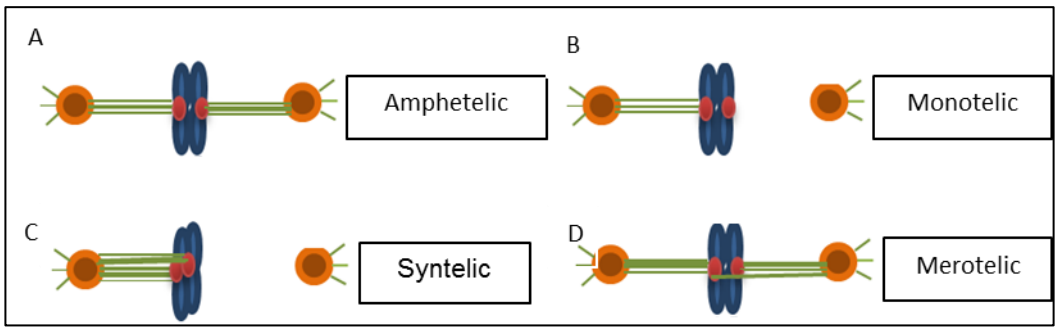

Figure 1.5 Four main k-mt attachments that occur during mitosis

A) Amphitelic: Both kinetochores bind to microtubules that are emanating from opposite poles. B) Monotelic: One kinetochore binds to microtubules of the pole it is facing. C) Syntelic: Both kinetochores are attached to microtubules of the same pole. D) Merotelic: One or both kinetochores attach to microtubules arising from both poles. Microtubules (green), centrosomes (orange), kinetochores (red), and chromosomes (blue).

Once the SAC has been properly established, robust SAC maintenance must ensue so that premature entry into anaphase does not occur.

1.5.2 - The role of SAC proteins in checkpoint maintenance

The same kinases that are required for establishment of the checkpoint, are also needed for the maintenance of the SAC. Direct inhibition of SAC kinases, such as Aurora B (Ditchfield et al., 2003; Hauf et al., 2003; Santaguida et al., 2011), MPS1 (Santaguida et al., 2010), or Haspin (De Antoni et al., 2012) can abruptly override a SAC induced cell cycle arrest. This results in mitotic exit without undergoing chromosome segregation, known as checkpoint override, indicating that these kinases are required for maintenance of the checkpoint. In particular, Aurora B, MPS1 and Haspin small molecule inhibitors, Hesperadin, Reversine and 5-Iodutubercidin, respectively, can cause SAC override of nocodazole arrested cells, either as single agents or synergistically when used, in combination, at concentrations which partially inhibit the kinases (De Antoni et al., 2012;

Santaguida et al., 2011; Saurin et al., 2011). Inhibition of the SAC kinases, Aurora B or MPS1, can also cooperate with depletion of a kinetochore protein, HEC1, to cause a checkpoint override (Saurin et al., 2011). Using a system in which prolonged activation of the SAC occurred, due to constitutively active MAD1, inhibition of Aurora B or MPS1 resulted in an override of the checkpoint arrest (Maldonado and Kapoor, 2011). This further implicates Aurora B and MPS1 in SAC maintenance.

PLK1 was not demonstrated to be required for checkpoint maintenance using this system (Maldonado and Kapoor, 2011). Inhibition of PLK1, unlike the inhibition of Aurora B, MPS1 and Haspin, is not sufficient to override the SAC induced cell cycle arrest, indicating that PLK1 is not strictly essential for the checkpoint (Li et al., 2015). The biological relevance of PLK1 in SAC maintenance was only recently uncovered by inhibiting PLK1 while also partially inhibiting Aurora B (Li et al., 2015; O'Connor et al., 2015). One study demonstrated that the major targets of PLK1 during SAC maintenance are a set of proteins that are also MPS1 targets, including MELT repeats of KNL1 and MPS1 auto-phosphorylation sites (von Schubert et al., 2015). In RPE-1 cells, PLK1 cooperates with MPS1 in the maintenance of the SAC and the combined inhibition of these two kinases causes a SAC override (von Schubert et al., 2015). *Caenorhabditis elegans*, does not have MPS1 and instead PLK1 substitutes for MPS1, by phosphorylating KNL1 to allow BUB1/BUB3 recruitment to the kinetochore (Espeut et al., 2015).

Cells arrested in mitosis with PLK1 inhibitors have been shown to have low levels of Aurora B at the kinetochores (Raab et al., 2015), suggesting that PLK1 dependent SAC override is associated with a mechanism dependent on Aurora B. However, another publication instead indicated that PLK1 inhibitors do not affect Aurora B localisation at the kinetochores (von Schubert et al., 2015), suggesting that the role of PLK1 in SAC maintenance is not dependant on Aurora B. Thus, the role of PLK1 in maintenance of the SAC is unclear.

Several sub-complexes of the SAC, function in both the establishment and maintenance of the checkpoint, to sense tension and correct erroneous k-mt attachments.

1.5.3 - The SAC effector: The mitotic checkpoint complex

The presence of unattached kinetochores during early mitosis catalyses the formation of the main SAC effector, the mitotic checkpoint complex (MCC) as shown in Figure 1.6. Three SAC subunits, BUB3, BUBR1 and MAD2, in complex with CDC20 (Sudakin et al., 2001), the activator of the E3 ubiquitin ligase APC/C, form the MCC. This leads to APC/C inactivation, stabilisation of Cyclin B and Securin which then blocks metaphase to anaphase progression (Musacchio and Salmon, 2007). Activation of MAD2 at unattached kinetochores is the most critical step in the formation of this complex. MAD2 exists as two different conformations, open-MAD2 (O-MAD2) and closed-MAD2 (C-MAD2). MAD2 is only active when it is in its closed form. Formation of C-MAD2 is catalysed by MAD1-MAD2 complexes which in turn, promotes the formation of MAD2-CDC20 complexes, followed by binding of CDC20 to BUBR1 (Luo et al., 2002; Sironi et al., 2002). MAD2 and BUBR1 bind to two distinct sites on CDC20 to synergistically inhibit the APC/C by preventing CDC20 from binding to the APC/C (Fang, 2002; Tang et al., 2001).

Once the last stable bipolar k-mt attachment occurs, formation of the MCC ceases. This results in SAC inactivation and the inhibition of CDC20, the co-activator of the SAC, is relieved (Lara-Gonzalez et al., 2012). This then causes polyubiquitination and degradation of Cyclin B and Securin followed by progression into anaphase and mitotic exit (Musacchio and Salmon, 2007; Nigg, 2001). Securin degradation results in the activation of Separase, which cleaves the cohesion complex at the centromeres of sister chromatids to allow proper segregation of sister chromatids to occur. Degradation of Cyclin B inactivates CDK1, which causes exit from mitosis (Nigg, 2001) as shown in Figure 1.6. Once this occurs, the SAC has become silenced. Thus, the SAC normally ensures faithful chromosome segregation and genome stability.

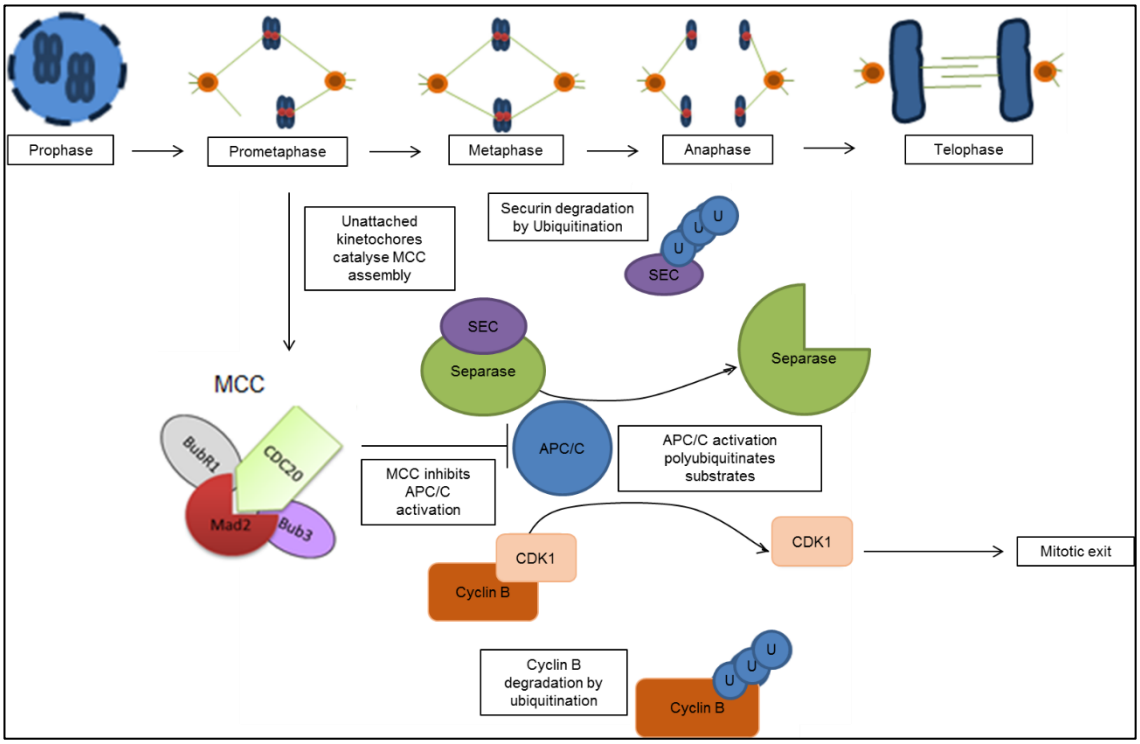

Figure 1.6 Timing of MCC formation and disassembly during mitosis

The stages of mitosis: prophase-telophase. Centrosomes (orange), microtubules (green), chromosomes (dark blue). The MCC forms during prometaphase and its disassembly occurs when all k-mt attachments are stable and bi-polar. CDC20 then activates the APC/C to allow polyubiquitination and degradation of Cyclin B and Securin and eventually mitotic exit occurs.

1.5.4 - The chromosomal passenger complex

The chromosomal passenger complex (CPC) which consists of Aurora B kinase and its three regulatory subunits: INCENP, Survivin and Borealin, localises to different structures during the various phases of mitosis, where it carries out different functions at each phase (Carmena et al., 2012b). During early prophase, it localises along the chromosome arms where it is involved in removing cohesion from the chromosome arms by phosphorylating Histone H3 on Ser 10 (H3S10Ph) and allows the enrichment of the CPC at the centromere (Hirota et al., 2005). During late prophase to metaphase, it localises to the centromere where it promotes bi-orientation of the mitotic spindle and functions in the error correction (EC) pathway through destabilising and repairing the

erroneous attachments, known as merotelic and syntelic attachments (Cimini, 2007). The CPC relocalises to the central spindle, to stabilise it, during anaphase, and then it moves to the equatorial cortex to regulate accurate execution of cytokinesis (Carmena and Earnshaw, 2003; Carmena et al., 2012b). In the latter years, the CPC has been shown to be required for SAC establishment and maintenance (Carmena et al., 2012b).

1.5.5 - Silencing the SAC

Once bi-orientation occurs, tension between sister kinetochores increases which leads to SAC inactivation. Several mechanisms contribute to silencing of the checkpoint.

As discussed in detail in Introduction section 1.5.1, activation of the SAC requires recruitment of many checkpoint proteins to the kinetochore. Thus, to extinguish the SAC, these proteins need to be removed from the kinetochore. As the microtubules fill the k-mt attachment sites, the SAC proteins MAD1 and MAD2 are stripped from the kinetochores towards the minus ends of the microtubules, by the minus-end motor protein dynein-dynactin, the RZZ complex and Spindly, leading to SAC inactivation (Musacchio, 2015). Constitutive MAD1 targeting to the kinetochore causes MAD2 to remain at the kinetochore, preventing SAC silencing, even after proper alignment occurs (Maldonado and Kapoor, 2011). Another report demonstrated that inhibition of dynein prevents removal of MAD2 from the kinetochores (Howell et al., 2001). Furthermore, tethering MPS1 to the kinetochore prevents removal of MAD1 and MAD2 from the kinetochores, even though the chromosomes were aligned (Jelluma et al., 2010). Thus, removal of checkpoint proteins, facilitated by the dynein-dynactin complex, is a crucial step in silencing the SAC.

Kinase phosphorylation is required for activation and recruitment of checkpoint proteins which allows SAC activation to occur. Therefore, it is likely that dephosphorylation events by protein phosphatase activity lead to SAC inactivation. Indeed, protein phosphatases 1 and 2A (PP1 and PP2A) have been reported to counteract the activity of PLK1, Aurora B and MPS1 in the SAC, by removing phosphate groups from these

kinases (Emanuele et al., 2008; Foley et al., 2011). KNL1 has been demonstrated to recruit PP1 to the kinetochore, which opposes Aurora B phosphorylation and therefore prevents Aurora B function (Liu et al., 2010). In addition, PP2A has been shown to repress phosphorylation of Aurora B substrates (Foley et al., 2011). PP2A also counteracts MPS1 phosphorylation of KNL1, which can in turn lead to a reduction in the activity of downstream kinases including BUBR1 and BUB1 (Espert et al., 2014). Furthermore, PLK1 has been shown to promote silencing by phosphorylating BUBR1, promoting BUBR1 interaction with PP2A. This counteracts the activity of Aurora B, leading to silencing of the SAC (Suijkerbuijk et al., 2012). PP1 has also been shown to antagonise Aurora B at the kinetochore (Emanuele et al., 2008; Francisco et al., 1994). PP1 localises to the kinetochore by binding to KNL1 on the RVXF motif and its recruitment to the kinetochore has been proposed to be facilitated by CENP-E (Musacchio, 2011). Binding of PP1 to the RVXF motif on KNL1 counteracts Aurora B phosphorylation on the RVXF motif, leading to SAC silencing (Hendrickx et al., 2009; Musacchio, 2011). However, there is limited understanding of the regulation and balance between kinase and phosphatase activity at the kinetochores.

Disassembly of the MCC and dissociation of CDC20 from its inhibitors, allows CDC20 dependant activation of the APC/C, which contributes to SAC silencing. MCC disassembly is thought to be mediated by $p31^{comet}$, a SAC antagonist and a MAD2 interacting protein. $p31^{comet}$ mimics the structure of O-MAD2 and is therefore able to bind to C-MAD2. Binding of $p31^{comet}$ to C-MAD2 prevents O-MAD2 binding to C-MAD2 which blocks MAD2 activity (Yang et al., 2007). The APC/C ubiquitinylates components of the MCC, promoting its disassembly, leading to checkpoint inactivation (Lara-Gonzalez et al., 2012).

The checkpoint monitors k-mt attachments and remains active until bi-orientation occurs. How microtubule binding satisfies the SAC is not clear. However, a current model proposes that SAC signalling is regulated by competitive binding between SAC kinases and microtubules to HEC1. MPS1 and microtubules bind to the same site on HEC1. Once

microtubules attach to the HEC1, MPS1 can no longer bind to HEC1, leading to the removal of the SAC signal and progression through (Hiruma et al., 2015).

It is evident that there are several mechanisms that exist to contribute to checkpoint silencing but how these processes are coordinated is poorly understood. Thus, further elucidation of these processes is required to fully understand how the SAC is silenced.

1.5.6 - Deregulation of the SAC and cancer

A robust SAC is essential for sensing tension and correcting abnormal k-mt attachments and is therefore required for faithful chromosome segregation, which is necessary for maintaining genome stability. Defects in checkpoint function, weaken the SAC, which result in an increase in mis-aligned chromosomes and chromosome mis-segregation which can lead to genome instability through aneuploidy (Giam and Rancati, 2015).

Mutations and internal deletions have been found in the genes of BUB1, BUBR1 and MAD1 in some cancer cell lines (Cahill et al., 1998; Nomoto et al., 1999; Ohshima et al., 2000; Ru et al., 2002). The work of Cahill et al. 1998, showed that an allele that can code for a mutated BUB1 protein has a dominant-negative effect over the wild-type protein because when the mutated BUB1 allele was introduced into cells displaying microsatellite instability with an otherwise proficient checkpoint, it resulted in a defective checkpoint. However, a large number of aneuploid cell lines do not harbour mutations in checkpoint genes possibly because frequent chromosome loss or gain could cause cell death, due to the essential nature of SAC genes(Lopes and Sunkel, 2003). It is possible that the defect in SAC function, in cancer cell lines which do not appear to have mutations in checkpoint genes, may be due to altered expression levels of SAC genes (Bharadwaj and Yu, 2004).

SAC kinases, including PLK1, Aurora B and MPS1 are overexpressed in multiple cancer cell lines and tumours (Chieffi et al., 2006; Kurai et al., 2005; Ling et al., 2014; Strebhardt and Ullrich, 2006; Takai et al., 2005). Inhibitors or depletion of checkpoint kinases cause entry into an abortive mitosis which results in polyploidy and apoptosis due to ‘‘mitotic

catastrophe'' (Vitale et al., 2011) in TP53 deficient cancer cells (Guan et al., 2005; Jemaa et al., 2013).

Several inhibitors of SAC kinases have been tested in xenograph and pre-clinical models, where they have been shown to inhibit tumour growth, and some have progressed into clinical trials (Colombo et al., 2010; Guan et al., 2005; Kollareddy et al., 2012; Mross et al., 2008; Perez de Castro et al., 2008; Schoffski, 2009; Wilkinson et al., 2007). These inhibitors have been shown to synergise with taxol, a drug that targets microtubules, to reduce tumour growth in xenograph models (Curry et al., 2009; Jemaa et al., 2013). Further investigation into effective combination therapies would potentially benefit treatment of cancers, as it helps to overcome the problem of drug resistance from treatment with single pharmacological agents in cancer treatment (Longley and Johnston, 2005).

1.5.7 – Mode of action and specificity of kinase inhibitors used in this study

Various kinase inhibitors of PLK1, CDC7, Aurora B and MPS1 were central to the work in this thesis. GW843682X and BI6727 were used as PLK1 inhibitors (Lansing et al., 2007; Rudolph et al., 2009). GW843682X and BI6727 are chemically different but both inhibitors are ATP competitive PLK1 inhibitors. GW843682X targets PLK1 enzyme with an IC_{50} of 2.2 nmol/L, whereas BI 6727 has an IC_{50} of 0.87 nmol/L on the PLK1 enzyme (Lansing et al., 2007; Rudolph et al., 2009). GW843682X and BI 6726 also target PLK3 and BI 6727 targets PLK2 but at much higher concentrations (Lansing et al., 2007; Rudolph et al., 2009). PLK3 is involved in DNA replication, neuronal differentiation and is a mediator of apoptosis and many types of cellular stress (Helmke et al., 2016). PLK2 functions in centrosome duplication, cellular stress responses and neuronal differentiation (de Carcer et al., 2011).

PHA-767491 which is a dual CDC7/CDK9, was used as a CDC7 kinase inhibitor (Montagnoli et al., 2004). It is a well characterised ATP competitive CDC7 kinase inhibitor with an IC_{50} of 10 nM and 34 nM for and CDK9 respectively. As PHA-767491

targets CDK9 aswel as CDC7, a second and more specific and potent ATP competitive CDC7 kinase inhibitor, XL413 was also used (Koltun et al., 2012). XL413 has an IC_{50} of 7.7 nM for CDC7.

Hesperadin was used as a specific ATP competitive Aurora B kinase inhibitor. It has been shown to target six other kinases but it is not known to target other SAC kinases, Aurora A or Aurora C (Hauf et al., 2003).

The ATP competitive MPS1 inhibitor, Reversine, was utilised to inhibit MPS1 kinase. Reversine has an IC_{50} of 6 nM towards MPS1 and it inhibits Aurora B but with an IC_{50} of 98.5 nM (Santaguida et al., 2010).

Each of these kinase inhibitors are used frequently in published work and are well characterised and specific inhibitors of the mentioned kinases.

1.6 - Thesis aims

- Assess the role of PLK1 in SAC maintenance
- Investigate a possible role for CDC7 kinase in mitosis
- Characterise cell lines carrying mutations in either *DBF4* or *DRF1*

CHAPTER 2:

MATERIALS AND METHODS

2.1 - Commonly used buffers

Reagents used were obtained from Sigma-Aldrich unless otherwise stated. 6-carboxyfluorescein TEG-azide and 5-ethynyl-2'-deoxyuridine (EdU) were purchased from Berry & Associates. Buffers used in this thesis are presented in table 2.1.

Table 2.1 Details of buffers used in this study

Buffer	Composition	Application
Click reaction solution	10 μM 6-carboxyfluorescein TEG-azide, 10 mM sodium-L-ascorbate, 2 mM $CuSO_4$	EdU labelling of nascent DNA
Crystal violet	2% (w/v) Crystal violet, 25% methanol	Staining of cell colonies
CSK Buffer	10 mM PIPES pH 6.8, 100 mM or 300 mM NaCl, 300 mM Sucrose, 1.5 mM $MgCl_2$, 10 mM NaF, 0.5% triton-X. 1 mM DTT and protease and phosphatase inhibitors were added fresh	Cell lyse buffer
Laemmli sample buffer (5X)	60 mM Tris-HCl pH 6.8, 2% SDS, 10% glycerol, 5% β-mercaptoethanol, 0.01% bromophenol blue (Laemmli, 1970)	Sample preparation for SDS-PAGE

PBS	10 mM phosphate buffer, 137 mM NaCl, 2.7 mM KCl	Wash buffer
PBST	PBS, 0.5% tween 20	Wash buffer for immunoblotting
PBS-TX	PBS, 0.1% Triton X-100	Cell permeabilisation for immunofluorescence
Ponceau S stain	0.1% (w/v) Ponceau S, 5% (v/v) acetic acid	Reversible staining of nitrocellulose membrane
SDS-PAGE running buffer	25 mM Tris, 0.1% SDS, 190 mM glycine	SDS-PAGE gel running buffer
SDS-PAGE transfer buffer	25 mM Tris, 190 mM glycine, 20% methanol	Protein transfer onto nitrocellulose membrane
TGN buffer	50 mM Tris-HCL pH 7.5, 200 mM NaCl, 50 mM β-Glycerophosphate, 50 mM NaF, 1% Tween 20, 0.2% NP-40	Cell lyse buffer

2.2 - Antibodies

Details of primary antibodies used, including dilutions, used for immunofluorescence (IF), immunoblotting (IB) and flow cytometry (FC), are shown in Table 2.2. Secondary antibodies used for IF, IB and FC are shown in Table 2.3. All Alexa Fluor-conjugated secondary antibodies used for IF and FC were purchased from Invitrogen and secondary antibodies for IB were purchased from LI-COR Biosciences.

Table 2.2 Details of primary antibodies used for IF, IB and FC

Antigen	Species	Antibody Source	Application and antibody conditions
GAPDH	Rabbit	Santa Cruz (sc-25778)	(WB) 1:2000 in 5% Milk PBST
CDC7	Mouse	MBL International (K0070-3)	(WB) 1:1000 in 5% Milk PBST
Total MCM2	Mouse	AbD Serotec (MCA1859)	(WB) 1:1000 in 1% BSA PBST
pS0/41 MCM2	Rabbit	(Montagnoli et al., 2006)	(WB) 1:5000 in 1% BSA PBST
HEC1	Mouse	Gentex (Clone 9G2.23)	(WB) 1:1000 in 5% Milk PBST (IF) 1:1500 in 1% BSA-PBS-TX
H3S3Ph	Rabbit	Cell signalling (9714)	(WB) 1:1000 in 1% BSA PBST (IF) 1:400 in 1% BSA-PBS-TX
ZWINT-1	Rabbit	Bethyl (IHC-00095)	(WB) 1:1000 in 5% Milk PBST (IF) 1:100 in 1% BSA-PBS-TX
PLK1	Mouse	Santa Cruz (sc-56948)	(WB) 1:500 in 1% BSA PBST
PLK1	Mouse	Abcam (Ab17057)	(IF) 1:200 in 1% BSA-PBS-TX
T210 PLK1	Mouse	Abcam (39068)	(WB) 1:1000 in 1% BSA PBST (IF) 1:300 in 1% BSA-PBS-TX
pMPM2	Mouse	Millipore (05-368)	(WB) 1:1000 in 5% Milk PBST
Cyclin B	Mouse	Santa Cruz (sc-245)	(WB) 1:1000 in 5% Milk PBST

TCTP	Rabbit	Cell Signalling (8441S)	(WB) 1:1000 in 1% BSA PBST
pSer46 TCTP	Rabbit	Cell Signalling (5251S)	(WB) 1:1000 in 1% BSA PBST
pS53 MCM2	Rabbit	(Montagnoli et al., 2006)	(WB) 1:1000 in 1% BSA PBST
pS108 MCM2	Rabbit	(Montagnoli et al., 2006)	(WB) 1:1000 in 1% BSA PBST
pS139 MCM2	Rabbit	(Montagnoli et al., 2006)	(WB) 1:1000 in 1% BSA PBST
DBF4 clone 6F4/6	Mouse	Lab stock (1.8 mg/ml)	(WB) 1:1000 in 5% Milk PBST (IF) 1:180 in 1% BSA-PBS-TX
pSer317 CHK1	Rabbit	Cell Signalling (2344L)	(WB) 1:1000 in 1% BSA PBST
Total CHK1	Rabbit	Santa Cruz (sc-484)	(WB) 1:1000 in 5% Milk PBST
Strep	Mouse	Qiagen (34850)	(WB) 1:1000 in 5% Milk PBST
AIM-1	Mouse	BD Bioscience (611082)	(IF) 1:100 in 1% BSA-PBS-TX
pSer7CENP-A	Rabbit	Millipore (04-792)	(IF) 1:200 in 1% BSA-PBS-TX
Anti-Centromere	Human	Antibodies Incorporated (15-234)	(IF) 1:100 in 1% BSA-PBS-TX
CDC7	Mouse	(Tenca et al., 2007)	(IF) 1:50 in 1% BSA-PBS-TX
Pericentrin	Rabbit	Abcam (Ab4448)	(IF) 1:3000 in 1% BSA-PBS-TX

MAD1-488	Mouse	Gift from S. Taylor	(IF) 1:600 in 1% BSA-PBS-TX
H3S10Ph	Rabbit	Millipore 06-570	(FC) 1:50 in 1% BSA-PBS
TPX2	Rabbit	Bethyl A300-430	(IF) 1:100 1% BSA-PBS-TX

Table 2.3 Details of secondary antibodies used for IF, IB and FC

Secondary Antibodies	**Catalog number**	**Application and antibody conditions**
Anti-Rabbit IgG (680 LT)	926-68021	(WB) 1:10,000 in 5% Milk-PBST
Anti-Rabbit IgG (800 CW)	926-32211	(WB) 1:10,000 in 5% Milk-PBST
Anti-Mouse IgG (680 LT)	926-68020	(WB) 1:10,000 in 5% Milk-PBST
Anti-Mouse IgG (800 CW)	926-32210	(WB) 1:10,000 in 5% Milk-PBST
Anti-Mouse 488	A-11001	(IF) 1:300 in 1% BSA-PBS-TX
Anti-Rabbit 488	A-11034	(IF) 1:300 in 1% BSA-PBS-TX (FC) 1:50 in 1% BSA-PBS
Anti-Mouse 546	A-11003	(IF) 1:300 in 1% BSA-PBS-TX
Anti-Rabbit 546	A-11010	(IF) 1:300 in 1% BSA-PBS-TX
Anti-Human 647	A-21445	(IF) 1:300 in 1% BSA-PBS-TX

2.3 - Plasmids

The plasmids used in this study were generated in house and are detailed in Table 2.4.

Table 2.4 Details of plasmids used in this study

Plasmid name	Epitope tag (s)	Application
pAB1-CDC7	Flag-Strep (C-term)	Overexpression of CDC7
pAB1-DBF4	Flag-Strep (C-term)	Overexpression of DBF4
pAB1-DRF1	Flag-Strep (C-term)	Overexpression of DRF1
pLenti-CDH1-EF1-DBF4	Flag-Strep (C-term)	Lentiviral plasmid for the generation of stable cell lines overexpressing DBF4
pCDH-MCS-EF1-Neomycin	-	Cloning vector
pCDH-EF1-DBF4-MCS	Flag-Strep (C-term)	DBF4 containing plasmid for transfecting with lentiviral packaging and envelop plasmids
psPax2	-	Lentiviral packaging plasmid
pMD2.G	-	Lentiviral envelop plasmid
pRSV-Rev	-	Lentiviral packaging plasmid

2.4 - Cell culture methods

2.4.1 - Maintenance of cells

Osteosarcoma (U2OS) cells, from Noel Lowndes Laboratory, were first authenticated by STR analysis and subsequently certified by transposon profiling. U2OS cells were maintained in Dulbecco's modified Eagles medium (DMEM). HAP1 cells from Horizon Genomics were maintained in Iscove's modified Dulbecco's medium (IMDM). Human Embryonic Kidney (HEK) 293T cells, were obtained from American Type Culture Collection (ATCC) and host Flp-In T-REx HEK 293 cells were obtained from Invitrogen. HEK 293T cells, Flp-In T-REx HEK 293 Empty vector (EV), DBF4-Strep and DRF1-Strep cells were maintained in DMEM. Flp-In T-REx HEK 293 DBF4-Strep and DRF1-

Strep cell lines were generated similarly to Claspin Flp-In T-REx HEK-293 (McGarry et al., 2016) and cells were selected with Hygromycin (100 μg/ml) and Blasticidin (5 μg/ml). The protein of interest was induced with the addition of Doxycycline (1 μg/ml). All media were supplemented with 1% penicillin-streptomycin and heat inactivated 10% fetal bovine serum (FBS). Cells were cultured at 37°C with 5% CO_2.

2.4.2 - Growth curves

HAP1 wild-type (WT), DBF4 knockout (KO) and DRF1 KO cells were plated at a density of $6x10^4$/well in a 6-well dish and incubated for 24, 48 and 72 hours. The cells were then harvested, resuspended in a trypan blue and counted using the automated cell counter Countess (Invitrogen). Cell viability was determined by trypan blue exclusion.

2.4.3 - Drug treatment

The drugs used in this study and their targets are outlined in Table 2.5. The concentration used in each experiment is mentioned in the figure legend.

Table 2.5 Details of drugs used in this study

Name of drug	Drug target and reference	Source
Nocodazole	Microtubules (De Brabander et al., 1976)	Sigma Aldrich
MG132	Proteosome (Adams et al., 1998)	Sigma Aldrich
GW843682X	PLK1 (Lansing et al., 2007)	Tocris
BI 6727	PLK1 (Rudolph et al., 2009)	Stratech Scientific
Hesperadin	Aurora B (Hauf et al., 2003)	Axon Medchem
Reversine	MPS1 (Santaguida et al., 2010)	Cayman chemical
5-Iodotubercidin	Haspin (De Antoni et al., 2012)	Medchem

XL413	CDC7 (Koltun et al., 2012)	Made in house (Rainey et al., 2013)
PHA-767491	CDC7 (Montagnoli et al., 2008)	Tocris
Taxol	Microtubules (De Brabander et al., 1981)	Calbiochem
Etoposide	Topoisomerase II (Nitiss, 2009)	Sigma Aldrich
Hydroxyurea	Ribonucleotide reductase (Skoog and Bjursell, 1974; Skoog and Nordenskjold, 1971)	Sigma Aldrich
KU55933	ATM (Hickson et al., 2004)	Selleckchem
VE-821	ATR (Charrier et al., 2011)	Selleckchem
Mitomycin C	Alkylating agent (Gargiulo et al., 1995)	Sigma Aldrich
Cisplatin	Cross-linking agent (Loehrer and Einhorn, 1984)	Selleckchem
Aphidicolin	DNA polymerase α (Huberman, 1981)	Sigma Aldrich
Camptothecin	Topoisomerase I (Hsiang et al., 1985)	Selleckchem
RO-3306	CDK1 (Vassilev et al., 2006)	Millipore

2.4.4 - Colony formation assay

HAP WT and DBF4 KO cell lines were treated with HU or water, as a control. Eighteen hours later, cells were trypsinised, counted and replated in fresh media at a density of $1x10^3$ cells/10 cm dish. Seven days later the colonies that had formed from the cells which survived were fixed with 100% methanol for 24 hours, stained with crystal violet buffer and counted. Statistical analysis was performed using Graphpad Prism software.

2.4.5 - Alamar blue assay

HAP1 WT, DBF4 KO and DRF1 KO cells were plated in a 96-well plate at a density of $4x10^3$ cells/well. Cells were treated with either XL413, Etoposide, VE-821, KU55933, Cisplatin, Aphidicolin, Mitomycin C or Camptothecin for 24 hours. Alamar blue was added to cells at a final concentration of 0.112 M, 4 hours prior to the end of the drug treatment. Fluorescence was measured at an absorbance of 595 nm using a Wallac Victor 3 1420-012 (Perkin Elmer) and drug induced changes in cellular reductase activity were calculated.

2.5 - Basic DNA methods

2.5.1 - Mammalian genomic DNA extraction

Performed as per the Sigma-Aldrich Gene Elute ™ Mammalian DNA extraction miniprep kit, user manual instructions.

2.5.2 - Cell transfection using plasmid DNA

Plasmids used in this study are detailed in table 2.4.

DNA transfections in U2OS cells were carried out using JetPEI, Transfection reagent, from Polyplus, as per the manufacturers' recommendations. 1 µg of DNA and 4 µl JetPEI reagent were added to two separate tubes containing 150 mM NaCl solution, vortexed and centrifuged briefly. NaCl solution containing the JetPEI reagent was added to the DNA solution, vortexed and centrifuged. The DNA/JetPEI mixture was left at room temperature for 15 minutes before being added to the cells.

DNA transfections in HEK 293T cells were performed using JetPEI. psPAX2 (13 µg), pCDH-EF1-DBF4-MCS (13 µg), pMD2.G (5.6 µg) and pRSV-Rev (5.6 µg) were added to a tube containing 150 mM $NaCl_2$. 150 mM $NaCl_2$ and 41 µl of JetPEI were added to a separate tube. The tubes were then vortexed and centrifuged briefly. NaCl solution containing the JetPEI reagent was added to the DNA solution, vortexed and centrifuged. The DNA/JetPEI mixture was left at room temperature for 30 minutes before being added to the cells.

2.5.3 - *E. coli* transformation

50 µl of NEBα competent bacterial cells were allowed to thaw on ice. 1 µl of DNA was then added to the bacterial cells and mixed. The cells were incubated on ice for 30 minutes, heat shocked at 42 °C for 45 seconds and replaced on ice for 2 minutes. Cells were recovered with the addition of 100 µl of Luria Bertani (LB) media and incubated at 37 °C and rotation at 250 rpm for 1 hour. Cells were then plated onto LB/Amp (100 µg/ml) plates and incubated overnight at 37 °C.

2.5.4 - Plasmid amplification and purification

Single colonies from the *E. coli* transformation were picked and expanded in 5 ml of LB media containing Amp (100 µg/ml) in a shaking incubator and incubated overnight at 37°C. Plasmids were purified from this culture, using the GenElute Plasmid Miniprep Kit (Sigma-Aldrich), per the manufacturer's instructions. For maxi-preps, 200 µl of the initial 5 ml culture was added to 200 ml LB media and incubated overnight at 37 °C. Plasmid purifications were carried out, using the GenElute HP Plasmid Maxi prep Kit (Sigma-Aldrich), per the manufacturer's instructions.

2.5.5 - PCR and PCR purification

Primer sequences used for PCR amplification of DNA are detailed in table 2.6.

PCR amplifications of *DBF4* exon 3 and *DRF1* exon 4 from HAP1 cells lines were carried out using standard cycling conditions (initial denaturation: 95°C, 2 minutes; denaturation 95°C, 15 seconds; annealing 60°C for 15 seconds, extension: 72°C; 1 minute).

PCR amplification of the open reading frame (ORF) of the cDNA from pAB1-DBF4 plasmid was carried out using platinum *pfx* DNA polymerase protocol from Invitrogen with standard cycling conditions for this protocol (initial denaturation: 95°C, 2 minutes; denaturation 95°C, 15 seconds; annealing 56°C for 30 seconds, extension: 68°C; 2 minutes).

Qiagen QIAquick PCR purification kit was used for purification of PCR products.

Table 2.6 Details of primers used in this study

Primer	Primer sequence
DBF4 fwd 1	5’ - AGGAGCTCTTATACTTCCTCAGAGA - 3’
DBF4 rev 1	5’ - ACTCTACTGCCACCTTGCTATTAAA - 3’
DRF1 fwd 1	5’ - TGACAATTCTGCATTTGCTTTTTGG - 3’
DRF1 rev 1	5’ - CACCAAAGCCTACTTCCTTTGTTTA - 3’
DBF4 fwd 2	5’ - GCGAATTCGAACTCCGGAGCCATGAGG - 3’
DBF4 rev 2	5’-ATTCTTATGCGGCCGCCTATTTCTCAAACTGTGGATGGC-3’

Underlined sequence is an overhang.

2.5.6 - DNA sequencing

Sanger sequencing of DNA was performed by Eurofins Genomics with the appropriate sequencing primers.

2.6 - Lentiviral methods

2.6.1 - Lentiviral packaging plasmids

pCDH-CMV-MCS-EF1-Neomycin, psPax2, pMD2.G, pRSV-Rev plasmids were purchased from Addgene. DBF4 ORF cDNA was PCR amplified from the pAB1-DBF4 plasmid using primers containing overhangs (DBF4 fwd 2 and DBF4 rev 2, from Table 2.6) with compatible restriction sites (DBF4 fwd; EcoR1, DBF4 rev 2; NOT1), which allowed for cloning of the coding sequence into the pCDH-CMV-MCS-EF1-Neomycin lentiviral cloning plasmid. pCDH-CMV-MCS-EF1-Neomycin and the PCR amplified ORF of pAB1-DBF4 plasmid were then digested and the purified plasmids were ligated together and transformed into NEBα competent bacteria cells.

2.6.2 - Generation of lentivirus

HEK 293T cells were plated at a density of $5x10^6$ cells/15 cm dish and incubated at 37 °C, for 24 hours. Lentivirus for pLenti-CDH-EF1-DBF4 was generated by cotransfecting pCDH-EF1-DBF4-MCS-Neomycin plasmid (13 μg) with a 2nd generation lentiviral packaging system, psPax2 (13 μg), pMD2.G (5.6 μg) and pRSV-Rev (5.6 μg) plasmids, using JetPEI transfection reagent into the HEK 293T cells. The media was changed 6 hours after transfection. Twenty-four hours after transfection the media containing the lentivirus was collected and replaced with fresh media. Twenty-four hours after the addition of fresh media, the lentivirus containing media was again collected and pooled.

2.6.3 - Lentiviral transduction

Lentivirus was used to generate stable clones expressing DBF4 in the HAP1 WT and DBF4 KO cells line. WT and DBF4 KO cell lines were plated at a density of $8x10^5$ cells/well in 6-well dish. The cells lines were transduced the following day with increasing volumes of virus, either 0 μl, 60 μl, 120 μl, 240 μl or 480 μl virus in a total volume of 2 ml. After 24 hours, the media was replaced with media containing G418 (2 mg/ml). There was also a sample that was not transduced and to which no selection was added, as a control. Once all the cells in the control sample in the presence of G418, were dead, the percentage efficiency of each transduction was calculated (number of cells that survived in the transduced sample/number of cells in the control samples multiplied by 100). Polyclonal cell lines were then generated using the sample that had between 20-30% transduction efficiency.

2.7 - Protein manipulation methods

2.7.1 - Protein extraction and quantification methods

2.7.1.1 - Total protein extraction

Cell pellets were resuspended in CSK buffer with 300 mM NaCl and placed on ice for 10 minutes. Samples were then sonicated with the use of a probe sonicator for 1 second on 1 second off, ten times. Proteins were quantified by the Bradford assay (as described in 2.7.1.3).

2.7.1.2 - Soluble protein extraction

Cell pellets were resuspended in CSK buffer with 100 mM NaCl and placed on ice for 10 minutes. Samples were centrifuged at 3,200 rpm for 10 minutes. The soluble fraction was moved to a fresh tube and quantified using a Bradford assay (as described in 2.7.1.3). Typically, 20 µg of protein was prepared for each sample. Laemmli buffer was added to the prepared samples to a final dilution of 1x and samples were placed at 95°C for 5 minutes. The samples were ready to be loaded onto an SDS-PAGE gel.

2.7.1.3 - Protein quantification by Bradford assay

Adapted from the original Bradford assay description (Bradford, 1976). Protein concentration was determined by adding 180 µl of Bradford protein reagent to 1 µl of protein extract. The absorbance of each sample, at 595 nm, was measured using a Wallac Victor 3 1420-012 (Perkin Elmer). A standard curve was also prepared with a known range of concentrations of BSA (1 mg/ml – 5 mg/ml) in CSK buffer.

2.7.2 - Phosphatase Assay

Cells were lysed in TGN buffer (50 mM Tris-HCL pH 7.5, 200 mM NaCl, 50 mM β-Glycerophosphate, 50 mM NaF, 1% Tween 20, 0.2% NP-40) on ice for 20 minutes and centrifuged at 13,000 rpm for 20 minutes. 20 µg of extract was incubated with 100 units of λ phosphatase (Sigma). The reactions were stopped by the addition of 2x Laemmli buffer and by heating to 95°C for 5 minutes.

2.7.3 - Immunoprecipitation-kinase assay

For the immunoprecipitation-kinase assay, 1 mg of protein extract was incubated with 10 µg of anti-DBF4 (6F46-4) antibodies and 25 µl of protein G-Sepharose beads for 2 hours at 4 °C with end-over-end mixing followed by washing. After immunoprecipitation, the beads were equilibrated in kinase buffer (50 mM Hepes pH7.5, 10 mM MgCl2, 2 mM DTT) and incubated in 20 µl of the same buffer containing MCM2 N-terminal fragment (2 µg), 2.8 µM ATP and 1 µCi of [γ-^{32}P] ATP in the presence or absence of 100 nM XL413, a CDC7 kinase inhibitor. The reaction was performed at 30°C for 30 minutes and

stopped by addition of 25 µl of 2x Laemmli buffer and incubation at 95°C for 5 minutes. Samples were resolved by SDS-PAGE followed by immunoblotting onto a nitrocellulose membrane. Incorporation of γ-^{32}P was assayed by autoradiography.

2.8 - Sample preparation, electrophoresis and immunoblotting

2.8.1 - Sample preparation

Laemmli buffer was added, to 20 µg of protein extract, to a final dilution of 1x Laemmli buffer and samples were placed at 95°C for 5 minutes.

2.8.2 - SDS-PAGE protein gels

Ten % or 12.5 % polyacrylamide gels were routinely used for running protein samples on the Bio-Rad mini-PROTEAN system. Table 2.7 details the different components for the resolving and stacking gels used to make one SDS-PAGE gel. Resolving gels were allowed to set at room temperature with isopropanol overlaying the gel. Once set, the isopropanol was removed, the top of the gel was washed with dH_2O, the stacking gel poured and a 15-well comb was added immediately. Once the stacking gel had set, the gels were ready for running the protein samples. 2 µl of a pre-stained protein molecular weight marker (PageRuler™ Plus Prestained Protein Ladder-10 to 250 kDa) was loaded beside the protein samples. Electrophoresis was conducted at 60 V until the samples had entered the resolving gel and then at 100 V.

Table 2.7 Reagents used to prepare SDS-PAGE resolving and stacking gels.

Reagent	10% resolving gel	12.5% resolving gel	Stacking gel
H_2O	2760	1930	3605
30% Acrylamide/Bis-acrylamide 37:5:1	3340	4170	665
1 M Tris-HCl pH 8.8	3750	3750	-
1 M Tris-HCl pH 6.8	-	-	625
10% SDS	100	100	50
10% APS	50	50	25
TEMED	5	5	5

Volumes are in µl.

2.8.3 - Protein transfer

The SDS-PAGE gels were placed onto nitrocellulose membrane, which was placed between sheets of 2 mm blotting paper, all of which were pre-equilibrated in transfer buffer. This was contained within a transfer cassette and placed in a Mini Trans-Blot system (Bio-Rad) transfer apparatus surrounded with transfer buffer and an ice pack. Proteins were typically transferred for 2.5 hours at a current of 250 mA. The nitrocellulose membrane was then stained with Ponceau S stain. The Ponceau S stain was removed with PBS prior to immunoblotting.

2.8.4 - Immunoblotting

The nitrocellulose membrane was blocked in 5% milk-PBS for 1 hour at room temperature, unless otherwise stated. The membrane was incubated with primary antibodies for 18 hours at 4°C. Antibody conditions are detailed in Table 2.2. The nitrocellulose membrane was washed 3 times in PBST for 10 minutes prior to incubation

with secondary antibodies for 1 hour at room temperature. Conditions for secondary antibodies are detailed in Table 2.3. The nitrocellulose membrane was washed twice in PBST for 10 minutes, followed by a final 10-minute wash in PBS. Immunoreactive bands were visualised using an Odyssey Infrared Imaging System (Li-Cor Biosciences).

2.9 - Flow Cytometry

Table 2.2 and Table 2.3 detail the conditions for which the primary and secondary antibodies were used for FC.

2.9.1 - Detection of H3S10Ph by Flow cytometry

Cells were plated at a density $5x10^5$ cells/well in a 6-well dish. Cells were harvested and fixed with 70% ethanol, then permeabilised with 0.25% Triton-X 100 in PBS for 15 min, on ice. Cells were incubated with primary antibodies for 1 hour, washed with PBS and incubated with secondary antibodies for 1 hour. Cells were washed and resuspended in PBS or PI. Flow cytometry was carried out on a BD FACS Canto A and data was analysed using FlowJo software version 10.

2.9.2 - Detection of DNA content and DNA synthesis

Cells were plated at a density $5x10^5$ cells/well in a 6-well dish. Cells were labelled with EdU 30 minutes prior to harvesting and then fixed with 70% ethanol. Blocking was performed with 1% BSA in PBS for 15 minutes. Cells were resuspended in Click-iT reaction mix for 30 minutes. Cells were washed in 1% BSA in PBS with 0.5% Tween-20 and then resuspended in 500 µl of 1% BSA in PBS 0.1 mg/ml RNase and 1 µg/ml DAPI. Flow cytometry was carried out on a BD FACS Canto II and data was analysed using FlowJo software version 10.

2.10 - Microscopy

Table 2.2 and Table 2.3 detail the conditions for which the primary and secondary antibodies were used for IF.

2.10.1 - Immunofluorescence microscopy

Cells were fixed with 4% paraformaldehyde (PFA) for 10 min or with PTEMF (20 mM PIPES pH 6.8, 0.2% Triton X-100, 10 mM EGTA, 1 mM MgCl2, 4% PFA), and permeabilised with 0.1% Triton X-100. After blocking for 30 minutes, cells were incubated with primary antibodies, followed by 2 washes in PBS-TX for 10 minutes and incubated with secondary antibodies for 1 hour. Nuclei were stained with DAPI and coverslips were mounted using SlowFade Gold Antifade Reagent (S36936, Life Technologies). Imaging was performed on a Delta Vision microscope (Applied Precision, WA, USA) using a 100× objective lens, NA 1.40, and z-stacks taken every 0.3 μm across the cell. Images were deconvolved and projected using SoftWoRx (Applied Precision). Some imaging was carried out using an IX71 Olympus microscope using the 100x oil immersion objective lens. Images in any figure were acquired using the same settings and were imported into Adobe Photoshop CS after which pixel resolution and intensity levels were adjusted.

2.10.2 - High throughput imaging and analysis

Slides were imaged using a High Content Operetta system (PerkinElmer, London, UK) and a 60× WD objective lens. Between 42 and 72 fields of view were imaged per slide and 7 focal planes recorded for each field, with 1.2 μm between each plane, to ensure that the planes covered the height of the nucleus. Fluorophore excitation times were kept constant for all slides: 200 ms for DAPI (emission 410-480 nm), 400 ms for Alexa Fluor 488 (emission 500-550 nm), 600 ms for Alexa Fluor 546 (emission 560-630 nm) and 400 ms for DRAQ5 (emission 650-760 nm). Images were analysed using Harmony 3.1.1 (PerkinElmer). Images from each field were processed as a stack, where 5 focal planes per field were stacked using the maximum projection tool. Nuclei were detected using a Find Nuclei building block and the method C, with common threshold of 0.20, area >120

μm2, split factor of 10.0, individual threshold of 0.20 and contrast >0.0. To ensure only whole nuclei were analysed, border objects were excluded. Next, a combination of Morphology Properties, DAPI Intensity Properties and Number of DAPI spots were used to select mitotic cells only. The Morphology Properties (using the standard method) and the DAPI Intensity Properties were calculated for the remaining entire nuclei. A Find Spot building block was used to find spots in the DAPI channel, over the nucleus region of the Entire Cells population, using the method A, with Relative Spot Intensity >0.030 and a Splitting Coefficient of 1.0. To establish the Final Population of mitotic cells, a Select Population building block was used to include cells with the following characteristics: number of DAPI spots ≥15, nucleus area >120 μm^2 and <650 μm^2, and a Nucleus Ratio of Width to Length >0.4. In our experiments, CREST, which localises to the centromere, was used as a localisation marker for pSer7CENP-A and Aurora B. A Find Spots building block was used to identify CREST Spots in the DRAQ5 channel, over the nucleus area of the Final Population, using the Method A, with a Relative Spot Intensity >0.0 and Splitting Coefficient of 1.0. Aurora B spots and pSer7CENP-A spots, within the area of the CREST spots were then looked at. For this, the size of the CREST spots was increased by 2 pixels using a Select Region building block. Two Find Spots building blocks were used to look for Aurora B spots in the Alexa Fluor 488 channel and pSer7CENP-A spots in the Alexa Fluor 546 channel, both within the resized CREST spots, using the Method A, with Relative Spot Intensity >0.0 and a Splitting Coefficient of 1.0. This allowed each Aurora B and pSer7CENP-A spot to be matched to its original CREST spot. The outputs were Single Cell results for all properties calculated in the Analysis Sequence. Finally, to address the effect of Aurora B and PLK1 inhibition on the localisation of Aurora B and pSer7CENP-A at the centromere, the fluorescence intensity of each Aurora B and pSer7CENP-A spot was determined, after standardising it to the fluorescence intensity of its original CREST spot: following Harmony analysis, single cell results were used to match Aurora B and pSer7CENP-A spots to corresponding CREST spots, and to calculate the ratios of Corrected Spot Intensity pSer7CENP-A/CREST and Aurora B/CREST for each spot. The average ratio per treatment was then calculated. At least 680 mitotic cells

per treatment were included in the counts, and the number of CREST spots was at least 13,900 per treatment. Data shown are the mean and S.E.M. of 3 independent experiments.

For PLK1 foci quantification in mitotic cells, slides were imaged and analysed using the above protocol, and PLK1 spots were identified in the 488-channel using the method C.

2.10.3 - Time-lapse microscopy

Imaging was performed at 37°C using spinning disk confocal microscopy from a 3i Marianas™ system (Intelligent Imaging Innovations), equipped with an Axio Observer Z1 microscope (Zeiss), a CSU-X1 confocal scanner unit (Yokogawa Electric Corporation), Plan-Apochromat 20x objective lens, 1.4NA objectives (Zeiss) and Orca Flash 4.0 sCMOS Camera (Hamamatsu). Images were acquired using Slidebook Software 5.5 from Intelligent Imaging Innovations. Quantification of mitotic index was carried out based on the percentage of rounded-up cell in the population.

2.10.4 - Differential Interference Contrast (DIC) Microscopy

Images were captured using an Olympus CKX41 microscope with a CAchN 10x objective, 0.25 PhP and 0.30 NA with CellSens Entry software.

2.11 - Statistical analysis

Statistical analysis was performed using Microsoft Excel and Graphpad Prism software. Three experimental repeats were performed for each dataset. Data are presented using either standard error of the mean (S.E.M.) or standard deviation (S.D.) as indicated in the figure legends. Student's T-test was used to determine statistical significance between two groups.

CHAPTER 3:

REQUIREMENT FOR PLK1 KINASE ACTIVITY IN THE MAINTENANCE OF A ROBUST SPINDLE ASSEMBLY CHECKPOINT

3.1 - Introduction

The Spindle Assembly Checkpoint (SAC) is a complex feedback control pathway that is important to allow proper chromosome segregation to occur (Musacchio and Salmon, 2007). Anticancer drugs that interfere with microtubule dynamics lead to an extended mitotic arrest due to sustained activation of the SAC. During mitotic arrest induced by microtubule targeting drugs, the weakening of the SAC allows cells to progress through the cell cycle without accurate chromosome segregation occurring which can result in genome instability and eventually cell death (Gascoigne and Taylor, 2008; Topham and Taylor, 2013).

PLK1 plays major roles at many stages of mitosis, including entry into, progression through and exit from mitosis (Lindon and Pines, 2004; van Vugt and Medema, 2005). Recent work indicates that PLK1 is also involved in the SAC. PLK1 has been shown to phosphorylate Haspin thus promoting Histone H3 phosphorylation at Thr 3 (H3T3Ph), contributing to Aurora B recruitment to the kinetochores (Zhou et al., 2014). PLK1, through Survivin phosphorylation, has been shown to regulate Aurora B kinase activity (Chu et al., 2011).

As discussed in introduction section 1.5.2, it has been shown that cells arrested in mitosis with PLK1 inhibitors have low levels of Aurora B at the kinetochores, in HeLa cells (Raab et al., 2015). On the contrary, another publication showed that PLK1 inhibition does not affect Aurora B localisation at the kinetochores, in RPE-1 cells (von Schubert et al., 2015). Thus, the function of PLK1 in sustaining robust SAC signalling, warrants further investigation.

3.2 - Maintenance of Aurora B at kinetochores and CENP-A phosphorylation in nocodazole treated cells requires PLK1 activity

To establish the function of PLK1 in SAC maintenance, the effect of PLK1 inhibition on Aurora B maintenance at kinetochores, was determined in U2OS cells. U2OS are extensively used in the SAC field, are well characterised and their large size facilitates kinetochore localisation studies. The experiment was set up under conditions where microtubules were completely depolymerised, using a high concentration of nocodazole (Brito et al., 2008). Cells were treated with nocodazole for 12 hours, followed by treatment with either one of two chemically unrelated PLK1 inhibitors, which have different off-target effects, GW843682X (Lansing et al., 2007) or BI 6727 (Rudolph et al., 2009), in the presence of proteosome inhibition by MG132 to retain the cells in mitosis. These PLK1 inhibitors may have different effects so consistent results with the two inhibitors, would suggest that any observed phenotypes would be more convincing. After 3 hours of inhibition, cells were fixed and stained with anti-Aurora B antibodies and co-stained with CREST, to mark the position of the kinetochores. In control cells, Aurora B was clearly detectable at the kinetochores, while the addition of GW843682X or BI 6727 caused a partial decrease in Aurora B intensity at the kinetochores with an overall more diffuse staining pattern (Figure 3.1A). The decrease in Aurora B intensity and the diffuse localisation of Aurora B in the presence of PLK1 inhibitors was obvious with BI 6727 treatment but it was less marked with GW843682X. As a positive control, Aurora B localisation at the kinetochores was almost completely lost when cells were challenged with high doses of the Aurora B inhibitor, Hesperadin (Hauf et al., 2003) as shown in Figure 3.1A. Chromosomes are closer in proximity upon Hesperadin treatment.

To investigate the effect of PLK1 inhibition on the activity of Aurora B at the kinetochores, cells were immunostained with anti-pSer7CENP-A antibodies, an established intracellular marker of Aurora B activity (Zeitlin et al., 2001). As shown in Figure 3.1B, pSer7CENP-A was decreased in the presence of both GW843682X and BI 6727, although it was more evident following treatment with the latter, and it was almost completely abolished upon treatment with Hesperadin.

Although a marked effect on Aurora B and pSer7CENP-A was detected following BI 6727 treatment, the effect of GW843682X was more subtle. To quantitatively assess the effects of GW843682X, a Perkin-Elmer Operetta high-content system, was used. Briefly, the intensity of Aurora B staining at each kinetochore was normalised to the intensity of the corresponding CREST spot (Material and Methods 2.9.2). By normalising to CREST any technical variation in signal can be accounted for. By analysing over 6,000 foci in over 600 cells, a significant decrease in Aurora B intensity at the kinetochores was detected upon treatment with GW843682X (Figure 3.1C). Similarly, the analysis of pSer7CENP-A corrected spot intensity normalised to CREST confirmed that there was a significant decrease in Aurora B activity at the kinetochores (Figure 3.1D).

Thus, PLK1 inhibitors affect the maintenance of Aurora B localisation and activity at the kinetochores, in U2OS cells, under these experimental conditions.

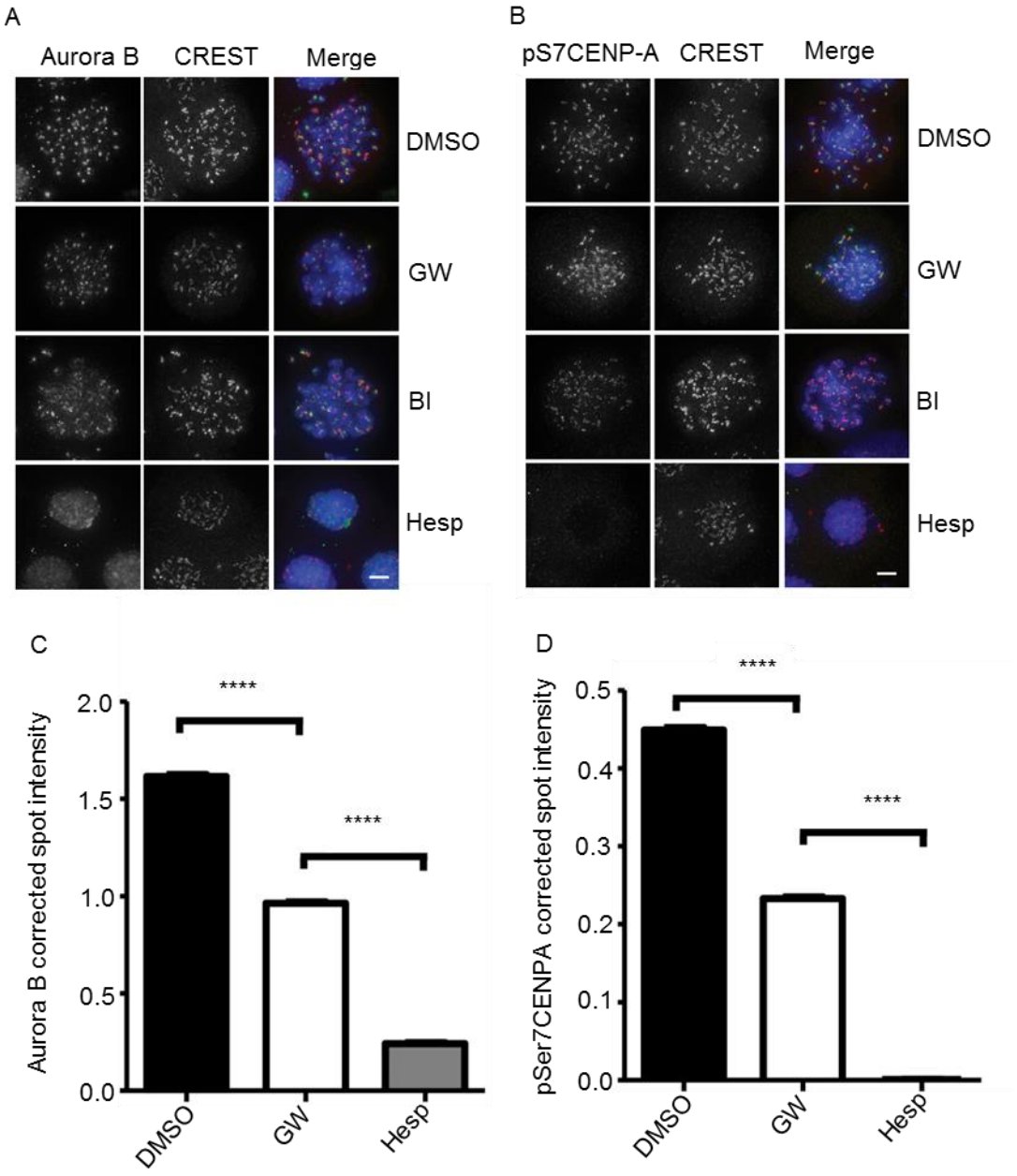

Figure 3.1 PLK1 inhibitors decrease Aurora B and pSer7CENP-A levels at the kinetochores

(A, B) U2OS cells were arrested in nocodazole for 12 hours, collected by mitotic shake-off and re-plated in the presence of 3.3 μM nocodazole and 10 μM MG132 with either 1 μM GW843682X, 100 nM BI 6727, 500 nM Hesperadin or DMSO for 3 hours. Cells were stained with (A) anti-Aurora B (green), CREST (red) and DAPI (blue) or (B) anti-pSer7CENP-A (green), CREST (red) and DAPI (blue) for immunofluorescence. Scale bar: 5 μm. (C, D) Quantification of Aurora B and pSer7CENP-A spot intensity in control, GW843682X and Hesperadin-treated samples were performed using an Operetta High

throughput system. Aurora B and pSer7CENP-A corrected spot intensity were normalised to CREST. At least 680 mitotic cells per treatment were included in the counts, and the number of CREST spots was at least 13,900 per treatment per repeat. N=3, error bars represent S.E.M., ****P<0.0001. One-tailed t-test was used.

3.3 - PLK1 and Aurora B inhibition reduce H3T3Ph levels

Decreased Haspin activity, with an associated loss of phosphorylation of Histone H3 on Threonine 3 (H3T3Ph) affects Aurora B recruitment to the kinetochores (Dai et al., 2005; Ghenoiu et al., 2013; Wang et al., 2010; Zhou et al., 2014). To examine whether the delocalisation of Aurora B by PLK1 inhibition was related to loss of H3T3Ph, cells were arrested in mitosis with nocodazole and treated with either of the PLK1 inhibitors or with the Aurora B inhibitor and stained with anti-H3T3Ph antibodies and CREST. H3T3Ph co-localisation with CREST was partially impaired when cells were treated with the PLK1 inhibitors, GW843682X or BI 6727, and the signal was less intense and more dispersed compared to the control. Cells treated with Hesperadin, reported to reduce H3T3Ph (Wang et al., 2011), acted as a positive control. The loss of H3T3Ph from the kinetochores upon Hesperadin treatment was more evident compared to PLK1 inhibition (Figure 3.2A). To investigate if H3T3Ph was simply delocalised or if the overall levels were reduced, immunoblotting analysis was carried out. Figure 3.2B demonstrates that H3T3Ph levels were reduced upon treatment with GW843682X and BI 6727 compared to the control. Similarly, Hesperadin treatment reduced H3T3Ph as previously reported (Wang et al., 2011).

This data indicates that PLK1 activity is required for continuous maintenance of H3T3Ph levels and its accumulation at the kinetochores.

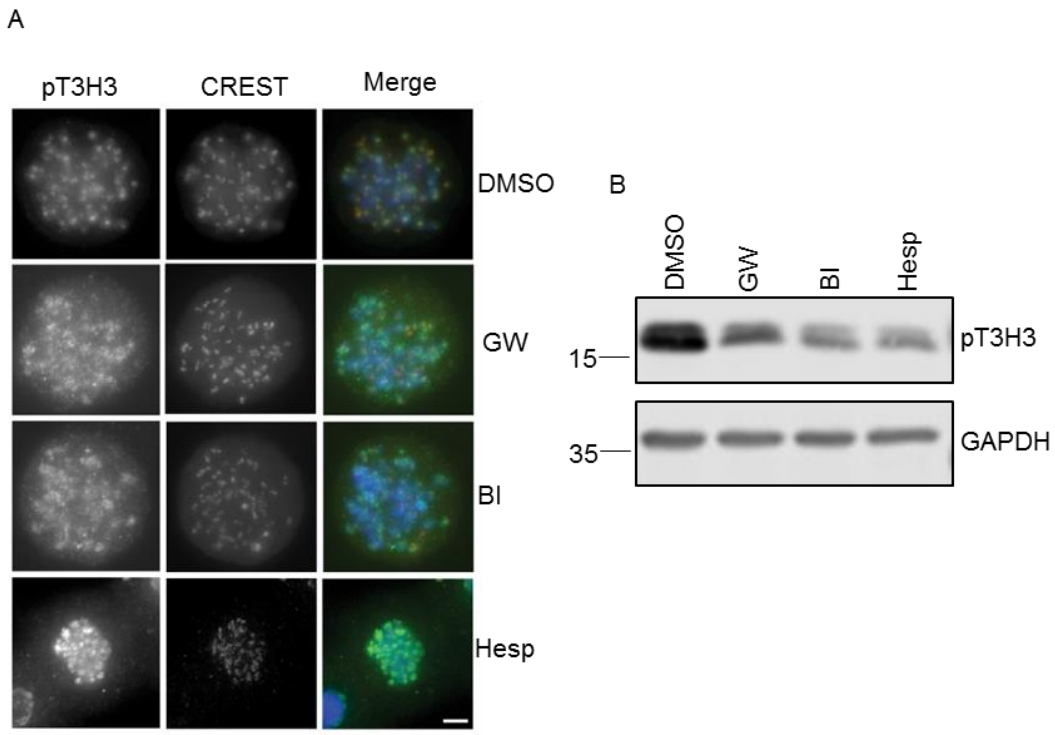

Figure 3.2 PLK1 inhibitors and an Aurora B inhibitor reduce H3T3Ph levels

(A) Nocodazole-arrested cells were treated with either 1 μM GW843682X, 100 nM BI 6727, 500 nM Hesperadin or DMSO for 3 hours in the presence of 10 μM MG132 and 3.3 μM nocodazole. Cells were stained with anti-H3T3Ph (green), CREST (red) and DAPI (blue). Scale bar: 5 μm. (B) Cells were treated with nocodazole as above followed by shake-off and re-plated in the presence of nocodazole and 10 μM MG132 and 1 μM GW843682X, 100 nM BI 6727, 500 nM Hesperadin, or DMSO for 3 hours. Proteins were analysed by immunoblotting with the indicated antibodies.

3.4 - Both PLK1 and Aurora B inhibitors cause PLK1 and outer kinetochore proteins to mis-localise

PLK1 recruitment to kinetochores is required for the formation of stable and bipolar kinetochore-microtubule (k-mt) attachments and its removal from the kinetochores is important for checkpoint silencing (Liu et al., 2012). To test whether PLK1 and Aurora B inhibitors affect PLK1 localisation during checkpoint maintenance, cells were arrested in mitosis with nocodazole and treated with the Aurora B or with either of the PLK1 inhibitors and stained with anti-PLK1 antibodies. Upon treatment with BI 6727, PLK1 became mis-localised from the kinetochore and the protein accumulated in larger foci,

compared to the control. The effect of GW843682X on PLK1 localisation was more subtle. Treatment with Hesperadin resulted in complete mis-localisation of the protein and its accumulation in larger foci (Figure 3.3A). These larger foci are often in proximity to CREST. Occasionally, they are also found outside of the chromosomes, indicating that these are unlikely to represent abnormal kinetochore recruitment of PLK1 (Figure 3.3B). It was observed that the number of large PLK1 foci increases upon treatment with either of the PLK1 inhibitors or the Aurora B inhibitor compared to the control (Figure 3.3C).

It is known that Aurora B is required for the recruitment of outer kinetochore proteins such as HEC1 (Emanuele et al., 2008) and ZWINT-1 (Kasuboski et al., 2011). To understand if the effect of PLK1 or Aurora B inhibition on their localisation, during maintenance, also correlates with errors in the recruitment of outer kinetochore proteins, cells were arrested in mitosis and treated with either of the PLK1 inhibitors or the Aurora B inhibitor, as before. Cells were then stained with anti-PLK1 antibodies, anti-ZWINT-1 antibodies and CREST. Both GW843682X and BI 6727 decrease ZWINT-1 kinetochore levels. As expected, ZWINT-1 foci were not detected upon Hesperadin treatment (Figure 3.3A). Similarly, HEC1 is mis-localised upon PLK1 inhibition. Again, Hesperadin treatment results in no detectable HEC1 foci at the kinetochores (Figure 3.3D). To investigate if ZWINT-1 and HEC1 were simply mis-localised or if overall levels were reduced, immunoblotting analysis was carried out. Overall HEC1 and ZWINT-1 protein levels were not affected upon treatment with the PLK1 or the Aurora B inhibitors compared to the control (Figure 3.3E). These results are consistent with published data which demonstrates that outer kinetochore protein localisation is affected upon treatment with a combination of low doses of two different Aurora B inhibitors under different experimental conditions (Emanuele et al., 2008). This data adds to this that HEC1 and ZWINT-1 proteins are mis-localised in the presence of PLK1 inhibition, under these experimental conditions.

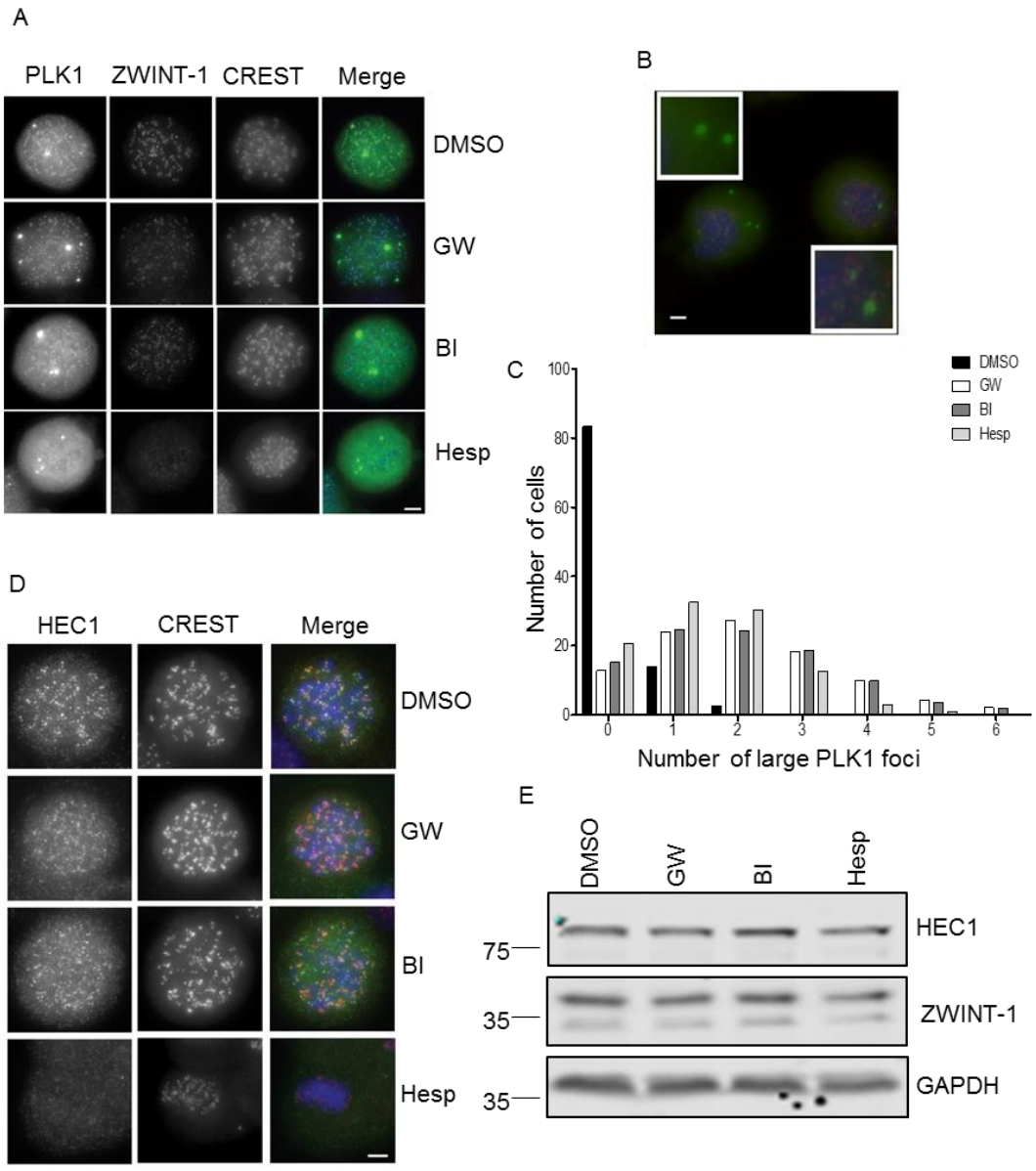

Figure 3.3 PLK1 inhibitors and an Aurora B inhibitor affect PLK1 localisation and the localisation of HEC1 and ZWINT-1 at kinetochores

Nocodazole arrested cells were treated with either 1 μM GW843682X, 100 nM BI 6727, 500 nM Hesperadin or DMSO for 3 hours in the presence of 10 μM MG132 and 3.3 μM nocodazole. Cells were stained with (A) anti-PLK1 (green), anti-ZWINT-1 (red) and CREST (blue). Scale bar: 5 μm. (B) Representative image of Hesperadin-treated cells co-stained with anti-PLK1 (green) CREST (red) and DAPI (blue). Scale bar: 5 μm. (C) Distribution of mitotic cells with large PLK1 foci after treatment with GW843682X, BI 6727, Hesperadin or DMSO as in A. At least 625 mitotic cells were counted for each

treatment per repeat. (D) Cells were treated as in A and stained with anti-HEC1 (green), CREST (red) and DAPI (blue). Scale bar: 5 μm. (E) Cells were treated with nocodazole as above followed by shake-off and re-plated in the presence of nocodazole and 10 μM MG132and either 1 μM GW843682X, 100 nM BI 6727, 500 nM Hesperadin or DMSO for 3 hours. Proteins were analysed by immunoblotting with the indicated antibodies.

The phosphorylation of the Polo T-loop is also required for the establishment of the SAC. Aurora B has been shown to phosphorylate Polo at T182 in *Drosophila*, which is equivalent to T210 of humans (Carmena et al., 2012a). To test whether an Aurora B inhibitor affects PLK1 activity during checkpoint maintenance, cells were arrested in mitosis with nocodazole, treated with the Aurora B inhibitor Hesperadin and stained with anti-pT210-PLK1 antibodies and CREST. pT210-PLK1 staining showed a similar, altered pattern to PLK1 when treated with an Aurora B inhibitor (Figure 3.4A). Immunoblotting analysis also indicates that the overall levels of pT210-PLK1 were reduced upon Hesperadin treatment (Figure 3.4B).

These results suggest that PLK1 and Aurora B may cooperate with each other in a positive feedback loop to regulate their localisation and activity during a prolonged cell cycle arrest in mitosis.

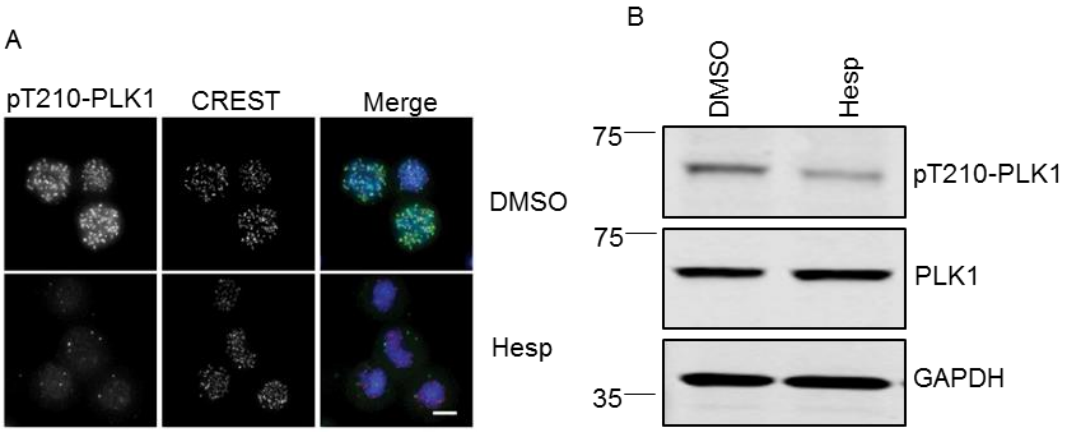

Figure 3.4 Aurora B inhibitor reduces pT210-PLK1 levels

(A) Nocodazole arrested cells were treated with 500 nM Hesperadin or DMSO for 3 hours in the presence of 10 μM MG132 and 3.3 μM nocodazole. Cells were stained with pT210-PLK1 (green), CREST (red) and DAPI (blue). Scale bar: 10 μm. (B) Cells were treated with nocodazole as above followed by shake-off and re-plated in the presence of nocodazole and 10 μM MG132 and either 500 nM Hesperadin or DMSO for 3 hours. Proteins were analysed by immunoblotting with the indicated antibodies.

3.5 - PLK1 inhibitors weaken the spindle assembly checkpoint

Having established that PLK1 inhibitors affect recruitment and activity of both PLK1 and Aurora B at the kinetochores, it was important to investigate if this would have consequences for SAC function.

To reiterate what was discussed in Introduction section 1.5.2, it has been shown that inhibition of SAC kinases, including Aurora B (Hauf et al., 2003; Santaguida et al., 2011), MPS1 (Santaguida et al., 2010) or Haspin (De Antoni et al., 2012) can abruptly override a SAC induced cell-cycle arrest. Thus, to examine whether PLK1 inhibition would result in override of the SAC under conditions in which SAC signalling is partially compromised, cells were treated with nocodazole for 12 hours, mitotic cells were collected by shake-off and re-plated in the continued presence of nocodazole. PLK1 inhibitors were added either as single agents or together with low doses of the Aurora B inhibitor, Hesperadin (100 nM). After 3 hours, cells were harvested, fixed, stained using antibodies against the mitotic marker H3S10Ph and scored using flow cytometry. More

than 80% of the cells in the DMSO treated control sample were H3S10Ph positive. This was similar following treatment with the PLK1 inhibitors, GW843682X or BI 6727. High doses of Hesperadin (500 nM), used as a positive control (Santaguida et al., 2011), resulted in the disappearance of H3S10Ph positive cells. A low dose of Hesperadin (100 nM) only caused a reduction from approximately 85% to approximately 45% in the number of H3S10Ph positive cells (Figure 3.5A). Since Aurora B can phosphorylate Histone H3 on Ser 10 (H3S10Ph), it was verified by flow cytometry that the low levels of Hesperadin used, did not reduce the intensity of H3S10Ph positive cells (Figure 3.5B). Importantly, the addition of PLK1 inhibitors in combination with low doses of Hesperadin, almost completely abolished H3S10Ph staining.

Differential interference contrast (DIC) images, were also captured, of the cells, following drug treatment. It was observed that there was a loss of the typical round shaped morphology of mitotic cells in the samples that displayed a reduction of H3S10Ph positive cells (Figure 3.5C), suggesting that in these cells, the mitotic cell cycle arrest was overridden.

To further verify that PLK1 and Aurora B inhibition cooperate to cause a SAC override, two other mitotic markers, Cyclin B (Pines and Hunter, 1991) and pMPM2 (Davis et al., 1983) levels were examined by immunoblotting. The MPM2 antibody recognises phosphorylated epitopes on multiple mitotic proteins. Analysis of protein levels revealed that both Cyclin B and pMPM2 were dramatically reduced in the presence of combined inhibition of PLK1 and Aurora B compared to the control or to when PLK1 inhibitors or low levels of Hesperadin were used as single agents. Cyclin B and pMPM2 levels were also reduced in the presence of high doses of Hesperadin, used as a positive control. This result confirms that the checkpoint has been overrode.

Altogether, these data indicate that PLK1 and Aurora B inhibition cooperate to cause a SAC override.

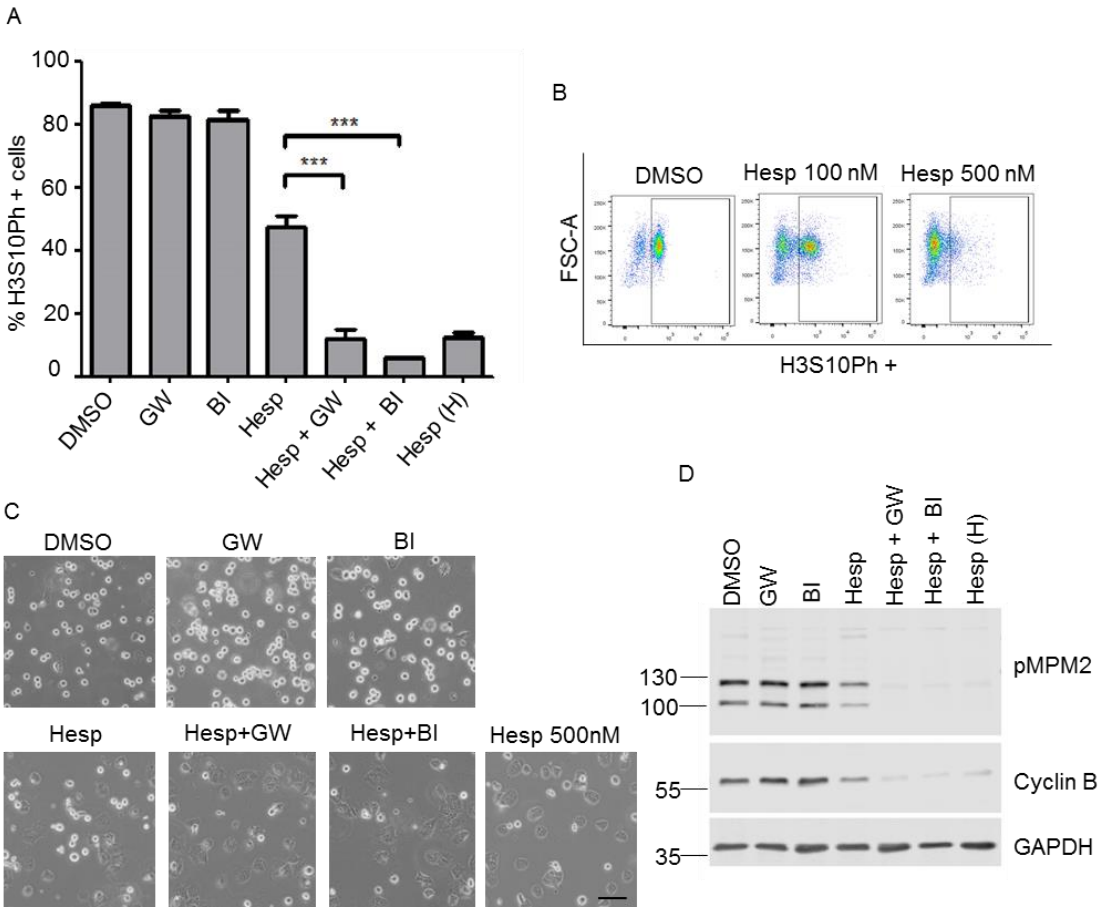

Figure 3.5 PLK1 inhibitors and an Aurora B inhibitor cooperate to weaken the checkpoint

(A) Cells were treated with nocodazole for 12 hours, collected by mitotic shake-off and re-plated in the presence of nocodazole and either 1 μM GW843682X (GW), 100 nM BI 6727 (BI), 100 nM Hesperadin (Hesp), both 1 μM GW843682X and 100 nM Hesperadin (Hesp+GW), both 100 nM BI 6727 and 100 nM Hesperadin (Hesp+BI), or 500 nM Hesperadin (Hesp H), as positive control, for 3 hours. Cells were then collected, stained with anti-Histone H3 pSer10 antibodies and analysed by flow cytometry. 10,000 cells were counted for each treatment per repeat. Error bars are S.D., ***P<0.001, N=3. One-tailed t-test was used. (B) Gating strategy used to quantify data in (A). (C) DIC images of (A), captured at the time of harvesting the cells. Scale bar: 50 μm. (D) Cells were treated as in (A) and immunoblotting analysis was carried out using the indicated antibodies.

As mentioned, inhibition of MPS1 (Santaguida et al., 2010) or Haspin (De Antoni et al., 2012) can weaken the SAC to cause a checkpoint override. To assess if PLK1 inhibitors can override the SAC when either MPS1 or Haspin is partially inhibited, a similar

experimental strategy to Figure 3.5A, was used. More than 80% of the cells in the control sample were H3S10Ph positive and the PLK1 inhibitors, GW843682X or BI 6727 did not change this outcome. High doses of the MPS1 inhibitor, Reversine (500 nM), used as a positive control, resulted in the disappearance of H3S10Ph positive cells. Low doses of Reversine (100 nM), only caused a reduction from approximately 85% to approximately 60% in the number of H3S10Ph positive cells (Figure 3.6A). However, unlike Hesperadin, the combination of GW843682X or BI 6727, with low doses of Reversine did not show a statistically significant increase in the fraction of H3S10Ph negative cells compared to Reversine alone (Figure 3.6A). DIC images were also captured of the cells following drug treatment. It was observed that in the samples that displayed a reduction of H3S10Ph positive cells, that some cells had reattached to the plates (Figure 3.6B), suggesting that in these cells the mitotic cell cycle arrest was overridden. Like Reversine, there was no statistically significant increase in H3S10Ph negative cells when GW843682X was combined with low doses of the Haspin inhibitor, 5-Iodotubercidin (5-Itu), compared to low doses of 5-Itu alone (Figure 3.6C). Again, DIC images were captured of cells treated with each drug. It was shown that in the samples that showed a reduction of H3S10Ph positive cells there was also a loss of the mitotic phenotype (Figure 3.6D), suggesting that in these cells the mitotic cell cycle arrest was overridden.

These results indicate that upon disruption of microtubules in U2OS cells, PLK1 functions to cooperate with Aurora B but not with MPS1 or Haspin to maintain a mitotic cell cycle arrest.

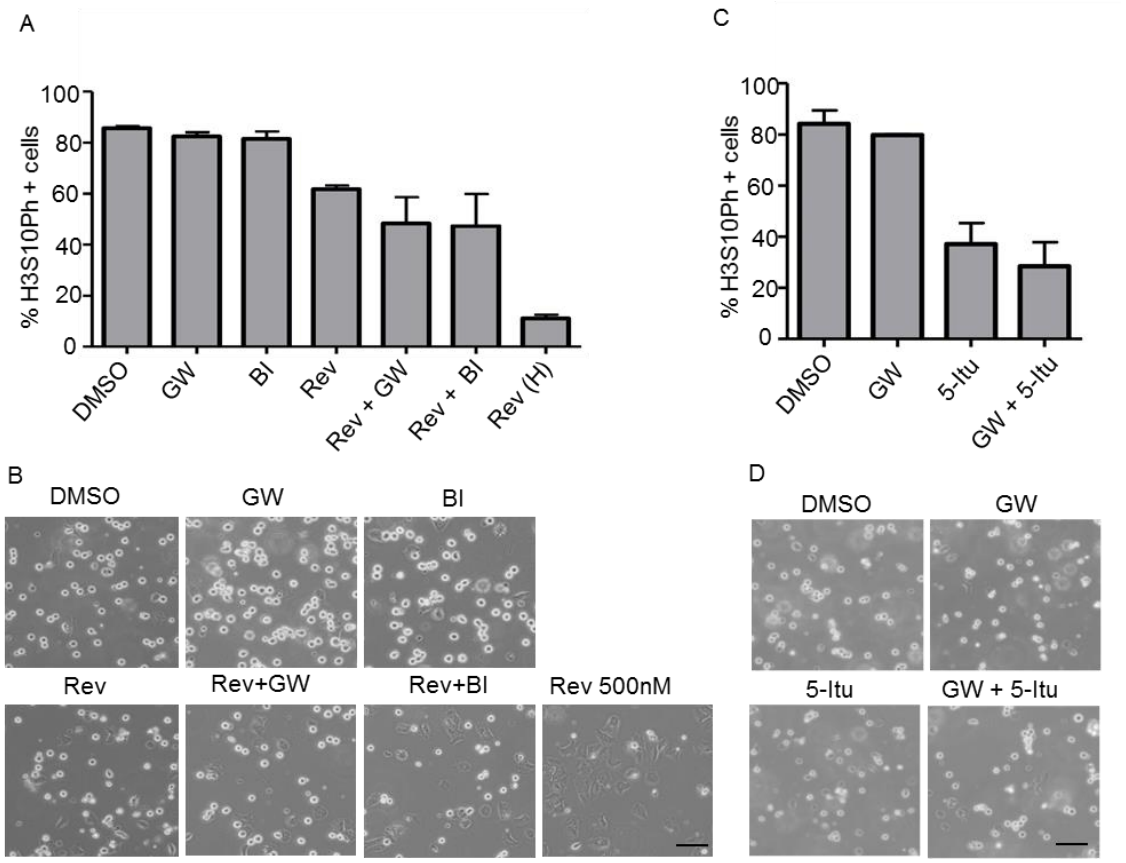

Figure 3.6 Effect of PLK1 inhibitors in combination with inhibitors of MPS1 or Haspin

Nocodazole-arrested cells were re-plated in the presence of nocodazole (A) 1 μM GW843682X (GW), 100 nM BI 6727 (BI) or 100 nM Reversine (Rev), both GW843682X and 100 nM Reversine (Rev+GW), both BI 6727 and 100 nM Reversine (Rev+BI), a high dose (500 nM) Reversine [Rev (H)] or DMSO, as a control. After 3 hours cells were collected, stained and analysed by flow cytometry. 10,000 cells were counted for each treatment per repeat. Error bars are S.D., N=3. (B) DIC images of (A). Scale bar: 50 μM. (C) Nocodazole-arrested cells were re-plated in the presence of nocodazole and 1 μM GW843682X (GW), 10 μm5-Itu or both GW843682X and 5-Itu (GW+5-Itu) for 3 hours. Cells were then stained and analysed as in A. Error bars are S.D., N=2. (D) DIC images of (C), scale bar: 50 μM.

3.6 - Discussion and Future Perspectives

The effects of PLK1 inhibition on the localisation of key SAC proteins and their effects as single agents, or in combination, on the maintenance of the mitotic cell cycle arrest in nocodazole treated cells was assessed using two chemically distinct PLK1 inhibitors. It was confirmed that PLK1 contributes to the maintenance of the SAC and that PLK1

inhibition affects the localisation and activity of Aurora B at the kinetochores (Figure 3.1A-D and Figure 4.10). PLK1 activity was not only required to establish Aurora B localisation, as previously shown (Raab et al., 2015), but it is also required for its maintenance, in U2OS cells (Figure 4.10). This is different from what has been reported by another group who have shown that PLK1 activity is not required for recruitment of Aurora B to the kinetochores in RPE-1 cells. However, it is important to note that PLK1 kinase inhibition only partially reduces Aurora B activity and kinetochore localisation. This is consistent with the existence of multiple and redundant mechanisms promoting Aurora B tethering, which involve Haspin phosphorylation Thr 3 of Histone H3 and BUB1 phosphorylation of Histone H2A on T120, that recruits Borealin through Shugoshin (Chu et al., 2011; Dai et al., 2005; Kawashima et al., 2010; Tsukahara et al., 2010). The presence of the multiple, redundant pathways, which may vary depending on the cell types may account for the discrepancies in the above, mentioned reports.

In this chapter, it has been shown that Haspin activity is reduced when PLK1 is inhibited (Figure 3.2A-B and Figure 4.10), which is consistent with published work (Zhou et al., 2014). This suggests that the effect of PLK1 inhibition on Aurora B and its activity, under the experimental set up used in this work, may be at least partially medicated through Haspin activity at the kinetochores (Figure 4.10). Similarly, PLK1 activity is continuously required for its own tethering at kinetochores (Figure 3.3A-C) which is in line with previous work which demonstrated that PLK1 phosphorylates a Polo Box Domain-binding protein, PBIP1, at T78 to create a phospho-binding domain for the Polo Box Domain (PBD) of PLK1 itself (Kang et al., 2006).

It was observed that Hesperadin treatment causes the chromosomes in the cells arrested with nocodazole to become more compacted compared to the control. This may be due to the role of Aurora B in chromosome condensation (Gadea and Ruderman, 2005).

The higher potency of BI 6727 compared to GW843682X could account for the more evident effects of BI 6727, observed in this study, on checkpoint kinases, compared to GW843682X. GW843682X targets PLK1 enzyme with an IC_{50} of 2.2 nmol/L, whereas

BI 6727 has an IC_{50} of 0.87 nmol/L on the PLK1 enzyme (Lansing et al., 2007; Rudolph et al., 2009). GW843682X and BI 6726 also target PLK3 and BI 6727 targets PLK2 but at much higher concentrations (Lansing et al., 2007; Rudolph et al., 2009).

Outer kinetochore proteins, ZWINT-1 and HEC1 are mis-localised when PLK1 is inhibited (Figure 3.3D-E). This data indicates that inhibition of PLK1 or Aurora B causes incomplete kinetochore recruitment of HEC1 and ZWINT-1, which may be required for accurate recruitment of PLK1 and for the maintenance of Aurora B at the kinetochores. The large PLK1 foci are sometimes in proximity to CREST but are often found outside of chromosomes (Figure 3.3B). This may be because the outer kinetochore proteins are not properly recruited under these conditions. PLK1 may require correct outer kinetochore protein localisation for it to be accurately maintained at the kinetochore and possibly to prevent PLK1 protein aggregation. It is tempting to speculate that some of these larger PLK1 foci could also be localised at promyleocytic leukemia (PML) bodies as PLK1 can accumulate as foci that are similar to what was observed for PML bodies (Bernardi and Pandolfi, 2007). A future experiment testing this hypothesis could be performed using the same experimental set up as described for the experiment presented in Figure 3.2A and staining with antibodies against PML bodies.

It was found that Hesperadin, an inhibitor that has been described as specific for Aurora B (Hauf et al., 2003), reduced PLK1 tethering at most kinetochores (Figure 3.3A). It has been reported that, at least in *Drosophila*, Aurora B contributes to PLK1 activity by phosphorylating the PLK1 T-loop (Carmena et al., 2012a). However, recent work has demonstrated that Bora-Aurora A is responsible for phosphorylating the PLK1 T-loop at T210, in mitosis, in human cells (Bruinsma et al., 2014). This work demonstrated that, in nocodazole treated cells, overall phosphorylation of PLK1 at T210 is reduced by Hesperadin treatment (Figure 3.4A-B), suggesting that Aurora B may be partially responsible for maintaining PLK1 activity under these experimental conditions. This can occur by direct phosphorylation or indirectly by counteracting a PLK1 targeting protein phosphatase. Alternatively, the reduction in pT210-PLK1 may simply be related to PLK1

displacement from kinetochores and therefore the impossibility of being phosphorylated by a kinetochore resident kinase.

The similarities in the phenotype observed upon PLK1 inhibition and Hesperadin-mediated inhibition of Aurora B, suggest that these kinases may be part of a positive feedback loop acting at the kinetochores during SAC maintenance. This idea is reinforced by the observation that PLK1 inhibition, together with reduced Aurora B activity, has a strong effect in promoting SAC silencing, consistent with recently published data, under different experimental settings (Li et al., 2015). Intriguingly, some small molecule inhibitors of PLK1, including BI 6727 that were used in this study, can cause a mitotic arrest at their effective concentrations but at much higher doses they were shown to mis-localise Aurora B (Raab et al., 2015). This is likely to be caused by off target effects that are revealed only when the compound is used at very high concentrations.

Although this work has revealed that PLK1 cooperates with Aurora B to maintain a strong SAC signal, in a positive feedback loop, which, from this study, indicates partial mediation through Haspin, the mechanism of action is not fully elucidated.

Protein phosphatases counteract the action of kinases by removing phosphate groups on key substrates. Previous findings in the field have shown that Aurora B prevents protein phosphatase 1 (PP1) localisation at the kinetochores (Emanuele et al., 2008; Liu et al., 2010). PLK1 indirectly regulates protein phosphatase 2A (PP2A), which in turn counteracts Aurora B activity (Foley et al., 2011; Meppelink et al., 2015; Nijenhuis et al., 2014; Suijkerbuijk et al., 2012). Thus, PLK1 activity could potentially be important to avoid abnormal levels of PPase activity at the kinetochores, thus explaining the positive PLK1-Aurora B feedback loop observed in this study. To test this, future experiments could be carried out to evaluate the effects of single or dual inhibition of PLK1 and Aurora B on PP1 and PP2 levels and activity at the kinetochores. Another experiment that could be performed to test this hypothesis could be to assess if partial reduction of PPase activity can restore the defects caused by PLK1 and Aurora B inhibition.

In future studies, it would be interesting to determine whether the SAC override caused by combined PLK1 and Aurora B inhibition, causes cells to enter a G1- or G2-like state. It is plausible that the cells which have bypassed the SAC have entered into a G1-like state as Cyclin B levels, which are known to be low in G1 (Pines and Hunter, 1991), are low when PLK1 and Aurora B are inhibited in combination with each other. To address this question in more detail, the Fluorescent ubiquitination cell cycle-based indicator (Fucci) system (Sakaue-Sawano et al., 2008), which can easily distinguish between G1 and S/G2/M-phases, could be utilised.

This work was unable to confirm the recent finding that demonstrated that MPS1 and PLK1 inhibition cooperates to cause checkpoint override (von Schubert et al., 2015). Intriguingly, a trend in promoting SAC override was observed but the data did not reach statistical significance. These discrepancies may be explained by either difference in PLK1 inhibitors used in the two studies (GW843682X and BI 6727 versus TAL) and/or the relevance of the two pathways in the different cell types (U2OS versus RPE-1) or simply due to the difference in the experimental setup used. This could be tested by performing an experiment in both cell lines, using the three different PLK1 inhibitors for each experimental set up.

This body of research, conducted with chemical inhibitors, has revealed that PLK1 and Aurora B can cooperate to maintain a robust SAC. Although the use of such compounds is associated with potential off target effects they were a necessity for this work. During this study, attempts were made to perform siRNA experiments to deplete PLK1, to validate these findings. However, these attempts were unsuccessful due to the high level of toxicity which is likely due to the essential function of PLK1 in mitosis. To overcome this problem, in future studies, genetic editing tools could be used, such as an analog sensitive PLK1 cell line (Burkard et al., 2007). Alternatively, experiments could be performed to rescue the defects observed in this study by using overexpression constructs or using a viral transfection and transduction system. These experiments could validate that PLK1 is important for SAC maintenance.

In conclusion, this work has revealed that PLK1 is important for the maintenance of robust SAC signalling, by cooperating with Aurora B, in a positive feedback loop. PLK1 inhibitors are being developed as anticancer agents and it is important to understand how they can be best used either as single agents or in effective combination therapies. This work could contribute to the understanding of how PLK1 inhibition can affect the fate of cells arrested in mitosis and may provide a rational for testing mitotic kinase inhibitors in multidrug approaches.

CHAPTER 4:

PLK1 AND CDC7 KINASE ACTIVITIES COOPERATE TO MAINTAIN A ROBUST SPINDLE ASSEMBLY CHECKPOINT

4.1 - Introduction

Cell division cycle 7 (CDC7) kinase is activated by one of two regulatory subunits, DBF4 or DRF1. It has well established roles in the initiation of DNA synthesis at origins of replication (Sclafani and Holzen, 2007) and in the replication stress checkpoint (Costanzo et al., 2003; Day et al., 2010; Rainey et al., 2013).

Cdc7p and its regulatory subunit Dbf4p has been shown to localise to centromeres in yeast (Natsume et al., 2013). This facilitates the recruitment of cohesion loaders onto centromeres in G1 and helps to maintain accurate sister chromatid cohesion (Natsume et al., 2013). More recently, human DBF4 has been shown to localise at centromeres during S-phase (Wu et al., 2016).

Interestingly, it has been reported that Dbf4p is a negative regulator of Cdc5p (the *Saccharomyces cerevisiae* ortholog of PLK1) which prevents inappropriate mitotic exit in the presence of mis-aligned spindles (Miller et al., 2009).

As discussed in introduction sections 1.4 and 1.5 and in the published work of chapter 3, PLK1 has many roles in mitosis and it has been demonstrated to function in SAC establishment and maintenance in human cells (Chu et al., 2011; Li et al., 2015; O'Connor et al., 2015; Raab et al., 2015; von Schubert et al., 2015; Zhou et al., 2014).

Owing to the link between Dbf4p and Cdc5p in yeast, it seemed plausible that a relationship may exist in higher eukaryotes, between these two protein kinases. CDC7 kinase has not been reported to have a role in mitosis in humans. The only indication of a role of CDC7 in mitosis is the failure to execute proper chromosome segregation when CDC7 is depleted (Montagnoli et al., 2004; Yoshizawa-Sugata et al., 2005). However,

this has not been further investigated. Therefore, the aim of this work was to investigate if CDC7 kinase, functions in mitosis, in human cells, by analysis of the localisation of CDC7 and its regulatory subunits and by assessing CDC7 kinase activity, during mitosis, in U2OS cells.

4.2 - CDC7 localises to centrosomes during interphase and mitosis

Previous reports have shown that CDC7 is a mainly nuclear protein during interphase (Jiang and Hunter, 1997; Jiang et al., 1999; Montagnoli et al., 2002). However, due to the lack of specific immunological reagents for CDC7, not much is known about its precise localisation. Further still, its localisation in mitosis has not been described. Thus, to identify the localisation of endogenous CDC7, in both interphase and mitosis, asynchronous U2OS cells were fixed using PTEMF, prior to staining with anti-CDC7 monoclonal antibodies (Tenca et al., 2007). Interestingly, by co-staining with a marker of the pericentriolar material (PCM), pericentrin (PCNT) (Doxsey et al., 1994), CDC7 protein was detected at the centrosomes during interphase and during all stages of mitosis (Figure 4.1A). This data suggests that CDC7 could be potentially localised at the centrosome.

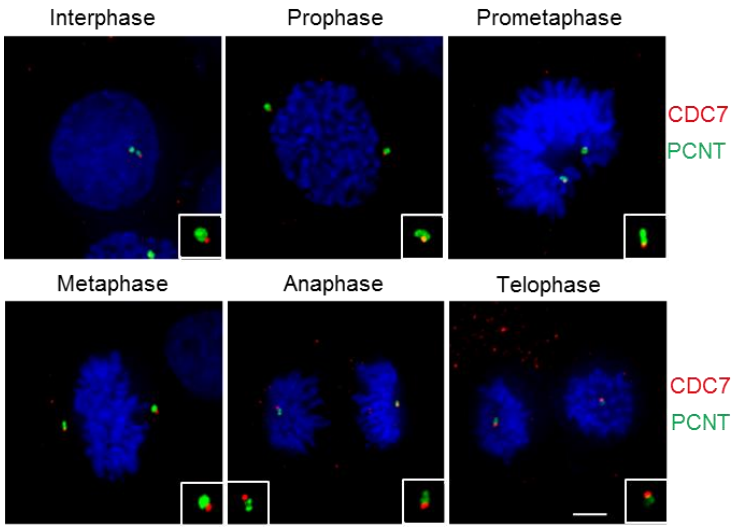

Figure 4.1 CDC7 localises to centrosomes during interphase and mitosis using monoclonal antibodies

Cells were fixed with PTEMF and stained with anti-CDC7 (red), anti-PCNT (green) and DAPI (blue). Scale bar: 5 μm.

4.3 - DBF4 localises to centrosomes during interphase and to the mitotic spindle during mitosis

DBF4 has also been described as a nuclear protein (Kumagai et al., 1999; Sato et al., 2003), but like CDC7, little is known about its specific localisation. Recent work from our lab, using a tagged version of DBF4, revealed that DBF4 localises to the centromeres in human cells (Wu et al., 2016). Dbf4p can also be recruited to the kinetochores in yeast (Natsume et al., 2013).

To determine the localisation of endogenous DBF4, U2OS cells were fixed and stained with monoclonal antibodies against DBF4, previously generated in house. By performing co-staining experiments with anti-PCNT, DBF4 protein was detected at centrosomes in interphase cells (Figure 4.2A). By carrying out co-staining experiments with anti-Targeting protein for Xenopus kinesin-like protein 2 (TPX2), a mitotic spindle marker (Wittmann et al., 1998), DBF4 protein was detected at the mitotic spindle during mitosis, using DBF4 monoclonal antibodies (Figure 4.2B). This data revealed novel localisations of DBF4.

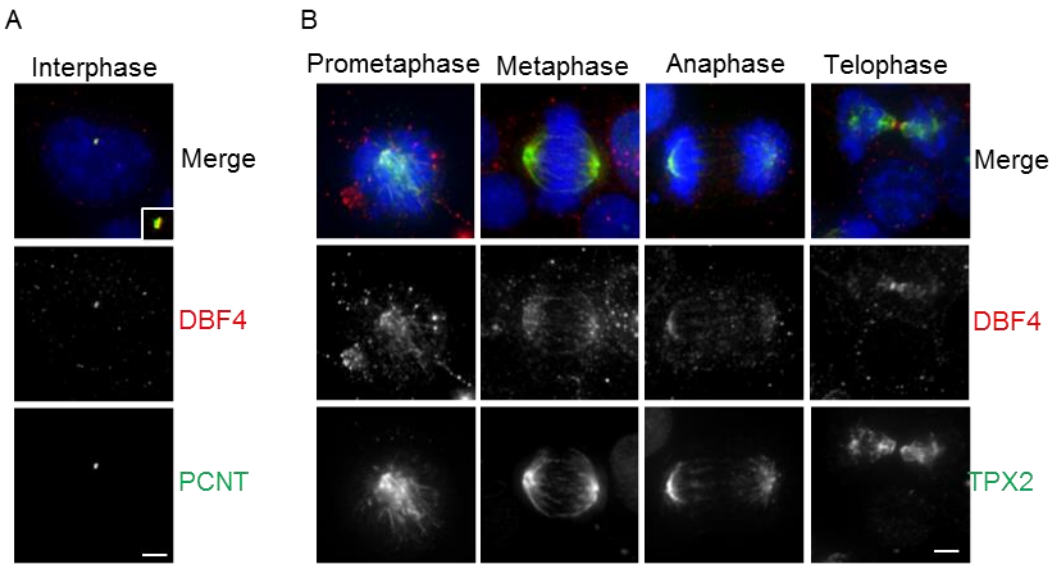

Figure 4.2 DBF4 localises to the centrosome during interphase and to the mitotic spindle during mitosis

Cells were fixed with PTEMF and stained with (A) anti-DBF4 (red), anti-PCNT (green) and DAPI (blue) or (B) anti-DBF4 (red), anti-TPX2 (green) and DAPI (blue). Scale bar: 5 μm.

4.3 - Overexpression of DRF1 but not DBF4 drives CDC7 to the centrosomes

Whilst CDC7 was detected at the centrosomes under these conditions, the previously reported nuclear localisation of the kinase was not observed (Jiang and Hunter, 1997; Jiang et al., 1999; Montagnoli et al., 2002). To further elucidate the localisation of CDC7, CDC7 was expressed with a C-terminal eGFP tag under a constitutive promoter. DBF4 was expressed with a C-terminal Strep tag under a constitutive promoter. As there was no DRF1 antibody available that was sensitive enough to detect endogenous DRF1, this second CDC7 regulatory subunit was also expressed with a C-terminal Strep tag under a constitutive promoter. In this experiment, CDC7, DBF4 or DRF1 protein were not detected in mitotic cells.

However, using this approach, CDC7-eGFP was detected in the nucleus of interphase cells, which is consistent with previous reports (Jiang and Hunter, 1997; Jiang et al., 1999; Montagnoli et al., 2002). DRF1-Strep was detected in the cytoplasm and at centrosomes,

suggesting a potential novel localisation of DRF1 at the centrosome. It has been shown that when DRF1 is expressed with a C-terminal eGFP tag, it can shuttle in and out of the nucleus (Kevin Wu thesis, National University of Ireland, Galway 2016). Interestingly, when cells were co-transfected with CDC7-eGFP and DRF1-Strep, CDC7-eGFP was no longer strictly localised to the nucleus (Jiang and Hunter, 1997; Jiang et al., 1999; Montagnoli et al., 2002). It could now be distinctly detected outside of the nucleus, at the centrosomes and in the cytoplasm (Figure 4.3A). Co-transfection of CDC7-eGFP and DRF1-Strep did not alter the localisation of DRF1 (Figure 4.3A).

To further determine the localisation of DBF4, this regulatory subunit was expressed with a C-terminal Strep tag. DBF4-Strep was detected in the nucleus of interphase cells when cells were transfected with DBF4-Strep, which was consistent with earlier reports (Kumagai et al., 1999; Sato et al., 2003). When cells were transfected with eGFP-CDC7 and DBF4-Strep, both eGFP-CDC7 and Strep were detected in the nucleus (Figure 4.3B).

This data indicates that DRF1 is possibly the main CDC7 regulatory subunit required to drive CDC7 to the centrosome.

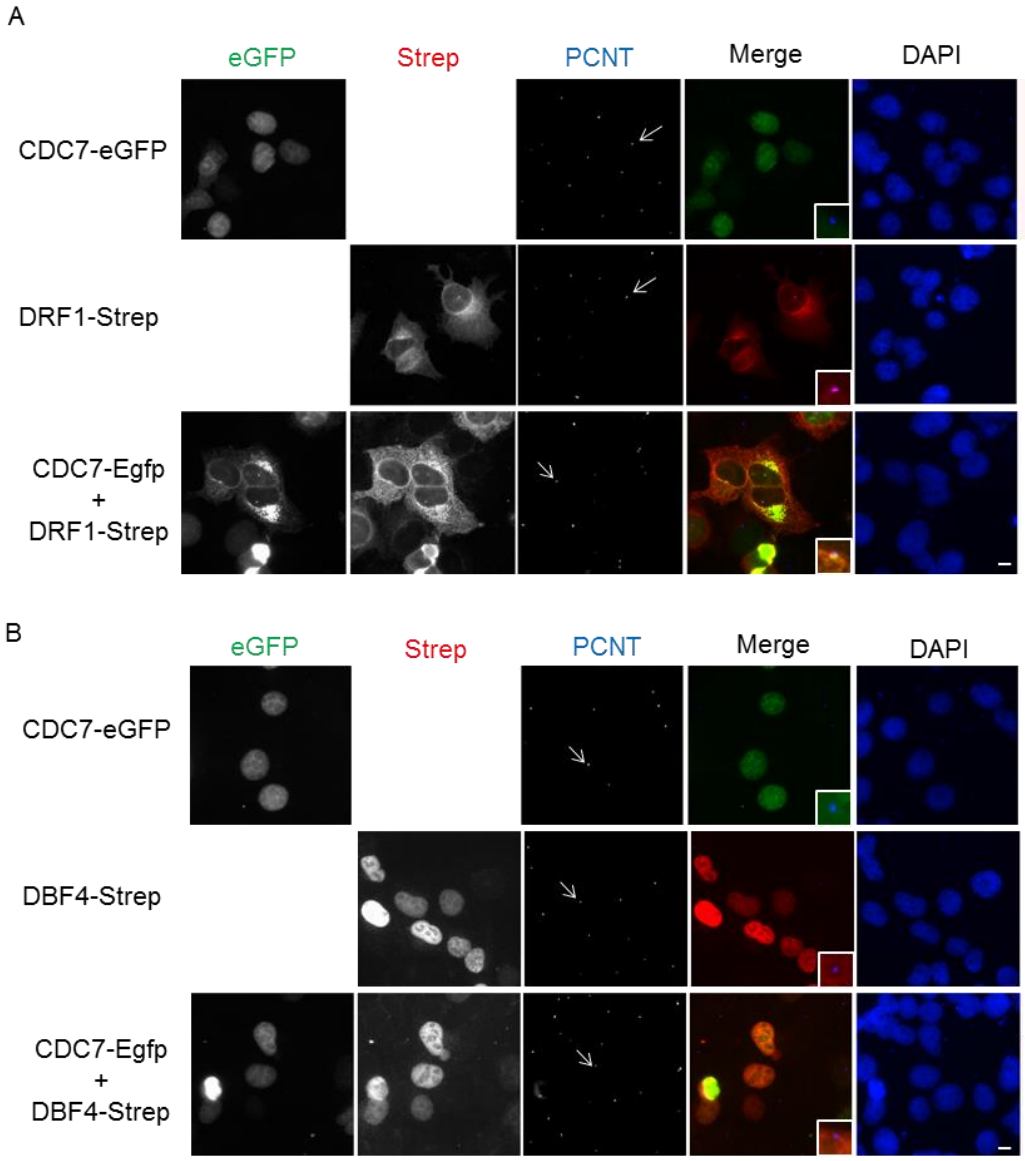

Figure 4.3 Overexpression of DRF1 but not DBF4 drives CDC7 to the centrosomes

Cells were transfected with (A) CDC7-eGFP (green in merge), DRF1-Strep (red in merge) or co-transfected with CDC7-eGFP (green in merge) and DRF1-Strep (red in merge) or (B) CDC7-eGFP (green in merge), DBF4-Strep (red in merge) or co-transfected with CDC7-eGFP (green in merge) and DBF4-Strep (red in merge). Arrows indicate centrosomes in the zoom image. Scale bar: 5 μm.

4.5 - CDC7 is an active kinase in mitosis that undergoes auto-phosphorylation

In budding yeast, Dbf4p, the regulatory subunit of Cdc7p has been suggested to be involved in the SPOC (Miller et al., 2009), which is a checkpoint in budding yeast that prevents premature mitotic exit when the spindles fail to align. For this reason, it was interesting to determine if human CDC7 plays a role in mitosis.

To begin to address this question, it was asked if the activity of CDC7 kinase could be measured in mitotic cells. Cells were arrested in mitosis using nocodazole for 16 hours and then harvested. The cells were lysed and protein extracts were prepared for immunoprecipitation, performed using DBF4 antibodies. The immunoprecipitated material was incubated with an N-terminal fragment of MCM2, which is known to interact with CDC7 kinase (Montagnoli et al., 2006; Ramer et al., 2013), and [γ-$_{32}$P] ATP and an *in vitro* kinase reaction was performed. In parallel, immunoprecipitated material was treated with the CDC7 kinase inhibitor, XL413 (Koltun et al., 2012), incubated with an N-terminal fragment of MCM2 and [γ-$_{32}$P] ATP and an *in vitro* kinase reaction was performed. Proteins were analysed by immunoblotting and incorporation of γ-^{32}P was assayed by autoradiography. CDC7 kinase could phosphorylate the MCM2 fragment in DMSO treated control cells and in nocodazole arrested cells (Figure 4.4A)*. The reaction was strongly inhibited by the presence of XL413, demonstrating that CDC7 itself is the main active kinase assayed in the immunoprecipitation. CDC7 was recovered in the immunoprecipitated material from both the DMSO treated control and the nocodazole treated samples (Figure 4.4A).

An altered electrophoretic mobility of CDC7 was observed, when cells were treated with nocodazole compared to the control (Figure 4.4A). This was thought to be most likely due to phosphorylation of CDC7 kinase. To address whether the altered electrophoretic mobility that was observed for CDC7 when cells were arrested in mitosis was due to phosphorylation, cells were arrested using nocodazole and then harvested. Cells were

* Experiment presented in Figure 4.4 A was performed by Dr. Michael Rainey.

lysed and protein extracts were treated with lambda (λ) phosphatase. Immunoblotting re-established that CDC7 protein had an altered electrophoretic mobility in the nocodazole arrested cells compared to the control. When protein extracts were treated with λ phosphatase, this altered electrophoretic mobility was not detected (Figure 4.4B) [†]. pSer40/41 MCM2, used as a control for phosphatase activity, was abolished in the presence of λ phosphatase (Figure 4.4B). This result indicated that the altered electrophoretic mobility of CDC7 that was observed, was due to phosphorylation of CDC7 kinase when the cells were arrested in mitosis using nocodazole.

[†] Experiment presented in Figure 4.4 B was performed by Gemma O'Brien and Dr. Michael Rainey.

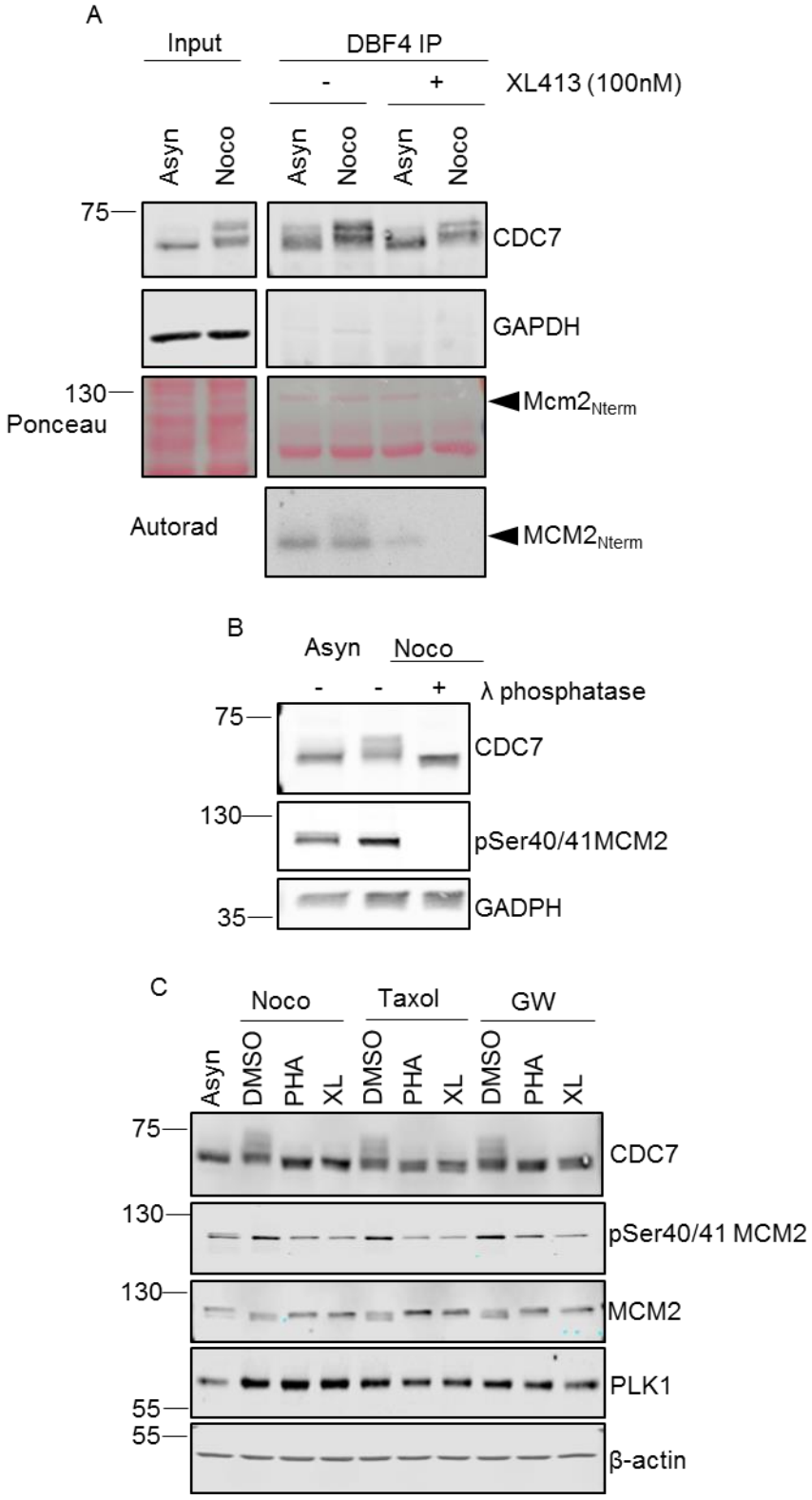
A
Input
DBF4 IP
-
+
XL413 (100nM)
Asyn
Noco
Asyn
Noco
Asyn
Noco
75
CDC7
GAPDH
130
Ponceau
Mcm2Nterm
Autorad
MCM2Nterm
B
Asyn
Noco
-
-
+
λ phosphatase
75
CDC7
130
pSer40/41MCM2
35
GADPH
C
Noco
Taxol
GW
Asyn
DMSO
PHA
XL
DMSO
PHA
XL
DMSO
PHA
XL
75
CDC7
130
pSer40/41 MCM2
130
MCM2
PLK1
55
55
β-actin

Figure 4.4 CDC7 is an active kinase in mitosis that undergoes auto-phosphorylation

(A) An immunoprecipitation, preformed using anti-DBF4 antibodies, was carried out from asynchronously growing cells or cells arrested in mitosis using 1 μM nocodazole for 16 hours. An *in vitro* kinase assay was performed on the immunoprecipitated material in the presence of an N-terminal fraction of MCM2 and [γ-$_{32}$P] ATP in the presence or absence of 100 nM XL413. Proteins were analysed by immunoblotting using the indicated antibodies and incorporation of γ-^{32}P was assayed by autoradiography. (B) Protein from nocodazole arrested cells were treated with λ phosphatase. Proteins were analysed by immunoblotting using the indicated antibodies. (C) Cells were arrested in mitosis with 1 μM nocodazole, 1 μM taxol or 1 μM GW843682X for 16 hours followed by 10 μM PHA-767491 or 5 μM XL413 for 3 hours. Proteins were analysed by immunoblotting with the indicated antibodies.

To determine if the phosphorylation of CDC7 kinase was due to auto-phosphorylation, cells were arrested in mitosis, using nocodazole, followed by treatment with one of two CDC7 kinase inhibitors, XL413 or PHA-767491 (Montagnoli et al., 2008). The altered electrophoretic mobility that was observed in the nocodazole arrested cells was abolished in the presence of either XL413 or PHA-767491 (Figure 4.4C)[‡], indicating that CDC7 kinase was undergoing auto-phosphorylation.

To confirm that CDC7 kinase auto-phosphorylation was not restricted to a nocodazole treatment, cell were challenged with one of two other drugs that arrest cells in mitosis, either taxol (De Brabander et al., 1981) or the PLK1 inhibitor GW843682X, followed by treatment with PHA-767491, XL413 or DMSO for 3 hours. In the presence of a taxol or GW843682X induced cell cycle arrest, the altered electrophoretic mobility was also present and this altered electrophoretic mobility was like that of the nocodazole arrested cells. Similar to the cells treated with nocodazole, followed by treatment using either of CDC7 kinase inhibitors, when the cells, treated with either taxol or GW843682X, were treated with PHA-767491 or XL413 (Figure 4.4C)[§], the altered electrophoretic mobility was abolished. This verified that CDC7 kinase auto-phosphorylation was not restricted to a nocodazole cell cycle arrest.

[‡] Experiment shown in Figure 4.4 C was performed by Dr. Kevin Wu and Gemma O'Brien.

To further assess CDC7 kinase activity directly, the levels of pSer40/41 MCM2, a specific biomarker of CDC7 kinase activity (Montagnoli et al., 2006), were monitored. pSer40/41 MCM2 levels accumulated to similar levels, in cells that were arrested in mitosis by either nocodazole, taxol or GW843682X and were similarly reduced upon the addition of either of the CDC7 kinase inhibitors, PHA-767491 or XL413 (Figure 4.4C).

Altogether, this data provides evidence that CDC7 kinase is active and undergoes auto-phosphorylation during a mitotic cell cycle arrest.

4.6 - CDC7 kinase and PLK1 inhibitors cooperate to cause a SAC override and this override is prevented by proteasome inhibition

So far, this study has shown that CDC7 can be detected at the centrosomes and it is possible that this localisation could indirectly affect the SAC. It was also demonstrated that CDC7 kinase is active in mitosis, in the presence of nocodazole, which causes microtubule depolymerisation, resulting in activation of the SAC. Furthermore, published reports have indicated that *Saccharomyces cerevisiae*, Dbf4p negatively regulates Cdc5p, to prevent premature mitotic exit (Miller et al., 2009). As clearly demonstrated by us and by multiple other labs (Chu et al., 2011; Li et al., 2015; O'Connor et al., 2015; Raab et al., 2015), and as extensively discussed in chapter 3, it has been shown that PLK1 plays a role in the SAC.

Thus, to explore a potential role for CDC7 in the SAC, either alone or in combination with PLK1, cells were arrested in mitosis using nocodazole for 16 hours, followed by treatment with one of two CDC7 kinase inhibitors, PHA-767491 or XL413 as single agents, the PLK1 inhibitor, GW843682X as a single agent, PHA-767491 in combination with GW843682X, XL413 in combination with GW843682X or DMSO as a control. After 6 hours, cells were harvested and stained with antibodies against the mitotic marker H3S10Ph and analysed using flow cytometry, as described in material and methods

section 2.9.1. [**]Figure 4.5A shows that approximately 60% of cells in the DMSO treated control sample were H3S10Ph positive. Single treatment with the CDC7 inhibitors, PHA-767491 or XL413 or with the PLK1 inhibitor, GW843682X caused a slight reduction of approximately 10% of H3S10Ph positive cells compared to the control sample. However, when either PHA-767491 or XL413 were used in combination with GW843682X, there was a statistically significant reduction in the percentage of H3S10Ph positive cells to approximately 25% compared to the controls. A loss of the mitotic morphology was observed in samples treated with a combination of either of the two CDC7 kinase inhibitors and the PLK1 inhibitor (Figure 4.5B), suggesting that the SAC has been overrode. These results indicated that CDC7 kinase and PLK1 may cooperate to maintain a robust SAC, thus, preventing SAC override.

To ensure that pharmacological inhibition of CDC7 had not grossly impaired PLK1 kinase activity, cells were arrested in mitosis, using nocodazole, for 16 hours and then treated with the PLK1 and CDC7 kinase inhibitors, as in Figure 4.6A, for 6 hours. Immunoblotting analysis demonstrated that neither PHA-767491 nor XL413 affected overall PLK1 kinase activity, as monitored by phosphorylation of one of its substrates, TCTP on Ser 46 (Cucchi et al., 2010; Yarm, 2002). GW843682X slightly decreased pSer40/41 MCM2, a marker of CDC7 kinase activity and it also affected MCM2 migration on SDS-PAGE (Figure 4.5C)[††]. This is consistent with the MCM complex interacting with PLK1 (Tsvetkov and Stern, 2005) and MCM2 being a potential target in *Xenopus* (Trenz et al., 2008). Combined inhibition of CDC7 and PLK1 did not have an additive effect on pSer40/41 MCM2 or on pSer46 TCTP. Thus, CDC7 kinase inhibition does not appear to directly affect PLK1 activity.

[**] Experiment presented in Figure 4.5 A and B were performed by Dr. Michael Rainey and Dr. Agnieszka Kaczmarcyk.

[††] Experiment shown in Figure 4.5 C was performed by Dr. Agnieszka Kaczmarcyk.

To investigate if the SAC override that occurred due to combined inhibition of CDC7 kinase and PLK1, was dependent on proteasome activity, as proteasome activity is required for anaphase progression, nocodazole arrested cells were treated with either DMSO as a control, PHA-767491 in combination with GW843682X, XL413 in combination with GW843682X, PHA-767491 in combination with GW843682X and the proteasome inhibitor MG132 or XL413 in combination with GW843682X and MG132. DIC imaging revealed that, again, in the DMSO control sample, cells had a rounded shaped morphology which was consistent with that of mitotic cells. In the presence of CDC7 kinase inhibition with either PHA-767491 or XL413 in combination with GW843682X, some cells had reattached to the plate which suggests that the SAC was weakened (Gascoigne and Taylor, 2008; Taylor and Stark, 2001). When MG132 was added to the cells treated with either PHA-767491 or XL413 in combination with GW843682X, nearly all the cells had a round-shaped morphology, indicating that these cells were in mitosis. Thus, this data is consistent with the requirement of proteasome activity to allow SAC override to occur (Figure 4.5D)[‡‡].

[‡‡] The experiment presented in Figure 4.5 D was performed by Dr. Michael Rainey.

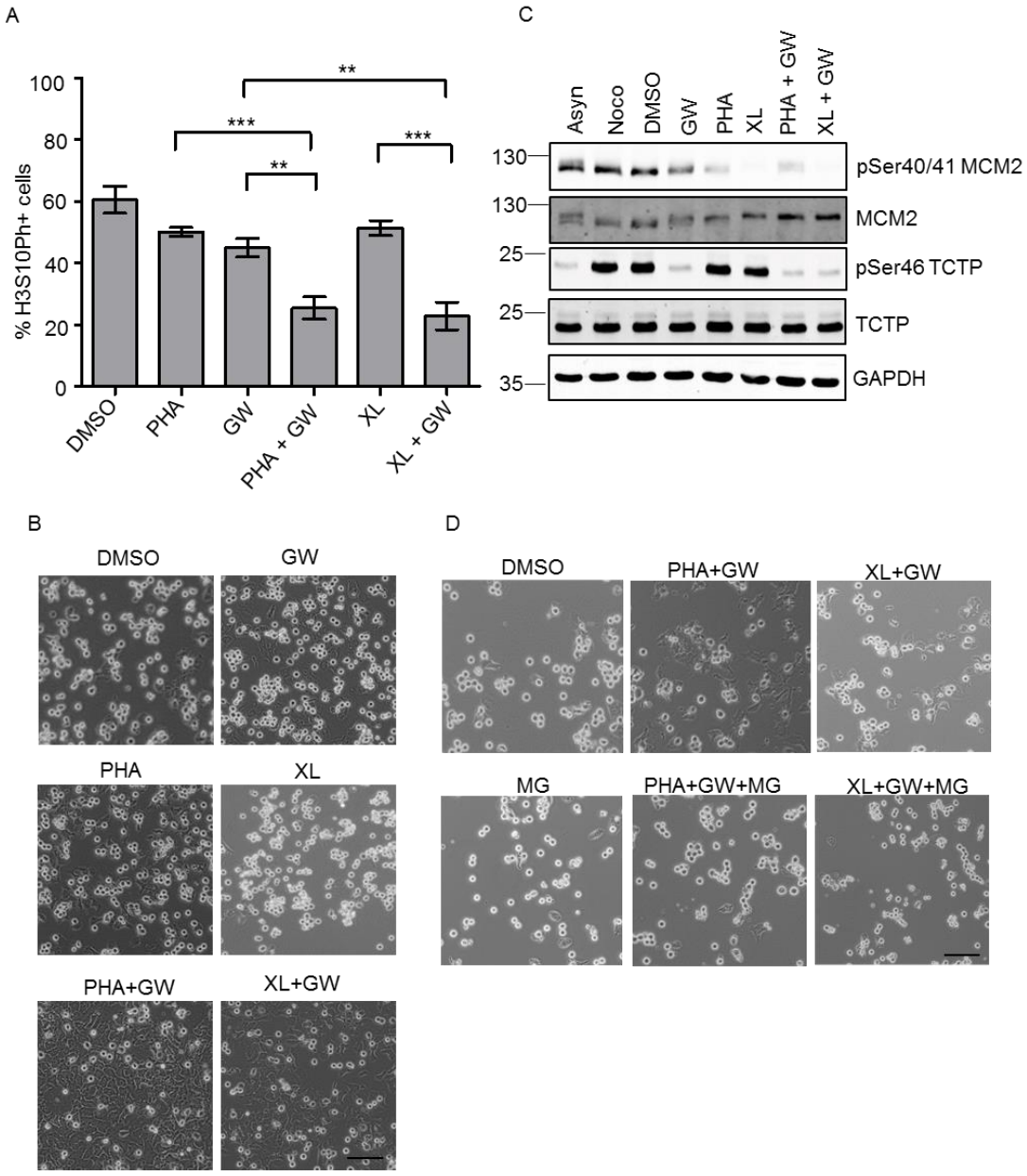

Figure 4.5 CDC7 kinase and PLK1 inhibitors cooperate to cause a SAC override and this override is prevented by proteasome inhibition

(A) Cells were arrested in mitosis with 1 μM nocodazole for 16 hours prior to treatment with 10 μM PHA-767491 or 5 μM XL413, 1 μM GW843682X, both 10 μM PHA-767491 and 1 μM GW843682X or both 5 μM XL413 and 1 μM GW843682X for 6 hours. Cells were then harvested, stained with anti-H3S10Ph antibodies and analysed by flow cytometry. 10,000 cells were counted for each treatment per repeat. N=3, error bars indicate S.D., ***P<0.001, ** P<0.01. (B) DIC images of (A) captured at the time of harvesting

the cells. Scale bar: 50 μm. (C) Cells were arrested and drug treated as in (A). Immunoblotting analysis was carried out using the indicated antibodies. (D) Cells were arrested as in (A) followed by treatment with 10 μM PHA-767491 in combination with 1 μM GW843682X or 10 μM XL413 in combination with 1 μM GW843682X in the presence or absence of 10 μM MG132 for 6 hours. DIC images were then captured. Scale bar: 50 μm.

4.7 - CDC7 kinase inhibitors cooperate with a second PLK1 inhibitor to promote SAC override

To help eliminate the possibility of off-target effects associated with the use of a single chemical agent, a second chemically distinct PLK1 inhibitor, BI6727, was used to examine whether PLK1 and CDC7 kinase inhibitors were cooperating to weaken the SAC. Cells were arrested using nocodazole, for 16 hours, followed by treatment with DMSO as a control, PHA-767491, XL413 or BI 6727 as single agents, PHA-767491 in combination with BI 6727 or XL413 in combination with BI 6727. When cells were treated with PHA-767491, XL413 or BI 6727, there was a similar amount of cells with a round-shaped morphology compared to the DMSO treated control (Figure 4.6A). However, when either of the CDC7 kinase inhibitors were used in combination with BI 6727 some cells lost their round-shaped morphology and reattached to the plates (Figure 4.6A). This suggested that the SAC was weakened. This data together with the data in Figure 4.5, suggests that phenotypes that are observed are unlikely due to off-target effects of the inhibitors and that CDC7 kinase and PLK1 are cooperating to maintain a robust checkpoint.

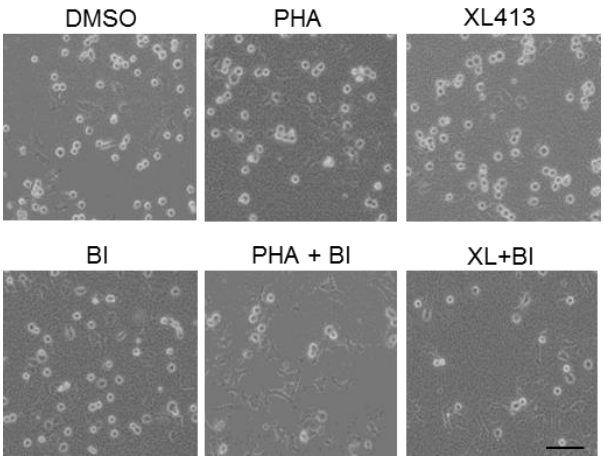

Figure 4.6 CDC7 kinase inhibitors cooperate with BI 6727 to cause a SAC override

Nocodazole arrested cells were treated with 10 μM PHA-767491, 5 μM XL413, 100 nM BI 6727, both 10 μM PHA-767491 and 100 nM BI 6727 or 5 μM XL413 and 100 nM BI 6727. DIC images were then captured. Scale bar: 50 μm.

4.8 - SAC override can occur when the checkpoint is fully challenged but this override is not as efficient as MPS1 inhibition dependant SAC weakening

The previous experiments described in this chapter were performed using 1 μM nocodazole. However, at this concentration complete microtubule depolymerisation does not occur (Brito et al., 2008). To test the efficiency of the SAC override, conditions in which microtubules are completely depolymerised and in which the checkpoint is fully challenged, the dose of 3.3μM nocodazole, was utilised (Brito et al., 2008). Cells were arrested in mitosis using nocodazole for 16 hours. These cells were then treated with either DMSO as a control, XL413, GW843682X or XL413 in combination with GW843682X for 3 hours. The percentage of cells in mitosis was visually scored based on cell round-up. Figure 4.7A shows that approximately 70% of cells for all treatments were in mitosis at hour 0. After 3 hours of treatment with DMSO this percentage did not change. Treatment with XL413 or GW843682X also did not change this outcome (Figure 4.7A). Treatment of cells with both XL413 and GW843682X in the presence of either 1 μM or 3.3 μM nocodazole caused a reduction to approximately 40% of cells in mitosis

after 3 hours (Figure 4.7A). This data demonstrated that SAC override caused by dual CDC7 and PLK1 inhibition can occur when the checkpoint is fully engaged.

To examine whether the SAC override caused by combined inhibition of CDC7 kinase and PLK1 was as efficient as a SAC override caused by inhibition of a major checkpoint kinase, cells were arrested in mitosis followed by treatment with an MPS1 inhibitor, Reversine, for 3 hours, which is known to cause checkpoint override (Santaguida et al., 2010). Three hours of treatment with Reversine resulted in less than 10% of cells being retained in mitosis (Figure 4.7A)[§§]. Therefore, the checkpoint weakening caused by combined inhibition of CDC7 kinase and PLK1 was not as efficient as SAC override caused by MPS1 inhibition.

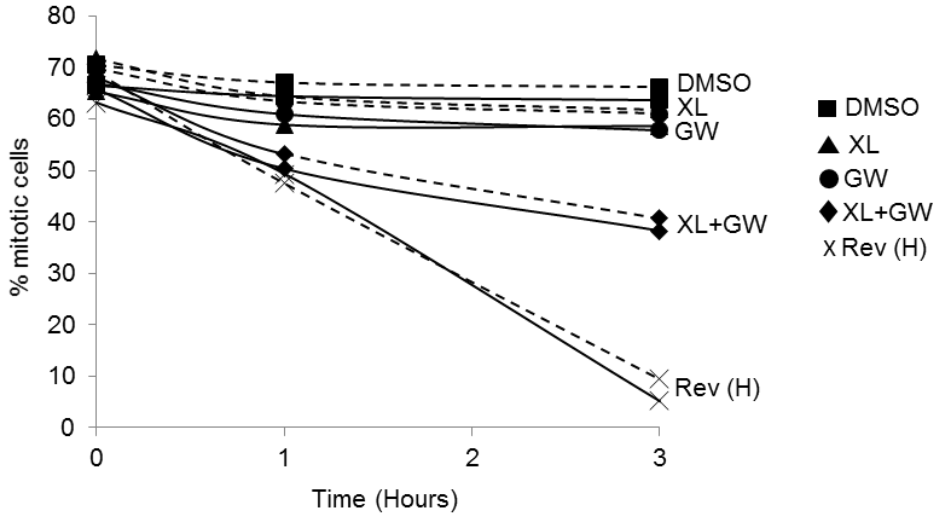

Figure 4.7 SAC override can occur when the checkpoint is fully challenged but this override is not as efficient as MPS1 inhibition dependent SAC weakening

Cells were arrested in mitosis with 1 μM (dashed line) or 3.3 μM (continuous line) nocodazole for 16 hours followed by treatment with 5 μM XL413, 1 μM GW843682X, 5 μM XL413 and 1 μM GW843682X or 500 nM Reversine. Time lapse microscopy was performed over 3 hours and mitotic cells were scored morphologically.

[§§] Experiment presented in Figure 4.7 was performed by Dr. Stefano Maffini.

4.9 - CDC7 and Aurora B or MPS1 kinases inhibition do not cooperate to weaken the SAC

As identified in this work, CDC7 kinase cooperates with PLK1 (Figure 4.6A and Figure 4.7A) and PLK1 specifically cooperates with Aurora B (Chapter 3 section 3.5) to maintain a robust SAC. Thus, it seemed possible that the effect observed, could be mediated through Aurora B as PLK1 regulates Aurora B localisation and its activity (Chapter 3, section 3.2). To examine whether CDC7 kinase inhibition in cooperation with Aurora B inhibition weakened the SAC, cells were treated with nocodazole for 12 hours, followed by 3 hours of treatment with DMSO as a control, XL413, low doses of the Aurora B inhibitor Hesperadin (100 nM), XL413 in combination with low doses of Hesperadin, or high doses of Hesperadin alone (500 nM) as a positive control. Cells were harvested, stained with antibodies against the mitotic marker H3S10Ph and scored using flow cytometry. Figure 4.8A shows that more than 80% of cells in the DMSO treated control sample were H3S10Ph positive. Treatment with XL413 did not change this outcome while high doses of Hesperadin, used as a positive control, resulted in a decrease to below 20% of H3S10Ph positive cells. Low doses of Hesperadin caused a reduction from approximately 80% to approximately 50% of H3S10Ph positive cells. In samples treated with a combination of XL413 and low doses of Hesperadin, there was no significant reduction in H3S10Ph positive cells observed (Figure 4.8A). DIC imaging of Figure 4.8A, revealed that the cells in the DMSO treated control sample, had a mitotic morphology, while treatment with a high dose of Hesperadin caused most cells to lose their mitotic morphology and reattach to the plates. The mitotic morphology was retained when cells were treated with XL413. Treatment with low doses of Hesperadin or combined treatment with XL413 and a low dose of Hesperadin caused some cells to exit mitosis (Figure 4.8B).

Similarly, the effect of CDC7 kinase inhibition in combination with MPS1 inhibition on SAC maintenance was also explored, as MPS1 is another major checkpoint kinase which functions downstream of Aurora B (Santaguida et al., 2010). Low doses of the MPS1 inhibitor, Reversine (100 nM), caused a partial reduction from approximately 80% to approximately 60% in the percentage of cells that were H3S10Ph positive while high

doses of Reversine (500 nM) caused a reduction to below 20% in the percentage of H3S10Ph positive cells. In samples treated with a combination of XL413 and a low dose of Reversine, there was no significant decrease in the percentage of H3S10Ph positive cells (Figure 4.8A). Again, some cells had re-attached to the plates in the samples which displayed a reduction in the percentage of H3S10Ph positive cells. (Figure 4.8B), suggesting that these cells had bypassed the checkpoint.

This data suggests that CDC7 does not cooperate with Aurora B or MPS1 to maintain robust SAC signalling.

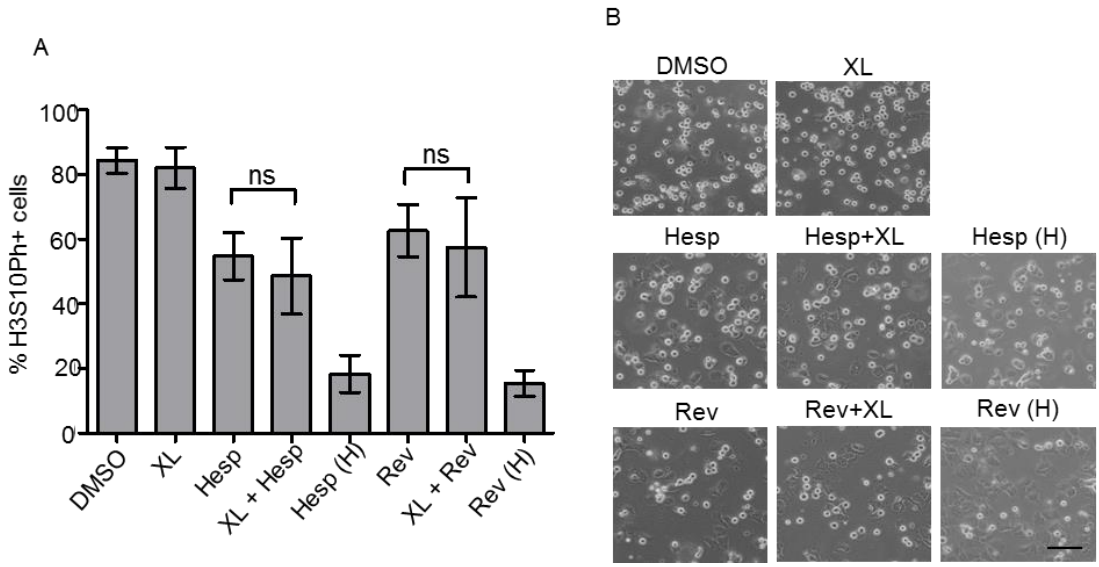

Figure 4.8 CDC7 and Aurora B or MPS1 kinases inhibition do not cooperate to cause a SAC override

(A) Cells which were arrested with 3.3 μM nocodazole were re-plated in the presence of nocodazole with DMSO, 5 μM XL413 (XL), 100 n M Hesperadin (Hesp), 100 nM Reversine (Rev), both 5 μM XL413 and 100 n M Hesperadin (XL+Hesp), 500 nM Hesperadin (Hesp (H)), 100 nM Reversine (Rev), 5 μM XL413 and 100 nM Rev (XL+Rev) or 500 nM Reversine (Rev (H)) for 3 hours. N=3, error bars indicate S.D., ns=not significant. (B) DIC images of (A). Scale bar 50 μM.

4.10 - Cooperation of CDC7 kinase and PLK1 inhibition is not sufficient to cause a checkpoint bypass when the cells are treated with nocodazole for a short period of time

The previous section demonstrated that CDC7 and PLK1 cooperate to maintain a robust SAC during a nocodazole induced cell cycle arrest. However, it is known that cells which spend a long time in mitosis can adapt to these conditions (Brito et al., 2008). To accurately measure the time spent in mitosis, different biological conditions were utilised, which induced a stronger SAC. Cells were arrested in G2-phase using the CDK1 inhibitor, RO-3306 (Vassilev et al., 2006) for 18 hours. This allowed all the cells to be synchronised in the same stage of the cell cycle. The cells were then released from the G2-phase block and into conditions which caused partial or complete microtubule depolymerisation (Brito et al., 2008). For this, nocodazole concentrations of 100 nM, 1 μM or 3.3 μM nocodazole were used and simultaneously, treated with either DMSO, XL413, GW843682X, XL413 in combination with GX843682X or as positive controls, high doses or either Reversine (500 nM) or Hesperadin (500 mM) were utilised. Cells were imaged by time-lapse microscopy for 350 minutes. The length of time that the cells spent in mitosis was scored based on cell round-up. In the DMSO treated control samples, for all nocodazole concentrations, cells were retained in mitosis for 350 minutes. However, when cells were treated with either Reversine or Hesperadin, cells only spent approximately 100 minutes in mitosis (Figure 4.9A). Treatment with XL413, GW843682X or a combination of XL413 and GW843682X did not result in exit from mitosis prior to 350 minutes (Figure 4.9A).

This data combined with the previous result, suggests that CDC7 and PLK1 cooperate to play a minor role in the maintenance of a robust SAC signal.

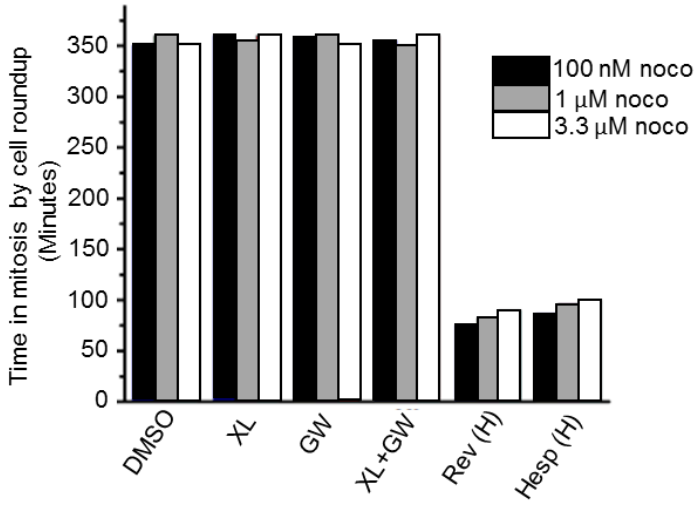

Figure 4.9 Cooperation of CDC7 kinase and PLK1 inhibition is not sufficient to cause a checkpoint bypass when the cells are treated with nocodazole for a short period of time

Cells were arrested using 9 μM RO-3306 for 18 hours followed by release into media containing either 100 nM, 1 μM or 3.3 μM nocodazole with 5 μM XL413, 1 μM GW843682X, both 5 μM XL413 and 1 μM GW843682X, 500 nM Reversine (Rev (H)) or 500 nM Hesperadin (Hesp (H)). Cells were imaged by time-lapse microscopy for 350 minutes. Mitotic cells were scored based on cell roundup. N=2.

4.10 - Discussion and future perspectives

This study provides the first indications of a potential role for CDC7 kinase in mitosis (Figure 4.1). Specifically, using monoclonal antibodies CDC7 appears to localise at the centrosomes, with no nuclear signal detected. This contrasted to a previous report which demonstrated that CDC7 is a nuclear protein (Jiang and Hunter, 1997; Jiang et al., 1999; Montagnoli et al., 2002). Consistent with these reports, this study found that an eGFP tagged version of CDC7 localised to the nucleus (Figure 4.3A-B). However, localisation at specific structures had not been described. This data suggests that CDC7 may play a role in the nucleus and at the centrosome.

Technically, methods of slide preparation, with regards to extraction of soluble proteins, can help account for the detection of CDC7 at the centrosome versus in the nucleus. Extraction of soluble proteins, followed by monoclonal antibody detection of CDC7,

facilitated, for the first time, detection of CDC7 at the centrosome, potentially suggesting a novel role for the kinase in centrosome biology. The cells in which CDC7 was ectopically expressed were not subjected to extraction. However, although there are differences in the extraction methods used in these experiments, together they suggest that CDC7 could be localised at the centrosome. Experiments using a tagged CDC7 and pre-extraction, may be used to confirm CDC7 centrosomal localisation.

Interestingly, ectopic expression of DRF1, but not DBF4, appeared to drive CDC7 to the centrosomes (Figure 4.3A and B). This data suggests that the role that CDC7 may play at the centrosome is mainly regulated by DRF1. It is unknown whether DRF1 and DBF4 are functionally different from each other. This data strengthens the idea that they do indeed play functionally different roles. Following the discovery of DRF1, it has been shown that DRF1 has little amino acid sequence similarity to DBF4 outside of the N-, M- and C-motifs (Montagnoli et al., 2002). It is likely that through the unconserved C-terminus regions of DBF4 and DRF1, that CDC7 could be differentially regulated or that they target CDC7 kinase to different substrates. Adding to this hypothesis, it is known that DBF4 and DRF1 cannot bind to CDC7 simultaneously (Montagnoli et al., 2002).

To date, very little is known about the function of the second CDC7 regulatory subunit, DRF1, but it has been reported to be a nuclear protein (Montagnoli et al., 2002; Yoshizawa-Sugata et al., 2005). In contrast to this, using DRF1-Strep fusion proteins, this work has revealed novel localisations of DRF1 at the centrosomes and in the cytoplasm with a small fraction of DRF1 located in the nucleus (Figure 4.3A). This is consistent with the work of a recent PhD thesis from our lab, which demonstrated that DRF1 can shuttle in and out of the nucleus in interphase cells (Wu thesis, National University of Ireland, Galway 2016). The use of different tags could account for the differences in localisation observed in this work compared to the work published in Montagnoli et al., 2002. The development of specific immunological reagents for the detection of endogenous DRF1 would avoid the need for epitope tagging which may affect the localisation of the protein.

As of yet, CDC7 and its regulatory subunits have no known role at the centrosome. However, the replication complexes of MCM and ORC, which are known CDC7 interacting partners during replication, have been reported to localise to the centrosome but their role there is unknown (Ferguson et al., 2010; Knockleby and Lee, 2010; Lu et al., 2009; Prasanth et al., 2004). This work, demonstrates that CDC7 can be detected at the centrosomes which could link CDC7 along with the MCM2 and ORC complexes to a role at the centrosome. Preliminary work has demonstrated that depletion of CDC7 can cause centrosomal amplification, suggesting that CDC7 may function in the regulation of accurate centrosome duplication (Cuffe, O'Connor, Santocanale and Morrison, unpublished).

To further support a role for CDC7 in mitosis, the work in this chapter, revealed a localisation of endogenous DBF4 at the spindles in mitotic cells, using DBF4 monoclonal antibodies and extraction of soluble proteins (Figure 4.2). To date, the only other hint of localisation of this protein in mitosis is at the kinetochores in telophase cells, in yeast (Natsume et al., 2013) and at the spindle pole bodies in filamentous fungi (De Souza et al., 2014).

DBF4 has predominantly been described as a nuclear protein (Kumagai et al., 1999; Sato et al., 2003). In this chapter, using DBF4-Strep fusion proteins, diffuse nuclear staining of DBF4 was also revealed which was consistent with previous reports. Until this year, the precise nuclear localisation of DBF4 in human cells had not been shown. A recent publication from our lab, demonstrated that ectopically expressed DBF4, localises to the centromere, when soluble DBF4 was pre-extracted (Wu et al., 2016). Extracting soluble proteins allows the detection of proteins bound to specific structures. The work presented in this chapter and the work from Wu et al. 2016, used different methods of extraction and fixation which may account for differences in the DBF4 localisation observed. An alternative reason for these discrepancies, could be due to the differences in the localisation of ectopic DBF4 versus endogenous DBF4. Future experiments comparing these extraction methods may be used to confirm these results. Moreover, it cannot be

excluded that the antibody might recognise different proteins under these experimental conditions. Depletion of DBF4, using siRNAs, could verify if the antibody is specific for DBF4. Furthermore, it would be interesting to determine if DBF4 is on the spindle itself. This could be performed using nocodazole or using cold-treatment which would cause depolymerisation of the spindles. Spindle localisation of DBF4 suggests a potential role for DBF4 in proper microtubule formation and accurate chromosome segregation. Again, depletion of DBF4 by utilising siRNAs could address this.

CDC7 kinase activity is regulated during the cell cycle. It is associated with replication but the kinase is still active in mitosis, suggesting that it may have a role here (Montagnoli et al., 2006). This is consistent with previous observations of mild mitotic defects in cancer cells depleted of either CDC7 or its regulatory subunits (Montagnoli et al., 2004; Yoshizawa-Sugata et al., 2005). In this work, it was revealed that CDC7 is an active kinase during mitosis, where it is auto-phosphorylated (Figure 4.4A-C). It demonstrated that during mitosis CDC7 is able to phosphorylate MCM2 leading to a hypothesis that the importance of CDC7 kinase activity and its phosphorylation of MCM2 extends beyond an extensively described role of CDC7 kinase in S-phase (Montagnoli et al., 2006; Ramer et al., 2013).

This research documented the first indication of a function of CDC7 during mitosis, specifically by cooperating with PLK1 to maintain a robust SAC signal (Figure 4.5A-B). Combined inhibition of CDC7 kinase and PLK1 during a nocodazole induced cell cycle arrest, in which the checkpoint was partially or fully challenged, resulted in a SAC override which was dependent on proteasome activation. However, it is likely that cooperation between CDC7 and PLK1 in the maintenance of a robust SAC is minimal as it does not occur under conditions in which cells have not spent a prolonged period of time in mitosis (Figure 4.9). Furthermore, the CDC7 and PLK1 inhibition dependent SAC override is not as efficient as a checkpoint override caused by inhibition of MPS1, a major SAC kinase (Figure 4.7). Perhaps CDC7 cooperates with PLK1 to recruit SAC kinases or to regulate their activity at the kinetochore. It is also possible that there is a delayed

mitotic entry in the presence of a PLK1 inhibitor, due to the role of PLK1 in the positive feedback loop for CDK1 activation. Therefore, timings of mitotic entry in the control and in the presence of PLK1 inhibition are not comparable. Another possibility could be that PLK1 and CDC7 could compete for binding to DBF4 because Dbf4p has been shown to interact with Cdc5p (Miller et al., 2009). In this case PLK1 could bind more DBF4 when CDC7 is inhibited. However, this is unlikely as PLK1 was never detected in mass spectrometry from our lab, which attempted to identify DBF4 interacting proteins. Due to its minor role in the checkpoint it was difficult to study its function there. Another genetic approach, such as the use of an analog sensitive CDC7 cell line (Wan et al., 2006), could be used to verify the role of CDC7 kinase in SAC maintenance, as it would limit off target effects and perhaps complete inhibition would enhance a phenotype.

CDC7 inhibition in combination with inhibition of either of the major checkpoint kinases, Aurora B or MPS1, that are well known to cause a checkpoint override, even when they are only partially inhibited (De Antoni et al., 2012; Santaguida et al., 2010), did not result in a SAC override (Figure 4.8A-B). This provides initial evidence that CDC7 kinase is involved in the maintenance of the SAC specifically in combination with PLK1.

Chemical inhibitors, although useful, do have limitations, such as off target effects and incomplete inhibition. This work attempted to limit the possibility that the phenotypes that were observed, were due to off target effects of the chemical inhibitors, by using two different CDC7 kinase and PLK1 inhibitors.

Due to strong apoptotic death in cancer cells preferentially over normal cells, the emergence of inhibitors of both CDC7 kinase and PLK1 are being pursued as anticancer agents. However, the task of kinase inhibitor development is associated with resistance of cancer cells, over time, to these inhibitors. To overcome resistance or to increase efficacy of treatment, combination therapies are being explored, to offer a therapeutic advantage (Ito et al., 2012; Natoni et al., 2013). Therefore, it is important to understand how these kinase inhibitors can be best used either as single agents or in effective combination therapies. A CDC7 kinase inhibitor has shown a dramatic synergy with

taxanes in eradicating carcinogen-induced breast carcinomas in rats (Montagnoli et al., 2010), although, to date the underlying mechanism is not known.

This work contributes to the understanding of the function of CDC7 outside of DNA replication. Thus, in cancer therapies CDC7 kinase inhibitors could target CDC7 kinase during replication and mitosis.

In conclusion, this study, reveals a novel role for CDC7 kinase in mitosis. Specifically, it implicates CDC7 kinase in cooperation with PLK1 in the maintenance of the SAC. This work also reveals a potential novel role for CDC7 in centrosome function, possibly through its regulatory subunit, DRF1.

This data, in particular the work describing a role for CDC7 during SAC maintenance, adds to the complexity of the SAC feedback control pathway (Figure 4.10).

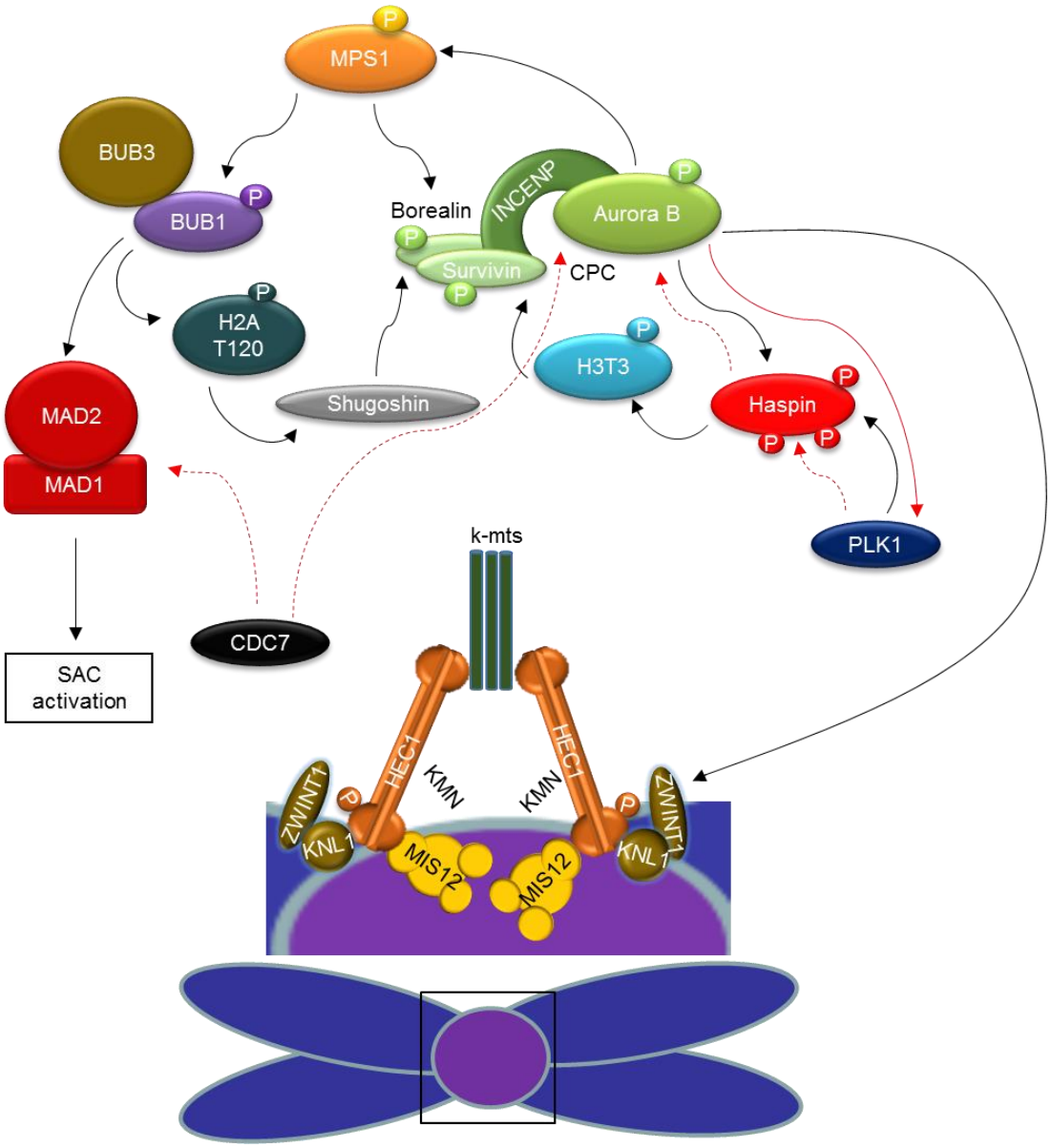

Figure 4.10 Proposed model of the roles of PLK1, Aurora B and CDC7 kinases in SAC maintenance

In this work, it has been shown that Aurora B kinase activity is important for the maintenance of PLK1 at the kinetochore (continuous red arrow). PLK1 is required for Aurora B localisation and activity during SAC maintenance, partially mediated through Haspin (broken red arrow). Further study into the role of CDC7 kinase in the maintenance of the SAC is required to understand where CDC7 kinase acts during checkpoint maintenance. Preliminary evidence suggests that it could act on Aurora B or MAD1/MAD2.

CHAPTER 5:

CHARACTERISATION OF HAP1 CELL LINES CARRYING A MUTATION IN EITHER *DBF4* OR *DRF1*

5.1 - Introduction

Although CDC7 kinase has been well characterised with respect to DNA replication and DNA replication stress (Costanzo et al., 2003; Day et al., 2010; Rainey et al., 2013; Sclafani and Holzen, 2007), there is a limited understanding of the roles of its regulatory subunits, DBF4 and DRF1.

Studies have shown that DBF4 and DRF1 are mutually exclusive in their binding to CDC7 kinase (Montagnoli et al., 2002). Both DBF4 and DRF1 have been shown to be nuclear proteins (Kumagai et al., 1999; Montagnoli et al., 2002; Sato et al., 2003) with recent work identifying DBF4 at the kinetochores/centromeres (Natsume et al., 2013; Wu et al., 2016). In chapter 4, it was detected at the centrosome during interphase and at the spindle during mitosis. Dbf4p has been demonstrated to be phosphorylated by Mec1p/Tel1p in yeast, which is required to prevent replication in the presence of replication stress (Lee et al., 2012). DRF1 has been shown to be important for replication initiation during early development in *Xenopus* (Silva et al., 2006).

In human cells, the role for both proteins are even less well characterised. The amino acid sequence of DBF4 and DRF1 are conserved in the N-, M- and C-motifs, but are poorly conserved outside of these regions (Montagnoli et al., 2002; Yoshizawa-Sugata et al., 2005).

Whether DBF4 and DRF1 are functionally distinct is an important question that remains unanswered, due to the lack of specific and sensitive immunological reagents against DRF1.

HAP1, is a near-haploid cell line, except for chromosome 15. This cell line was derived from a chronic myeloid leukemia cell line, KBM-7 (Carette et al., 2011), a near-haploid cell line, with the exception of chromosome 8 and 15. The HAP1 cell line provides an attractive cellular model to generate cell lines in which a particular gene is mutated, as there is only a single allele that needs to be targeted.

This study employed the use of HAP1 cell lines carrying a deletion in the gene encoding for either DBF4 or DRF1, to begin to address the functional differences of DBF4 and DRF1.

5.2 - Confirmation of the deletion in either *DBF4* or *DRF1*

The HAP1 cell line was edited by CRISPR/Cas9 resulting in either a 17 base pair (bp) deletion in the coding region of exon 3 of *DBF4* (Figure 5.1A) or a 2 bp deletion in the coding region of exon 4 of *DRF1* (Figure 5.1C). These cell lines were generated by and purchased from Horizon Discovery. These deletions should result in a frameshift in the sequence of either *DBF4* (Figure 5.1B) or *DRF1* (Figure 5.1D) open reading frames, which would result in the introduction of a premature stop codon (Figure 5.1B and D). The introduction of the premature stop codon in *DBF4* and *DRF1* is upstream of the CDC7 kinase binding motifs, the M- and C-motifs, (Figure 5.1B and 5.1D). Therefore, CDC7 kinase would be prevented from binding to the truncated DBF4 or DRF1 proteins.

A

```
DBF4     AGGAGCTCTTATACTTCCTCAGAGATCTAGGTTCAGAAAAATACAGTATAAAAACCACCAATTTACGAAA
DBF4 KO  AGGAGCTCTTATACTTCCTCAGAGATCTAGGTTCAGAAAAATACAGTATAAAAACCACCAATTTACGAAA

         TAATTGCATCAAATTGAAATTTTTTACTGTGCTTGGCATATGAAACAGTTTATGGTTTTTATGACCTAGT
         TAATTGCATCAAATTGAAATTTTTTACTGTGCTTGGCATATGAAACAGTTTATGGTTTTTATGACCTAGT

         TGAAAATACCTTGGTGGCATGTGCCTATAGTCCCAGCTGTTCAGAAGGCCAAGGCGGGAGGATCACTTGA
         TGAAAATACCTTGGTGGCATGTGCCTATAGTCCCAGCTGTTCAGAAGGCCAAGGCGGGAGGATCACTTGA

         GAACAGGGGGTTGAGGCTGCAGTGAGCTATGATTGTGCCACTGCACTCTAGCCTGGATAACACAGTGAGA
         GAACAGGGGGTTGAGGCTGCAGTGAGCTATGATTGTGCCACTGCACTCTAGCCTGGATAACACAGTGAGA

         CCGTGTTTCTTAAAACAAATTTATAAATAAAAATACTTTGTTCTCTTCTAGCGAGTTGAAGAATTTCTCA
         CCGTGTTTCTTAAAACAAATTTATAAATAAAAATACTTTGTTCTCTTCTAGCGAGTTGAAGAATTTCTCA

         GCAAAGATATCAGTTATCTTATTTCAAATAAGAAGGAAGCTAAATTTGCACAAACCTTGGGTCGAATTTC
         GCAAAGATATCAGTTATCTTATTTCAAATAAGAAGGAAGCTAAATTTGCACAAACCT------------

         TCCTGTACCAAGTCCAGAATCTGCATATACTGCAGAAACCACTTCACCTCATCCCAGCCATGATGGAAGT
         ----GTACCAAGTCCAGAATCTGCATATACTGCAGAAACCACTTCACCTCATCCCAGCCATGATGGAAGT

         TCATTTAAGTCACCAGACACAACTCAGAAGGGCTATATCCTGAAGATCTCCTGGTTTTTAATAGCAAGGT
         TCATTTAAGTCACCAGACACAACTCAGAAGGGCTATATCCTGAAGATCTCCTGGTTTTTAATAGCAAGGT

         GGCAGTAGAGT
         GGCAGTAGAGT
```

B

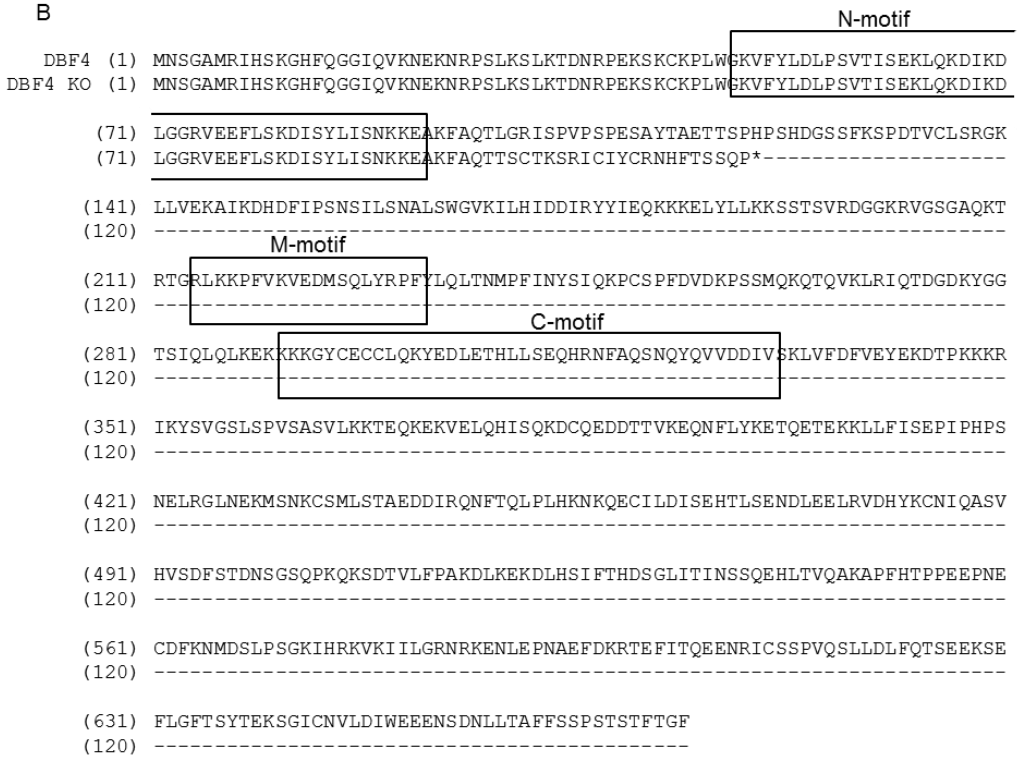

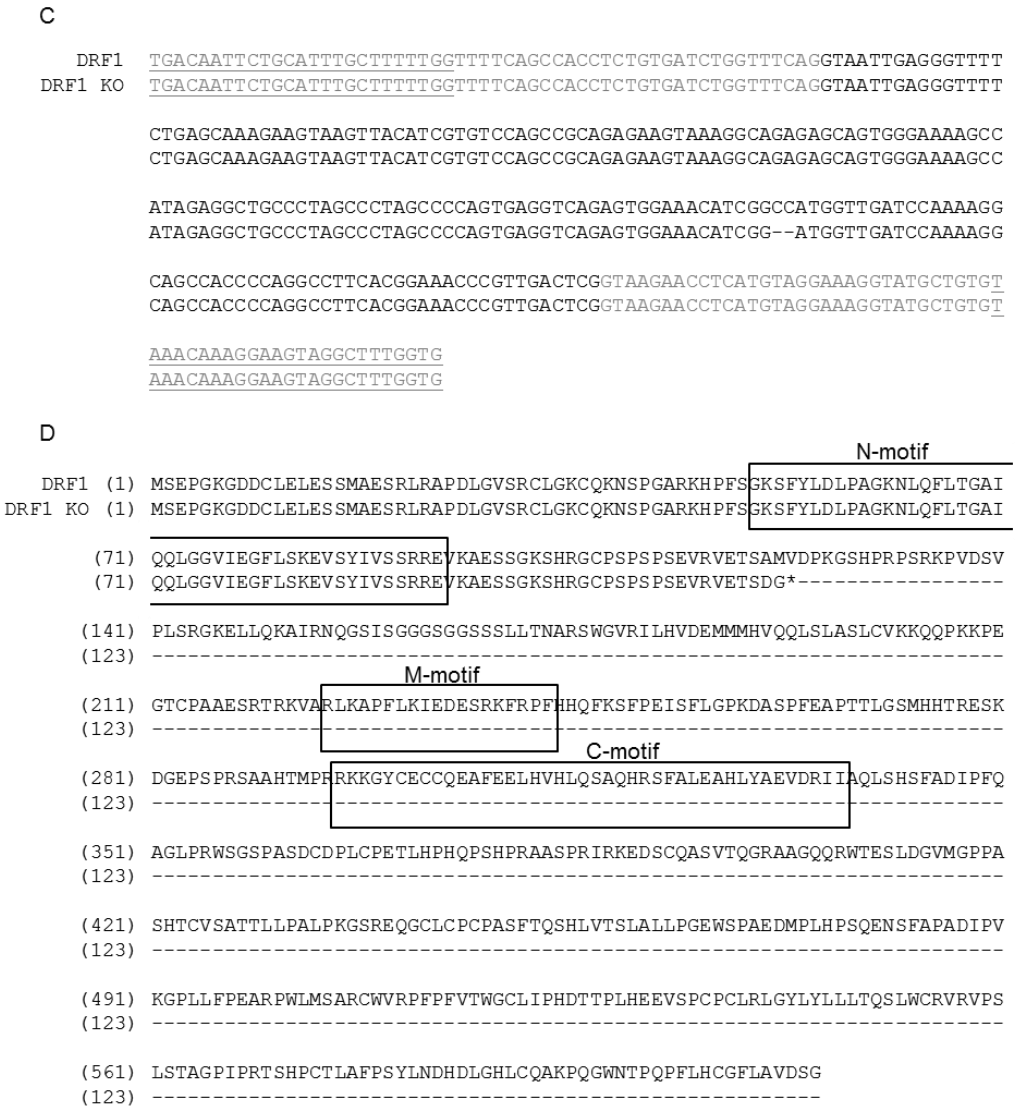

Figure 5.1 Nucleotide sequences of the exons containing the deletions in, and amino acids sequences of *DBF4* and *DRF1*

(A) Nucleotide sequence of exon 3 of *DBF4* (black) and the intronic regions flanking the exon (grey). PCR primers used to amplify the region (underlined), 17 bp deletion (dashed lines). (B) Amino acid sequence of DBF4, highlighting the N-, M- and C-motifs of DBF4. * represents the premature stop codon. (C) Nucleotide sequence of exon 4 of *DRF1* (black) and the intronic regions flanking the exon (grey). PCR primers used to amplify the region (underlined), 2 bp deletion (dashed lines). (D) Amino acid sequence of DRF1, highlighting the N-, M- and C-motifs of DRF1. * represents the premature stop codon.

To confirm that the deletion was present in the cell line in which exon 3 of *DBF4* was edited, this exon was sequenced. Genomic DNA was extracted from this edited cell line and from the wild type (WT) cell line, which was used as a control. Primers flanking exon 3 of *DBF4* were used to PCR amplify this region of *DBF4* in both cell lines (Figure 5.1A and Table 2.6). Sequencing confirmed a 17 bp deletion in *DBF4* in the edited cell line (Figure 5.1A). In the same manner, genomic DNA was extracted from the cell line in which exon 4 of *DRF1* was edited and primers flanking exon 4 of *DRF1* were used to PCR amplify this region of *DRF1* (Figure 5.1C and Table 2.6). Sequencing confirmed a 2 bp deletion in *DRF1* in the edited cell line (Figure 5.1C). In this thesis, these cell lines will be referred to as DBF4 knockout (DBF4 KO) or DRF1 knockout (DRF1 KO), due to the presence of the deletions.

To examine the effect of the deletion in *DBF4*, at the protein level, immunoblotting analysis was performed. As a control for these immunoblots, cell extracts were also prepared from Flp-In T-REx Human Embryonic Kidney (HEK) 293 cells overexpressing DBF4 (DBF4 OE), DRF1 (DRF1 OE) or transfected with empty vector (EV), (Kevin Wu thesis, National University of Galway, 2016). DBF4 protein levels in the DBF4 KO, DRF1 KO and WT cell lines were analysed using anti-DBF4 antibodies. An immunoreactive band for DBF4 was easily detected in the DBF4 OE cell line, the positive control. A low level of DBF4 was detected in the EV cell line. DRF1 OE cell line was included, to determine if overexpression of DRF1 affected DBF4 protein levels but an immunoreactive band for DBF4 was not detectable in this cell line. An immunoreactive band for DBF4 was detected in the WT and DRF1 KO cell lines but not in the DBF4 KO cell line (Figure 5.2A). These results indicate that DBF4 was eliminated or that there were undetectable amounts of DBF4 protein in the DBF4 KO cell line. However, verification of the deletion in the DRF1 gene at the protein level was not possible due to the lack of sensitive immunological reagents against DRF1.

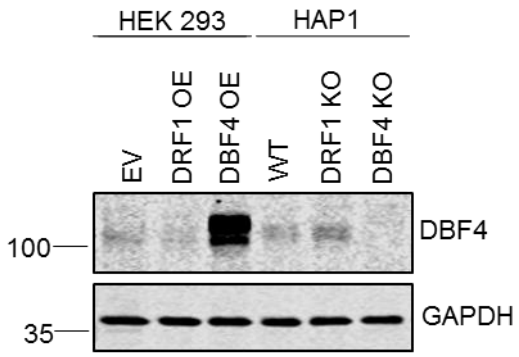

Figure 5.2 Effect of the deletion in *DBF4* at the protein level

WT, DBF4 KO, DRF1 KO cell lines and HEK 293 EV, DBF4 OE and DRF1 OE cell lines used as controls were analysed by immunoblotting using the indicated antibodies.

5.3 - Preliminary characterisation of cell lines carrying a mutation in either *DBF4* or *DRF1*

To characterise the DBF4 and DRF1 KO cell lines, cellular morphologies were examined. DIC images were captured of the WT, DBF4 KO and DRF1 KO cell lines. There were no noticeable morphological changes in the DBF4 KO cells compared to the WT. DRF1 KO cells instead were more rounded and possibly smaller. Specifically, the cytoplasm did not appear to stretch out as much compared to the WT (Figure 5.3A). However, as the DRF1 KO cells grew in clumps it was difficult to determine if these cells were smaller. Thus, overall cell size when cells were in suspension was then determined using the countess automated cell counter. The deletion in *DBF4* or *DRF1* did not cause a significant change in cell size compared to WT (Figure 5.3B). This data indicates that the deletion in *DRF1* but not *DBF4* effected cell morphology suggesting that perhaps DRF1 may play in cytoskeleton formation.

To determine whether the deletion in *DBF4* or *DRF1* affected cell growth or cell viability, growth curves were performed. Cell number and percentage of cell viability were examined by trypan blue exclusion using the Countess automated cell counter, at 0, 24, 48 and 72 hours after plating. Cell growth and cell viability were not affected in the DBF4

or DRF1 KO cell lines, at the time points examined, when compared to the kinetics of the WT control cells (Figure 5.3C and 5.3D).

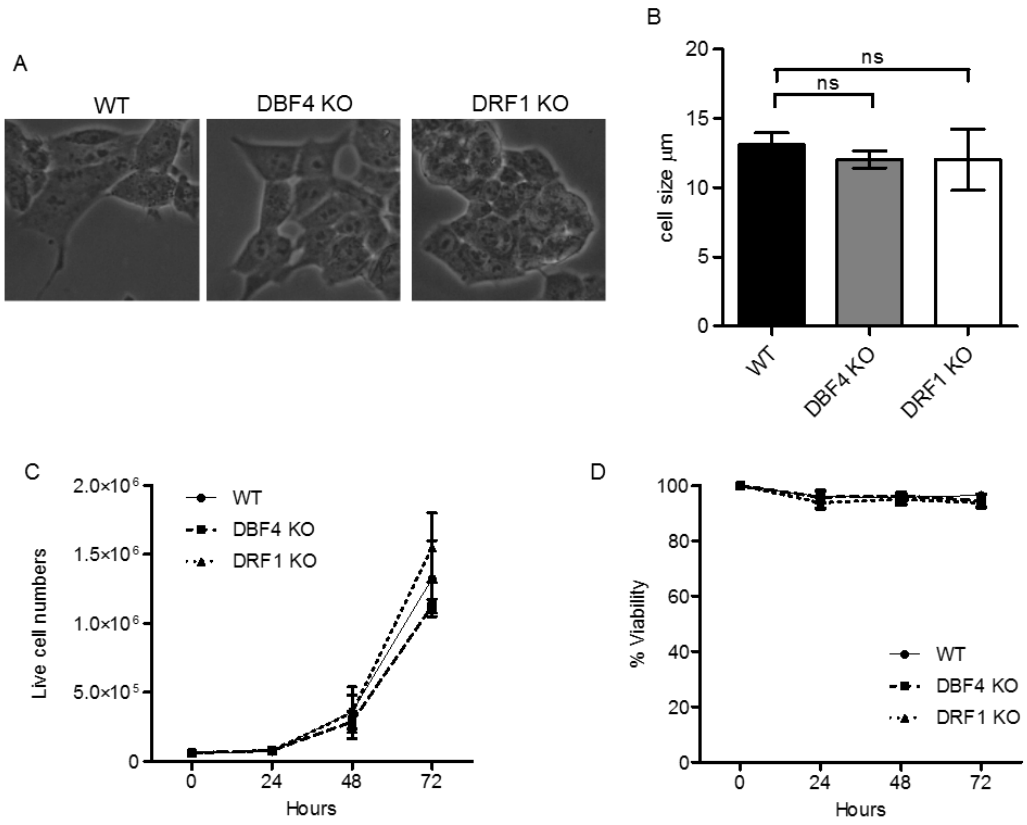

Figure 5.3 Preliminary characterisation of cell lines carrying a mutation in either *DBF4* or *DRF1*

(A) DIC images of morphology of cells in the WT, DBF4 KO and DRF1 KO cell lines. (B) Quantification of the cell sizes of (A) using a Countess automated cell counter. N=6, error bars=S.D., ns= not significant. (C) Growth curves or (D) cell viability for the WT, DBF4 KO and DRF1 KO cell lines were generated from live cell number, based on trypan blue exclusion 0, 24, 48 hr and 72 hours. N=4, error bars=S.D.

5.4 - Analysis of cell cycle parameters in cell lines carrying a mutation in either *DBF4* or *DRF1*

For cell cycle analysis experiments, cells were labelled with EdU, a thymidine analog, 30 minutes prior to harvesting. After fixing, the Click-iT reaction was performed as per Materials and Methods 2.9.2. It was observed that there was a population of cells that was diploid, in these HAP1 cell lines (Figure 5.4A). It appeared that, as the passage number of the cell line increases, the fraction of diploid cells in a population accumulates. Therefore, for all cell cycle analysis experiments in this chapter, apart from Figure 5.7A, cells with a DNA content higher than 2N, were gated out during the analysis (Figure 5.4B).

As discussed in the introduction, CDC7 kinase activity is essential for initiation of DNA replication in eukaryotes (Sclafani and Holzen, 2007). As CDC7 requires binding of either subunit for activation, the DBF4 KO and DRF1 KO cell lines were used to examine which of the subunits contribute to CDC7 kinase activity during S-phase. WT, DBF4 KO and DRF1 KO cells were labelled with EdU, 30 minutes prior to harvesting. The cells were then fixed, the Click-iT reaction was performed and DAPI was incorporated into the DNA. Flow cytometry analysis revealed that there was an accumulation of cells in S-phase, specifically late S-phase, in the DBF4 KO compared to WT (Figure 5.4C). A deletion in *DRF1* had no detectable effect on S-phase progression compared to the WT (Figure 5.4C). It should be noted that the cells labelled as G2-phase cells, in Figure 5.4C and in the proceeding figures, include both haploid G2-phase cells and diploid G1-phase cells, as they cannot be gated separately in these experiments. This data suggests that DBF4 is required for efficient progression through S-phase and that it may indicate that DBF4 has a predominant role for regulating CDC7 kinase during S-phase progression.

Chapter 4 revealed novel insights into potential roles for CDC7 kinase and its regulatory subunits in mitosis. For this reason, examination of mitotic index was carried out by analysing the percentage of H3S10Ph positive cells in the WT, DBF4 KO and DRF1 KO cell lines by flow cytometry. There was no statistical significant difference detected

between each cell line indicating that a deletion in *DBF4* or *DRF1* does not affect the percentage of cells in mitosis compared to the WT (Figure 5.4D).

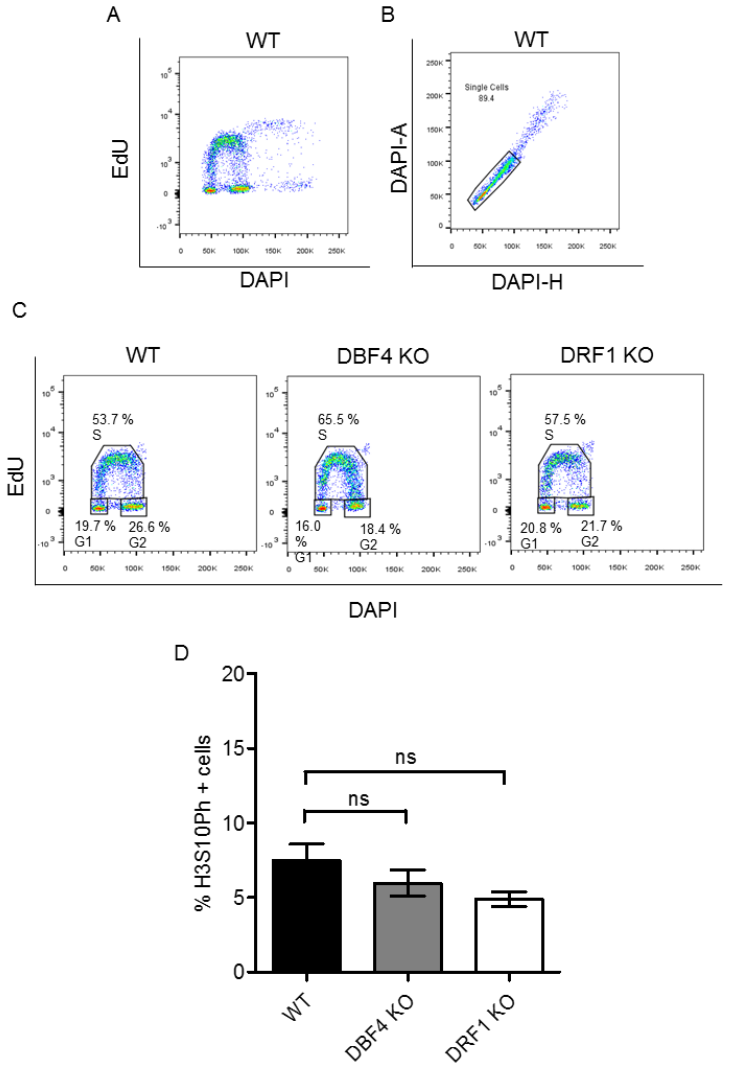

Figure 5.4 Analysis of cell cycle parameters in cell lines carrying a mutation either *DBF4* or *DRF1*

(A) WT cells were labelled with EdU, 30 minutes prior to harvesting. The Click-iT reaction was carried out and DAPI was incorporated into the DNA. Cell cycle analysis was carried out on a FACS CANTO II. (B) Gating strategy for eliminating cells with DNA content higher than 2N. (C) WT, DBF4 KO and DRF1 KO cells were labelled with EdU, 30 minutes prior to harvesting. The Click-iT reaction was carried out and DAPI was incorporated into the DNA. Cell cycle analysis was carried out on a FACS CANTO II. (D) WT, DBF4 KO and DRF1 KO cells were stained with H3S10Ph and analysed on a FACS CANTO II. The percentage H3S10Ph positive cells was quantified. N=3, error bars=S.D., ns=not significant.

5.5 - CDC7 kinase inhibition by XL413 in combination with a mutation in either *DBF4* or *DRF1* does not have an additive effect on the cell cycle

Although a deletion in *DBF4* prevents efficient S-phase progression, it does not fully block replication. This is possibly because of residual CDC7 kinase activity, due to compensatory effects of the subunits. To test whether the DBF4 KO and DRF1 KO cell lines are sensitive to further partial CDC7 kinase inhibition, the WT, DBF4 KO and DRF1 KO cell lines were treated with XL413 for 0, 6 or 24 hours. Thirty minutes prior to harvesting, EdU was added to the cells. The Click-iT reaction was performed and DAPI was incorporated into the DNA. The samples were then analysed by flow cytometry. An accumulation of cells in S-phase was observed in the DBF4 KO compared to the WT, as previously observed in Figure 5.5A. A deletion in *DRF1* did not have any detectable effect on S-phase progression. Treatment with the CDC7 kinase inhibitor, XL413 for 6 hours caused an accumulation of cells in late S-phase which have a lower rate of DNA synthesis, after 6 hours. These cells progressed to G2/M-phase after 24 hours, in the WT, DBF4 KO and DRF1 KO cell lines (Figure 5.5A). XL413 is dominant over the effect of a deletion in either *DBF4* or *DRF1*, suggesting that there is residual CDC7 activity in these cell lines.

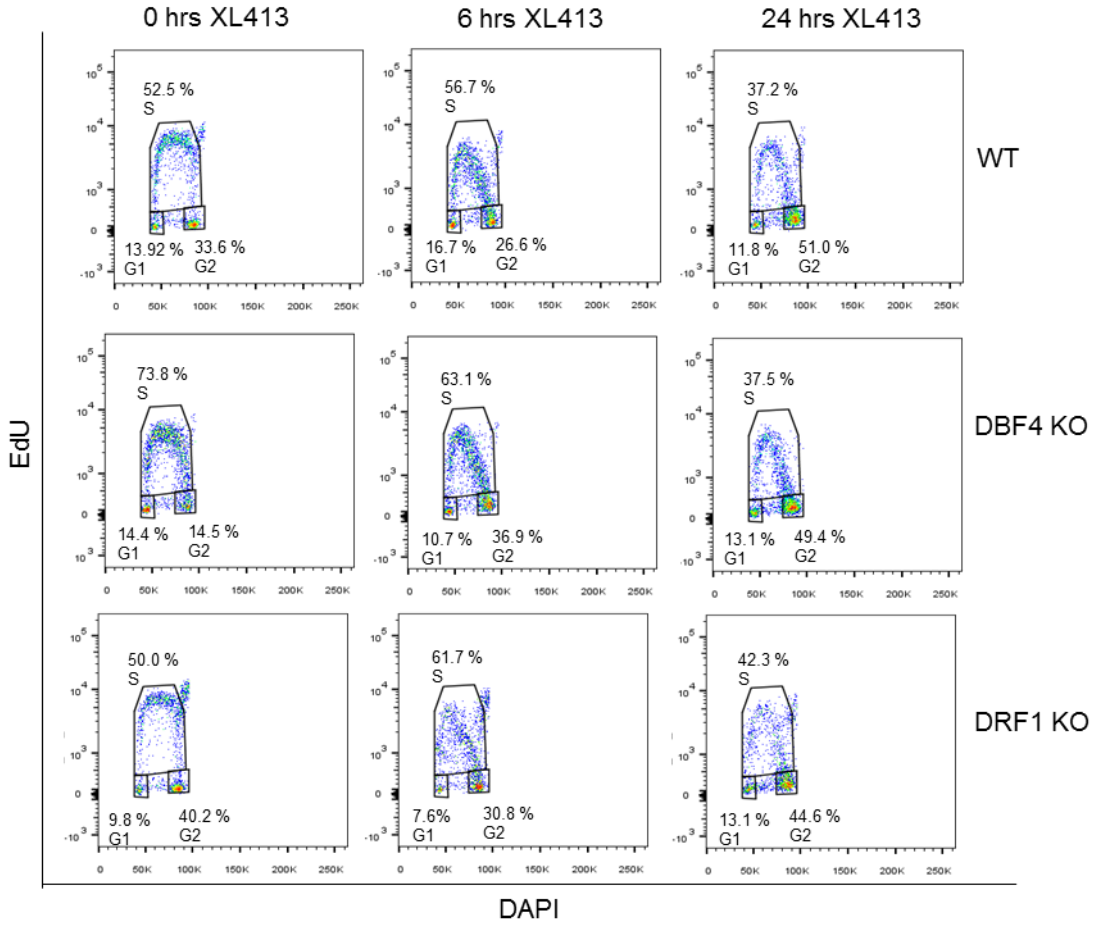

Figure 5.5 CDC7 kinase inhibition by XL413 in combination with a mutation in either *DBF4* or *DRF1* does not have an additive effect on the cell cycle

WT, DBF4 KO and DRF1 KO cells were treated with 10 μM XL413 or DMSO for 0, 6 or 24 hours. Cells were labelled with EdU 30 minutes prior to harvesting. The Click-iT reaction was performed and DAPI was incorporated into the DNA. Cell cycle analysis was carried out on a FACS CANTO II.

5.6 - Analysis of CDC7 kinase activity in cell lines carrying a mutation in either *DBF4* or *DRF1*

To examine whether disruption of the CDC7/DBF4 or CDC7/DRF1 complexes affected the stability of CDC7, immunoblotting analysis was performed on the WT, DBF4 KO and DRF1 KO cell lines, to examine the effect on CDC7 protein levels. WT, DBF4 KO and DRF1 KO cell lines contained similar CDC7 protein levels (Figure 5.6A), indicating

that the deletion in *DBF4* or *DRF1*, does not affect overall CDC7 protein levels. This suggests that the deletion in *DBF4* or *DRF1* does not cause CDC7 catalytic subunit degradation.

To further understand if there is residual kinase activity in the DBF4 KO and DRF1 KO cell lines, markers of CDC7 kinase activity were assessed. As discussed in the introduction, CDC7 kinase activity is required for phosphorylating the MCM2 helicase on Ser 40 and it has also been reported to contribute to phosphorylation of MCM2 on Ser 53, Ser 108 and Ser 139 (Montagnoli et al., 2006; Tsuji et al., 2006).

MCM2 is a phospho protein and the differentially phosphorylated form can be resolved on a polyacrylamide gel. Thus. the electrophoretic mobility of MCM2, in cells containing the deletions in either *DBF4* or *DRF1*, was assessed by immunoblotting analysis. An altered electrophoretic mobility of MCM2 was observed in the DBF4 KO compared to the WT (Figure 5.6B). Three hours of treatment with XL413 blocked CDC7 kinase phosphorylation and caused an altered electrophoretic mobility, which was comparable to the altered electrophoretic mobility observed in the DBF4 KO cell line, suggesting that CDC7/DBF4 is one of the major kinases that is responsible for phosphorylating MCM2. No detectable effect on total MCM2 was observed in the DRF1 KO cell line (Figure 5.6B).

The phosphorylation of MCM2 at specific sites was then examined. The deletion in *DBF4* reduced, but did not completely abolish, phosphorylation of MCM2 on Ser40/41 (Figure 5.6A). The overall level of phosphorylation of pSer53, pSer108 and pSer139 was not affected and the banding pattern was consistent with the position of total MCM2 in the DBF4 or DRF1 KO cell lines (Figure 5.6A-D). This is comparable with these sites being phosphorylated by other kinases. This data indicates that DBF4 may be the main regulatory subunit of CDC7 kinase required for phosphorylating MCM2 on Ser40.

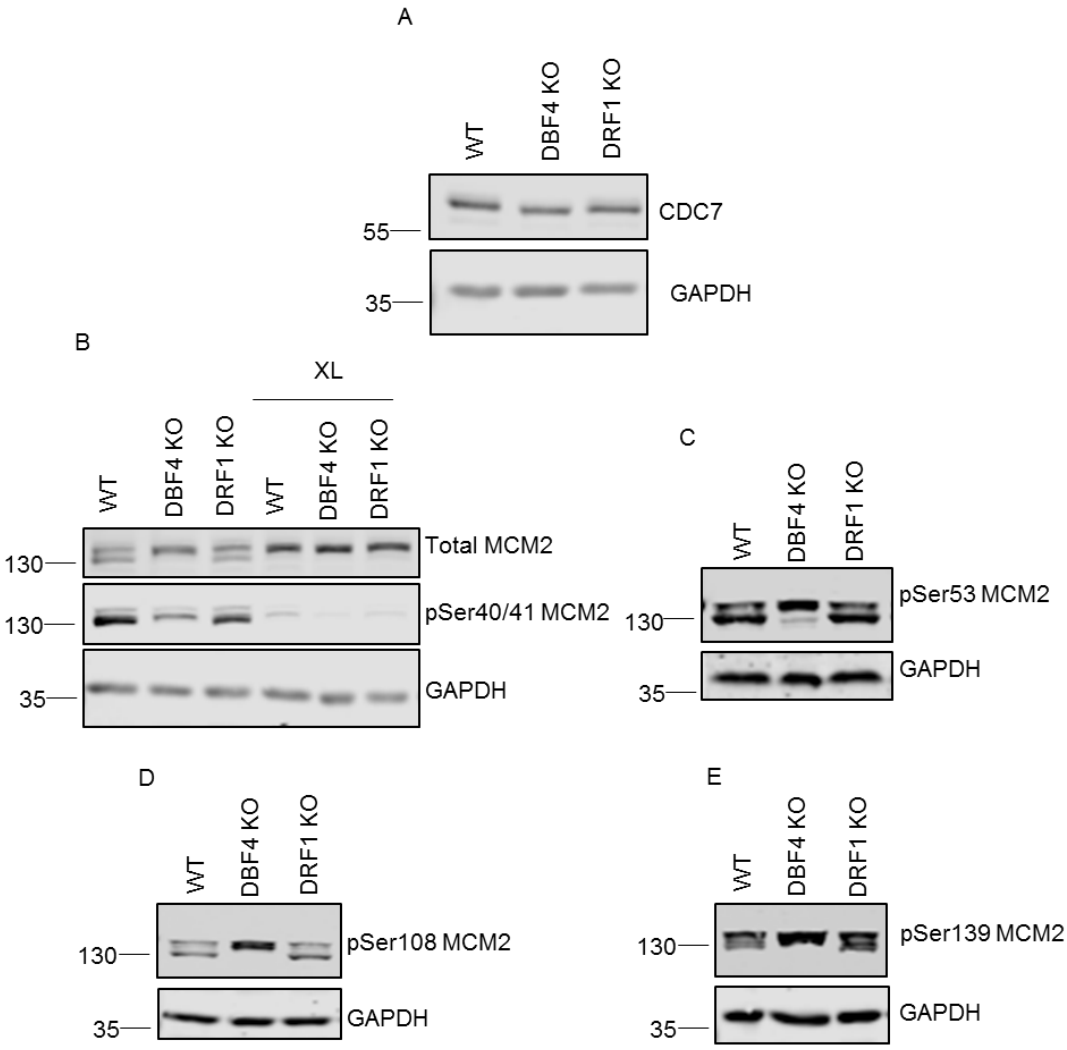

Figure 5.6 Analysis of CDC7 kinase activity in cell lines carrying a mutation in either *DBF4* or *DRF1*

(A) Immunoblotting analysis of WT, DBF4 KO and DRF1 KO cell lines using the indicated antibodies. (B) WT, DBF4 KO and DRF1 KO cell lines were treated with 10 μM XL413 or DMSO for 3 hours and proteins were analysed by immunoblotting using the indicated antibodies. (C-E) Immunoblotting analysis of WT, DBF4 KO and DRF1 KO, using the indicated antibodies.

5.7 - The defect in S-phase progression and the altered MCM2 electrophoretic mobility caused by a mutation in *DBF4* can be complemented by ectopic expression of DBF4

To determine whether the effects that were observed in the DBF4 KO cell line, were specifically due to the low levels or lack of DBF4 protein, DBF4 was transduced into the DBF4 KO cell line and WT cell line, as a control, as per Material and Methods 2.6.3[***]. Briefly, the HAP1 cell lines were transduced with virus that expressed the CDH-CMV-MCS-EF1 plasmid encoding for DBF4 tagged on the C-terminus with a dual Flag/Strep tag and neomycin resistance. After transduction, the cells were grown in the presence of G418, to kill any cells that were not transduced, generating a polyclonal cell line. The transduced DBF4 KO cell line expressing DBF4 will be referred to as DBF4 KO pCDH-DBF4 and the transduced WT cell line expressing DBF4 will be referred to as WT pCDH-DBF4. After transduction, cell cycle and immunoblotting analysis was performed to examine whether the defect in S-phase progression and the effect on MCM2 mobility observed in the DBF4 KO cell line could be complemented by ectopic expression of DBF4.

Firstly, to verify whether the defect in S-phase progression could be complemented with transduction of DBF4, WT, DBF4 KO, WT pCDH-DBF4 and DBF4 KO pCDH-DBF4 cells were labelled with EdU for 30 minutes. The cells were then harvested and fixed, the Click-iT reaction was performed as per Materials and Methods 2.9.2 and DAPI was incorporated into the DNA. Flow cytometry analysis revealed that there was an accumulation of cells in S-phase in the DBF4 KO compared to the WT control, as previously seen in Figure 5.6. WT pCDH-DBF4 cells resulted in approximately the same percentage of cells in S-phase compared to the WT control (Figure 5.7C). The percentage of cells that accumulated in S-phase in the DBF4 KO cell line was reduced in the DBF4 KO pCDH-DBF4 cell line (Figure 5.7A). It is worth to note that the cell lines, in particular

[***] The generation of these cell lines was conducted by Dr. Michael Rainey.

the WT pCDH-DBF4 cell line, have started to become diploid. Overall, this data suggests that DBF4 is indeed required for timely progression through S-phase.

To assess whether DBF4 had been transduced into the WT pCDH-DBF4 and DBF4 KO pCDH-DBF4 cell lines, immunoblotting was performed on the WT, DBF4 KO, WT pCDH-DBF4 and DBF4 KO pCDH-DBF4 cell lines. HEK293 EV DBF4 OE cell lines were used as controls for antibody detection. An immunoreactive band for Strep could be detected in the HEK 293 DBF4 OE cell line, used as a positive control, but not in the HEK 293 cells containing an empty vector (Figure 5.7B). An immunoreactive band for Strep was not detected in the WT or DBF4 KO cell lines as expected. An immunoreactive band for Strep was detected in the WT pCDH-DBF4 and DBF4 KO pCDH-DBF4 cell lines indicating that DBF4 was transduced into these cell lines (Figure 5.7B lanes 2 and 4).

To determine whether the altered electrophoretic mobility of MCM2, observed in the DBF4 KO cell line, was due to the low or absent expression of DBF4, immunoblotting analysis was performed on the WT, DRF1 KO, DBF4 KO, WT pCDH-DBF4 and DBF4 KO pCDH-DBF4 cell lines. Altered electrophoretic mobility of MCM2 was observed in the DBF4 KO cell line, as previously demonstrated (Figure 5.7C), and this altered electrophoretic mobility was reduced in the DBF4 KO pCDH-DBF4 cell line. The WT pCDH-DBF4 revealed a similar banding pattern for MCM2 compared to the WT (Figure 5.7C). Once again, deletion in the gene of DRF1 did not affect MCM2 (Figure 5.7C). This data suggests that DBF4 is required for complete phosphorylation of MCM2.

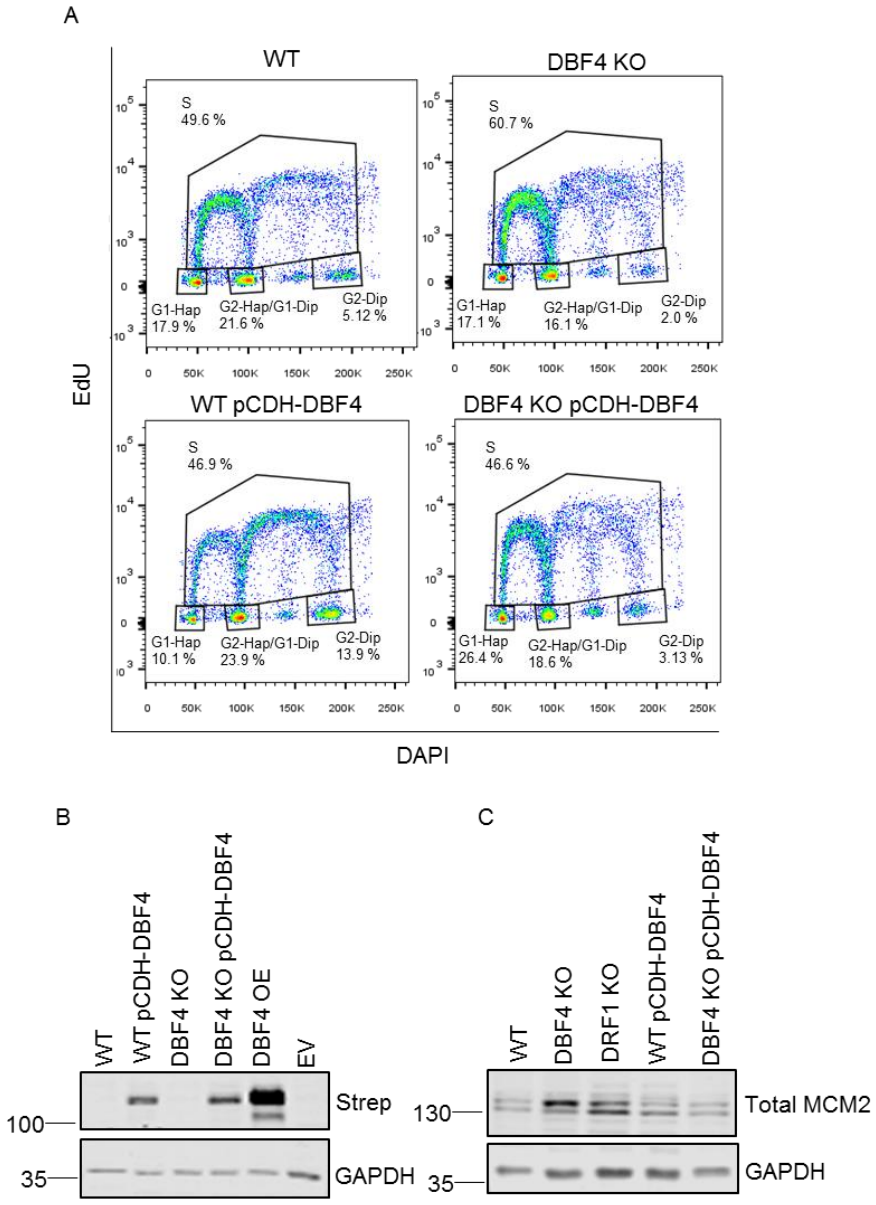

Figure 5.7 The defect in S-phase progression and the altered MCM2 electrophoretic mobility caused by a mutation in *DBF4* can be complemented by ectopic expression of DBF4

(A) WT, DBF4 KO, WT pCDH-DBF4 and DBF4 KO pCDH-DBF4 cell lines were labelled with EdU for 30 minutes prior to harvesting. Click-iT reaction was performed and DAPI was incorporated into the DNA. Cell cycle analysis was carried out using the FACS CANTO II. Immunoblotting analysis of (B) WT, WT pCDH-DBF4, DBF4 KO, DBF4 KO pCDH-DBF4, HEK 293 DBF4 OE (DBF4 OE) and HEK 293 EV (EV) cell lines or (C) WT, DBF4 KO, DRF1 KO, WT pCDH-DBF4, DBF4 KO pCDH-DBF4 cell lines, using the indicated antibodies.

5.8 - PLK1 inhibition alters the electrophoretic mobility of MCM2 but does effect S-phase progression

PLK1 has several known phosphorylation consensus sites on the MCM2-7 helicase complex (Trenz et al., 2008; Tsvetkov and Stern, 2005). Furthermore, as detailed in Chapter 4, a cooperativity between CDC7 and PLK1 in the maintenance of a robust SAC signal during mitosis was observed, leading to the postulation that PLK1 could be the other kinase responsible for driving S-phase progression when CDC7 kinase activity is compromised. To test this, the electrophoretic mobility of MCM2 was first accessed. WT and DBF4 KO cells were treated with the PLK1 inhibitors GW843682X or BI 6727 or with DMSO, as a control. After 3 hours, the cells were harvested. Immunoblotting analysis revealed, again that there was an altered electrophoretic mobility of MCM2 in the DBF4 KO cell line compared to the WT. A reduction in pSer40/41 MCM2 was also observed in the DBF4 KO cell line to the WT cell line (Figure 5.8A). Treatment with either G2843682X or BI 6727 resulted in an altered electrophoretic mobility of MCM2 compared to the control. However, treatment with GW843682X or BI 6727 did not affect pSer40/41 MCM2 (Figure 5.8A). This result suggests that PLK1 phosphorylates MCM2 but not on pSer40/41.

As PLK1 inhibition affected MCM2 phosphorylation, it was possible that the defect in MCM2 phosphorylation could affect S-phase progression. To explore this possibility, cells were treated as in Figure 5.8A. EdU was incorporated into the DNA for 30 minutes prior to harvesting. A Click-iT reaction was performed as per Materials and Methods section 2.9.2. There was an accumulation of cells in S-phase in the DBF4 KO compared to the WT, as observed in Figure 5.4C. Treatment with either GW843682X or BI 6727 caused an accumulation of cells in G2/M-phases (Figure 5.8B), consistent with what is reported in the literature (Lansing et al., 2007; Rudolph et al., 2009) but did not noticeably affect S-phase progression. Together, this data suggests that PLK1 phosphorylates MCM2 but that it does not obviously promote S-phase when CDC7 kinase activity is also compromised.

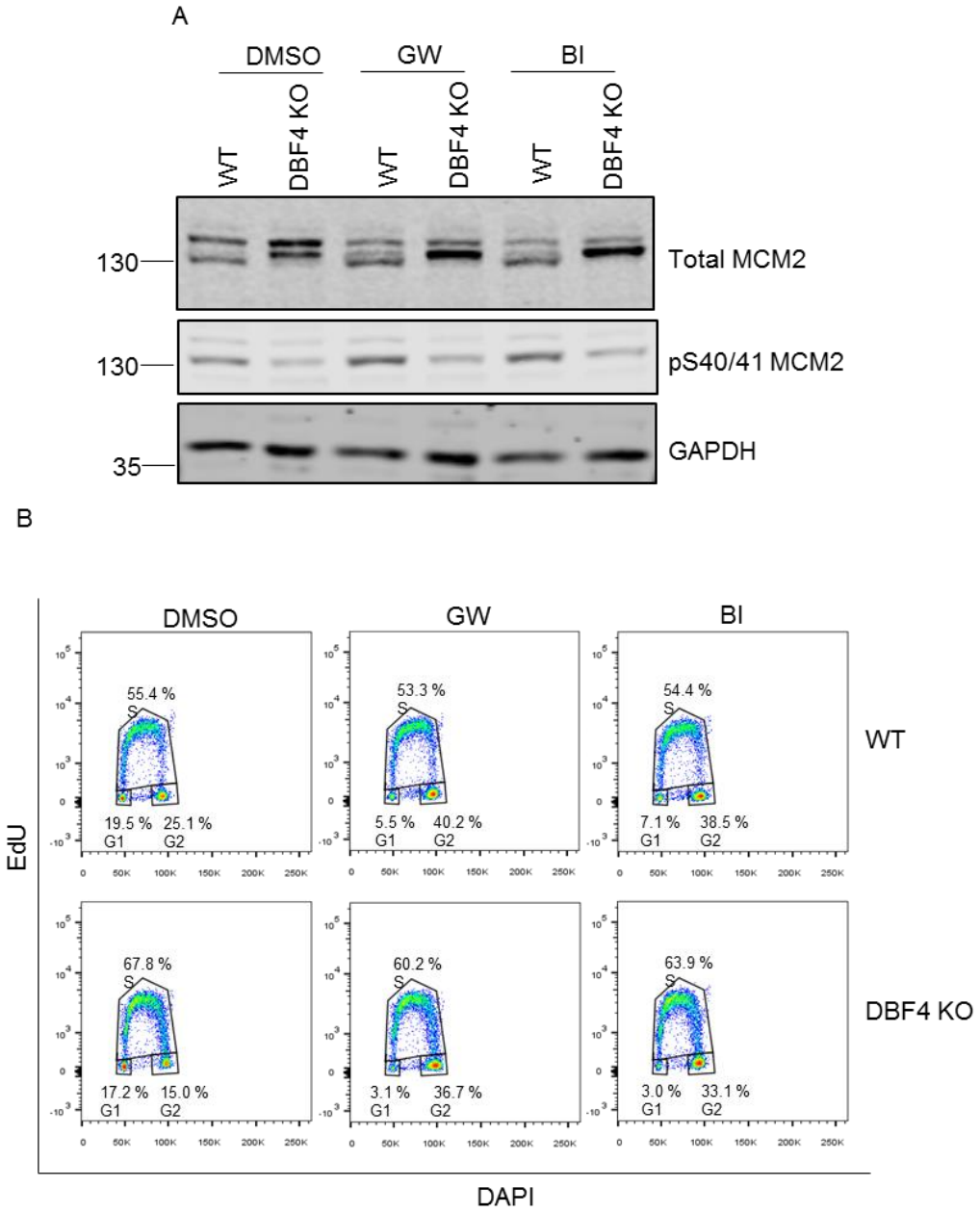

Figure 5.8 PLK1 inhibition alters the electrophoretic mobility of MCM2 but does not affect S-phase progression

(A) WT and DBF4 KO cell lines were treated with 1µM GW843682X, 100 nM BI 6727 or DMSO for 3 hours. Immunoblotting analysis was carried out using the indicated antibodies. (B) Cell lines were treated as in (A). Cells were labelled with EdU 30 minutes prior to harvesting. A Click-iT reaction was carried out and DAPI was incorporated into the DNA. Cell cycle analysis was performed using the FACS CANTO II.

5.9 - Characterisation of cell lines carrying a mutation in *DBF4* or *DRF1* in the replication stress checkpoint response

As discussed in the introduction, CDC7 kinase functions in the DNA replication stress response pathway (Costanzo et al., 2003; Day et al., 2010; Rainey et al., 2013). Specifically, inhibition of CDC7 kinase decreases Claspin phosphorylation, leading to a delay in CHK1 activation initiation (Rainey et al., 2013).

To examine if DBF4 or DRF1 contribute to the role of CDC7 kinase in the replication stress response, DBF4 and DRF1 KO cells were treated with 2 mM HU for 0, 0.5, 1 or 2 hours, after which, cells were harvested. WT cells were used as a control. Immunoblotting analysis revealed that CHK1 phosphorylation on Ser 317 (pSer317 CHK1), a marker of induction of the replication stress checkpoint (Zhao and Piwnica-Worms, 2001), increased in the presence of HU over time (Figure 5.9A). HU induced pSer317 CHK1, appeared to be decreased in the DBF4 KO cell line at 30 minutes compared to the control but this attenuation was not observed at 1 hour (Figure 5.9A). No effect was observed in the DRF1 KO cell line. Total CHK1 levels were not affected in the DBF4 or DRF1 KO cell lines compared to the WT (Figure 5.9A). This experiment was only carried out once. This suggests that DBF4 could be important for efficient induction of the replication stress checkpoint response.

To explore the relevance of DBF4 in the induction of the checkpoint response, the effect of prolonged replication stress, on cell viability, in the DBF4 KO cell line compared to the WT, was assessed using a colony formation assay, as described in Material and Methods section 2.4.4.

WT and DBF4 KO cells were treated with low and high doses of HU, as HAP1 cells appeared to be hypersensitive to HU. Briefly, cells were treated with 0 mM, 0.2 mM or 2.0 mM HU for 18 hours and then replated, in the absence of HU, incubated for 7 days and the number of surviving colonies were then scored. Treatment with low doses of HU showed a partial reduction in the number of colonies formed while treatment with high doses of HU showed a substantial decrease in the number of colonies formed, in both cell

lines. However, there was no statistical significance observed between the DBF4 KO and WT cell lines (Figure 5.9B). The decrease in the number of surviving colonies upon treatment of low doses or high doses of HU can be visualised in Figure 5.9C. This data, suggests that DBF4 does not play an important role in a cells ability to cope with replication stress, at least in HAP1 cells.

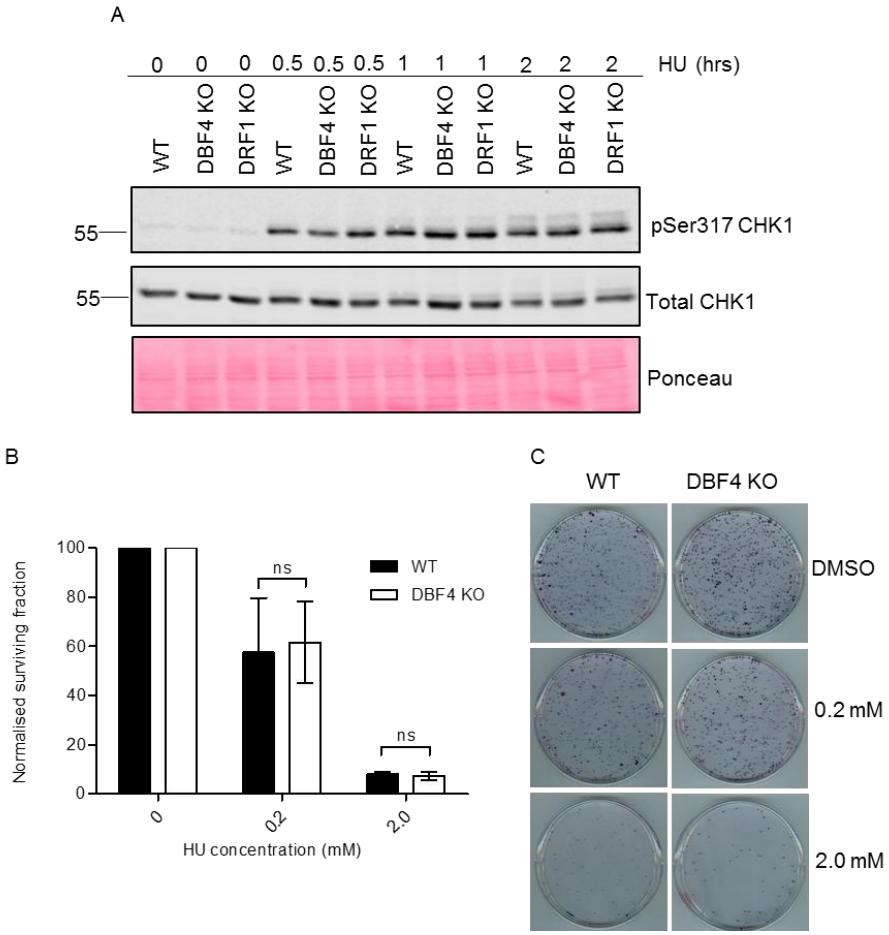

Figure 5.9 Characterisation of cell lines carrying a mutation in either *DBF4* or *DRF1* in the replication stress checkpoint

(A) WT, DBF4 and DRF1 KO cells were treated with 2 mM HU for 0. 0.5, 1 or 2 hours and proteins were analysed by immunoblotting using the indicated antibodies. (B) WT or DBF4 KO cell lines were treated with 0 mM, 0.2 mM or 2.0 mM HU for 18 hours and then replated. In each case the percentage of colony forming units (CFU), scored after 7 days, in the HU treated samples, were normalised to the untreated controls. Error bars represent S.D. (C) Examples of the colonies formed from each treatment from (B).

CDC7 kinase inhibition was shown to sensitise cells to HU (Rainey et al., 2013), a ribonucleotide reductase inhibitor, (Skoog and Bjursell, 1974; Skoog and Nordenskjold, 1971), and Etoposide (Rainey et al., 2013), a topoisomerase II inhibitor (Nitiss, 2009). In yeast, Dbf4p is known to be phosphorylated by Mec1p and Tel1p upon induction of the replication stress checkpoint response (Lee et al., 2012). Owing to these observations, it was considered whether the DBF4 KO or DRF1 KO cells were more sensitive to a range of drugs that target DNA replication and induce a replication stress response, compared to the WT. To examine this, WT, DBF4 KO and DRF1 KO cells were treated with varying doses of HU, Etoposide, XL413, a CDC7 kinase inhibitor (Koltun et al., 2012), KU55933 (KU), an ATM inhibitor (Hickson et al., 2004), VE-821, an ATR inhibitor (Charrier et al., 2011), Camptothecin, a topoisomerase I inhibitor (Hsiang et al., 1985), Cisplatin, a cross-linking agent (Loehrer and Einhorn, 1984), Mitomycin C, an alkylating agent (Gargiulo et al., 1995) or Aphidicolin, an inhibitor of DNA polymerase α (Ikegami et al., 1978). At hour 20 of treatment, alamar blue reagent was added to each well, as per Materials and Methods section 2.4.5. At hour 24 the fluorescent intensity was measured. Fluorescence intensity for each drug treatment was normalised to the control for that cell line. Normalised fluorescence decreased in WT, DBF4 KO and DRF1 KO cell lines as the concentration of any of the drugs increased. However, the DBF4 KO or DRF1 KO cell lines did not show any significant increase in sensitivity to any of the tested drugs compared to the WT control (Figure 5.10A-I). This data suggests that the deletion in either *DBF4* or *DRF1* does not sensitise cells to any of the tested drugs and does not contribute to reported, sensitisation to, Etoposide and HU, upon CDC7 kinase inhibition.

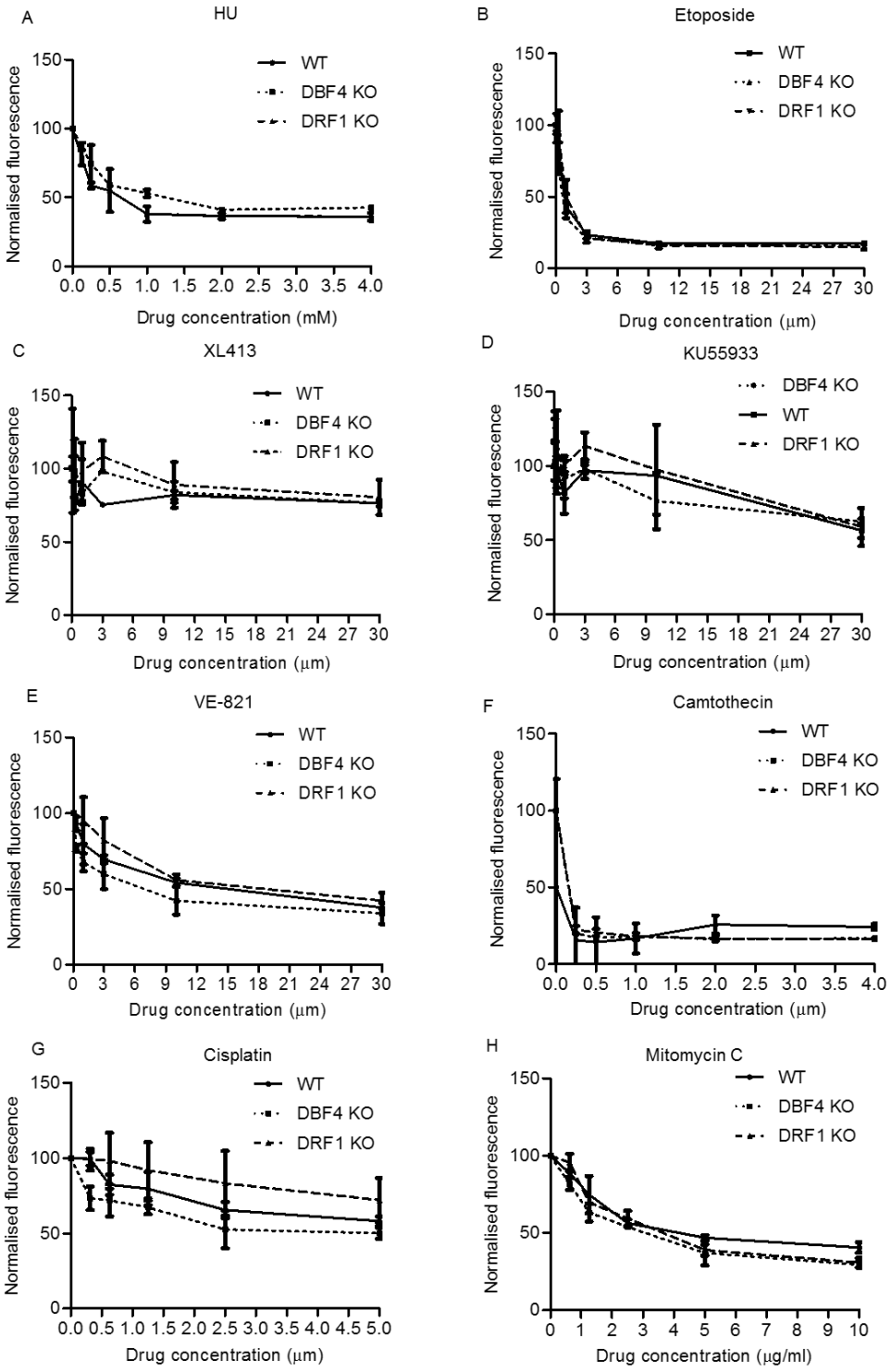
A
HU
WT
DBF4 KO
DRF1 KO
Normalised fluorescence
Drug concentration (mM)
B
Etoposide
Drug concentration (μm)
C
XL413
D
KU55933
E
VE-821
F
Camtothecin
G
Cisplatin
H
Mitomycin C
Drug concentration (μg/ml)

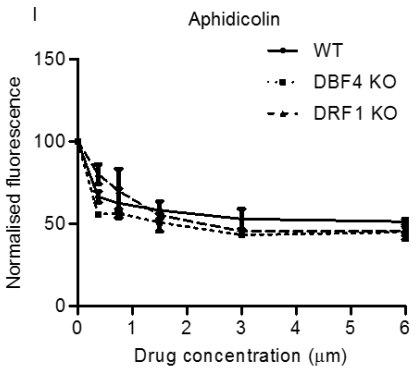

Figure 5.10 Analysis of the effect of drugs that target replication or induce the replication stress checkpoint on cell lines carrying a mutation in either *DBF4* or *DRF1*

(A-I) WT, DBF4 KO and DRF1 KO cell lines were treated with drugs at a range of concentrations as indicated in the graphs. An alamar blue assay was performed to measure cell proliferation. The fluorescence intensity was normalised to the control treatment in that cell line. N=3, error bars=S.D.

5.16 - Discussion and future perspectives

The primary scope of this chapter was to characterise HAP1 cell lines carrying a mutation in *DBF4* and *DRF1*, which were generated by Horizon Discovery.

The use of HAP1 cell lines proved difficult for cell cycle studies as a population of these cells became diploid and the fraction of diploid cells increased during each passage in culture. Thus, it was difficult to interpret the results due to the presence of a heterogeneous population of cells. Attempts to isolate homogenous cell populations by cell sorting proved unsuccessful despite technical optimisation efforts. The original advantage of using HAP1 cells was that there is only one allele for each chromosome that need to be disrupted. However, due to advancements in genetic editing tools in recent years, it has become easier to create homozygous deletions in two alleles.

The biology of why the haploid cells quickly become diploid is not yet understood. It was observed during these experiments, but never measured, that the DBF4 KO cell line did not become diploid as quickly as the WT cell line. A deletion in *DRF1* caused these cells to become became diploid faster than the WT cells. It is possible that accurate cell

division is not occurring in these cells. It is plausible that they are undergoing endo-reduplication (Lee et al., 2009). This is possible as CDC7 has a known role in endo-reduplication. Specifically, CDC7-DBF4 regulates CDT1 (Ballabeni et al., 2009), which is controlled by Geminin, a regulator of endo-reduplication (Melixetian et al., 2004). It is tempting to speculate that DBF4 plays a positive role in this process. Alternatively, errors during chromosome segregation or cytokinesis could be occurring.

This work confirmed that there is a mutation in the exonic region of *DBF4* which introduced a premature stop codon. As this premature stop codon is located upstream of the CDC7 binding domain, CDC7 cannot bind to DBF4 and therefore will not be activated by this regulatory subunit. Furthermore, DBF4 could not be detected at the protein level, suggesting that the protein has been eliminated. However, it is possible that DBF4 is expressed at a low level in this cell line and therefore cannot be detected. Exon skipping cannot be ruled out and this could result in potential functional effects. However, no consensus splice sites were noticed and no bands below the expected size for DBF4 were detected by immunoblotting suggesting that exon skipping has not occurred.

Although the DRF1 KO cell line contains a deletion in the exonic region of *DRF1*, which results in a frameshift and the introduction of a premature stop codon, it could not be confirmed whether DRF1 is eliminated at the protein level. This is because there are no sensitive and specific immunological reagents for DRF1. Attempts at testing multiple, commercially available antibodies of endogenous DRF1, proved futile. Investigation of the function of DRF1 will be limited until an antibody which can detect DRF1 becomes available.

In contrast to a previous report which indicates that *DBF4* is essential for growth in mouse ES cells (Yamashita et al., 2005), the ability to generate a cell line in which *DBF4* is eliminated, indicates that this gene is not essential, at least in the HAP1 cell line. It is possible that the difference observed between these results is because *DBF4* is essential in mice and perhaps it is not essential in humans or that *DRF1* could compensate for its loss in humans. To test this, a cell line in which both DBF4 and DRF1 are eliminated,

should be generated. Another possibility would be to deplete DRF1 in the DBF4 KO cell line. As it was inconclusive if DRF1 protein is eliminated in the DRF1 KO cell line, whether *DRF1* is essential remains unknown.

From analysis of the cell cycle, it appears that CDC7 kinase, activated by DBF4, is important for replication. Consistent with previous reports (Kumagai et al., 1999; Yamashita et al., 2005), this study reveals that DBF4 is required for accurate S-phase progression, specifically during late S-phase. In contrast to a previous report that indicates that depletion of DRF1 results in a defect in S-phase progression but that the effect is milder than the effect observed upon DBF4 depletion (Yoshizawa-Sugata et al., 2005), the work in this chapter did not reveal any role for DRF1 in S-phase progression. Although, the data in this section differs from the result of Yoshizawa-Sugata et al. 2005, both results agree in suggesting that DBF4 is the main CDC7 kinase regulator, during S-phase progression. DBF4 also appears to be required for phosphorylating MCM2 on Ser 40, consistent with the role of CDC7 kinase activity during replication and in the phosphorylation of the MCM2-7 helicase complex. Inhibition of CDC7 kinase, in the DBF4 KO cell line, did not completely block S-phase progression or MCM2 phosphorylation at Ser40. This suggests that there is another kinase, that also drives replication, or perhaps any residual kinase activity is enough to allow, a slow progression through S-phase.

This study, revealed a novel role of PLK1 in phosphorylating MCM2. These PLK1 dependent phosphorylation sites could be identified by mass spectrometry. Another hypothesis could be that PLK1 and DBF4 antagonise each other or that PLK1 and DBF4 compete for the same phosphorylation site on MCM2. This could be possible as Dbf4p has been shown to be a negative regulator of Cdc5p (Miller et al., 2009). PLK1 does not appear to be the kinase that drives replication in the absence of CDC7 kinase activity, consistent with a previous report that suggests that PLK1 can contribute to but is not required for replication (Song et al., 2011). On the contrary, several reports have suggested that PLK1 is involved in replication, in particular during replication stress

(Song et al., 2012). More work is required to investigate the function of PLK1 during replication and its cooperation with DBF4.

To examine whether DBF4 or DRF1 contributed to CDC7 kinase function during replication stress, CHK1 phosphorylation was examined. It was demonstrated that DBF4 could be potentially required for timely induction of the checkpoint, but not for its maintenance once establishment had occurred. This is consistent with published work demonstrating that CDC7 kinase activity is important for the induction of the checkpoint but not for robust checkpoint maintenance (Rainey et al., 2013).

Short term HU treatment hinted that DBF4 is required for an appropriate replication stress response. To extend the time frame of examining a DNA damage response, a clonogenic assay was performed, to examine whether the absence of DBF4 affected the ability of cells to form colonies following treatment with HU. However, no statistical significant difference was observed in the DBF4 KO cell line compared to the control.

Hypersensitivity of HAP1 cells to HU was observed in the clonogenic assay. This was not surprising as HU has been traditionally used as a chemotherapeutic agent for the treatment of CML for many years (Hehlmann et al., 1993). HAP1 cells are derived from KBM-7 cells which are a CML cell line (Andersson et al., 1987).

Another potential use of the cell lines containing a deletion in *DBF4* or *DRF1* would be to further assess the function of CDC7 kinase in mitosis, through examination of the contribution of DBF4 or DRF1. To examine the spindle localisation of DBF4 during mitosis and to verify if the protein that was detected using the monoclonal antibody for DBF4 (Figure 4.2) was DBF4. It is also important to examine which CDC7 regulatory subunit is required for recruitment of CDC7 to the centrosome and to address its role at the centrosome. Attempts have been made to identify the localisation of DBF4 in the HAP1 cell lines but they have been unsuccessful due to high levels of background staining. These cell lines also clump together making it difficult to analyse individual cells.

HAP1 cells are reported to have a fibroblast-like morphology. The DRF1 KO cell line revealed changes in cell morphology compared to the WT cell line. This could be specific to this clone due to off target effects of Cas9 in one clonal population and not another. To explore this possibility, other potential DRF1 KO clones should be examined. If this phenotype is reconfirmed, it could be speculated that DRF1 may play a role in proper formation of the cytoskeleton.

Cell lines containing gene mutations offer advantages over using siRNAs to target a protein of interest, as there is less associated off target effects. More importantly, a major advantage of this system is that a protein of interest is eliminated, whereas, it is only partially depleted when siRNAs are utilised. The depletion of a regulatory subunit, may be an inefficient strategy to study function because even if minimal protein levels remain, this may suffice to activate its binding partner.

In conclusion, it is likely that DBF4 is eliminated in the DBF4 KO cell line and that DBF4 plays a predominant role to regulate CDC7 kinase activity to allow efficient S-phase progression and phosphorylation of MCM2 to occur.

BIBLIOGRAPHY

Adams, J., Behnke, M., Chen, S., Cruickshank, A.A., Dick, L.R., Grenier, L., Klunder, J.M., Ma, Y.T., Plamondon, L., and Stein, R.L. (1998). Potent and selective inhibitors of the proteasome: dipeptidyl boronic acids. Bioorganic & medicinal chemistry letters *8*, 333-338.

Andersson, B.S., Beran, M., Pathak, S., Goodacre, A., Barlogie, B., and McCredie, K.B. (1987). Ph-positive chronic myeloid leukemia with near-haploid conversion in vivo and establishment of a continuously growing cell line with similar cytogenetic pattern. Cancer genetics and cytogenetics *24*, 335-343.

Ayares, D., Ganea, D., Chekuri, L., Campbell, C.R., and Kucherlapati, R. (1987). Repair of single-stranded DNA nicks, gaps, and loops in mammalian cells. Molecular and cellular biology *7*, 1656-1662.

Ballabeni, A., Zamponi, R., Caprara, G., Melixetian, M., Bossi, S., Masiero, L., and Helin, K. (2009). Human CDT1 associates with CDC7 and recruits CDC45 to chromatin during S phase. The Journal of biological chemistry *284*, 3028-3036.

Bastos, R.N., and Barr, F.A. (2010). Plk1 negatively regulates Cep55 recruitment to the midbody to ensure orderly abscission. The Journal of cell biology *191*, 751-760.

Bernardi, R., and Pandolfi, P.P. (2007). Structure, dynamics and functions of promyelocytic leukaemia nuclear bodies. Nature reviews Molecular cell biology *8*, 1006-1016.

Bharadwaj, R., and Yu, H. (2004). The spindle checkpoint, aneuploidy, and cancer. Oncogene *23*, 2016-2027.

Blow, J.J., and Dutta, A. (2005). Preventing re-replication of chromosomal DNA. Nature reviews Molecular cell biology *6*, 476-486.

Bonte, D., Lindvall, C., Liu, H., Dykema, K., Furge, K., and Weinreich, M. (2008). Cdc7-Dbf4 kinase overexpression in multiple cancers and tumor cell lines is correlated with p53 inactivation. Neoplasia *10*, 920-931.

Booher, R.N., Holman, P.S., and Fattaey, A. (1997). Human Myt1 is a cell cycle-regulated kinase that inhibits Cdc2 but not Cdk2 activity. The Journal of biological chemistry *272*, 22300-22306.

Boos, D., Sanchez-Pulido, L., Rappas, M., Pearl, L.H., Oliver, A.W., Ponting, C.P., and Diffley, J.F. (2011). Regulation of DNA replication through Sld3-Dpb11 interaction is conserved from yeast to humans. Current biology : CB *21*, 1152-1157.

Bradford, M.M. (1976). A rapid and sensitive method for the quantitation of microgram quantities of protein utilizing the principle of protein-dye binding. Analytical biochemistry *72*, 248-254.

Branzei, D., and Foiani, M. (2010). Maintaining genome stability at the replication fork. Nature reviews Molecular cell biology *11*, 208-219.

Brito, D.A., Yang, Z., and Rieder, C.L. (2008). Microtubules do not promote mitotic slippage when the spindle assembly checkpoint cannot be satisfied. The Journal of cell biology *182*, 623-629.

Bruinsma, W., Macurek, L., Freire, R., Lindqvist, A., and Medema, R.H. (2014). Bora and Aurora-A continue to activate Plk1 in mitosis. Journal of cell science *127*, 801-811.

Burkard, M.E., Randall, C.L., Larochelle, S., Zhang, C., Shokat, K.M., Fisher, R.P., and Jallepalli, P.V. (2007). Chemical genetics reveals the requirement for Polo-like kinase 1 activity in positioning RhoA and triggering cytokinesis in human cells. Proceedings of the National Academy of Sciences of the United States of America *104*, 4383-4388.

Byun, T.S., Pacek, M., Yee, M.C., Walter, J.C., and Cimprich, K.A. (2005). Functional uncoupling of MCM helicase and DNA polymerase activities activates the ATR-dependent checkpoint. Genes & development *19*, 1040-1052.

Cahill, D.P., Lengauer, C., Yu, J., Riggins, G.J., Willson, J.K., Markowitz, S.D., Kinzler, K.W., and Vogelstein, B. (1998). Mutations of mitotic checkpoint genes in human cancers. Nature *392*, 300-303.

Caldas, G.V., Lynch, T.R., Anderson, R., Afreen, S., Varma, D., and DeLuca, J.G. (2015). The RZZ complex requires the N-terminus of KNL1 to mediate optimal Mad1 kinetochore localization in human cells. Open biology *5*.

Carette, J.E., Raaben, M., Wong, A.C., Herbert, A.S., Obernosterer, G., Mulherkar, N., Kuehne, A.I., Kranzusch, P.J., Griffin, A.M., Ruthel, G., *et al.* (2011). Ebola virus entry requires the cholesterol transporter Niemann-Pick C1. Nature *477*, 340-343.

Carmena, M., and Earnshaw, W.C. (2003). The cellular geography of aurora kinases. Nature reviews Molecular cell biology *4*, 842-854.

Carmena, M., Pinson, X., Platani, M., Salloum, Z., Xu, Z., Clark, A., Macisaac, F., Ogawa, H., Eggert, U., Glover, D.M., *et al.* (2012a). The chromosomal passenger complex activates Polo kinase at centromeres. PLoS biology *10*, e1001250.

Carmena, M., Wheelock, M., Funabiki, H., and Earnshaw, W.C. (2012b). The chromosomal passenger complex (CPC): from easy rider to the godfather of mitosis. Nature reviews Molecular cell biology *13*, 789-803.

Chan, G.K., Liu, S.T., and Yen, T.J. (2005). Kinetochore structure and function. Trends in cell biology *15*, 589-598.

Charrier, J.D., Durrant, S.J., Golec, J.M., Kay, D.P., Knegtel, R.M., MacCormick, S., Mortimore, M., O'Donnell, M.E., Pinder, J.L., Reaper, P.M., *et al.* (2011). Discovery of potent and selective inhibitors of ataxia telangiectasia mutated and Rad3 related (ATR) protein kinase as potential anticancer agents. Journal of medicinal chemistry *54*, 2320-2330.

Cheeseman, I.M., Chappie, J.S., Wilson-Kubalek, E.M., and Desai, A. (2006). The conserved KMN network constitutes the core microtubule-binding site of the kinetochore. Cell *127*, 983-997.

Chen, Y.C., and Weinreich, M. (2010). Dbf4 regulates the Cdc5 Polo-like kinase through a distinct non-canonical binding interaction. The Journal of biological chemistry *285*, 41244-41254.

Chieffi, P., Cozzolino, L., Kisslinger, A., Libertini, S., Staibano, S., Mansueto, G., De Rosa, G., Villacci, A., Vitale, M., Linardopoulos, S., *et al.* (2006). Aurora B expression directly correlates with prostate cancer malignancy and influence prostate cell proliferation. The Prostate *66*, 326-333.

Chu, Y., Yao, P.Y., Wang, W., Wang, D., Wang, Z., Zhang, L., Huang, Y., Ke, Y., Ding, X., and Yao, X. (2011). Aurora B kinase activation requires survivin priming phosphorylation by PLK1. Journal of molecular cell biology *3*, 260-267.

Cimini, D. (2007). Detection and correction of merotelic kinetochore orientation by Aurora B and its partners. Cell Cycle *6*, 1558-1564.

Cimini, D., and Degrassi, F. (2005). Aneuploidy: a matter of bad connections. Trends in cell biology *15*, 442-451.

Colombo, R., Caldarelli, M., Mennecozzi, M., Giorgini, M.L., Sola, F., Cappella, P., Perrera, C., Depaolini, S.R., Rusconi, L., Cucchi, U., *et al.* (2010). Targeting the mitotic checkpoint for cancer therapy with NMS-P715, an inhibitor of MPS1 kinase. Cancer research *70*, 10255-10264.

Costanzo, V., Shechter, D., Lupardus, P.J., Cimprich, K.A., Gottesman, M., and Gautier, J. (2003). An ATR- and Cdc7-dependent DNA damage checkpoint that inhibits initiation of DNA replication. Molecular cell *11*, 203-213.

Cucchi, U., Gianellini, L.M., De Ponti, A., Sola, F., Alzani, R., Patton, V., Pezzoni, A., Troiani, S., Saccardo, M.B., Rizzi, S., *et al.* (2010). Phosphorylation of TCTP as a marker for polo-like kinase-1 activity in vivo. Anticancer research *30*, 4973-4985.

Curry, J., Angove, H., Fazal, L., Lyons, J., Reule, M., Thompson, N., and Wallis, N. (2009). Aurora B kinase inhibition in mitosis: strategies for optimising the use of aurora kinase inhibitors such as AT9283. Cell Cycle *8*, 1921-1929.

D'Angiolella, V., Palazzo, L., Santarpia, C., Costanzo, V., and Grieco, D. (2007). Role for non-proteolytic control of M-phase-promoting factor activity at M-phase exit. PloS one *2*, e247.

Dai, J., Sultan, S., Taylor, S.S., and Higgins, J.M. (2005). The kinase haspin is required for mitotic histone H3 Thr 3 phosphorylation and normal metaphase chromosome alignment. Genes & development *19*, 472-488.

Davis, F.M., Tsao, T.Y., Fowler, S.K., and Rao, P.N. (1983). Monoclonal antibodies to mitotic cells. Proceedings of the National Academy of Sciences of the United States of America *80*, 2926-2930.

Day, T.A., Palle, K., Barkley, L.R., Kakusho, N., Zou, Y., Tateishi, S., Verreault, A., Masai, H., and Vaziri, C. (2010). Phosphorylated Rad18 directs DNA polymerase eta to sites of stalled replication. The Journal of cell biology *191*, 953-966.

De Antoni, A., Maffini, S., Knapp, S., Musacchio, A., and Santaguida, S. (2012). A small-molecule inhibitor of Haspin alters the kinetochore functions of Aurora B. The Journal of cell biology *199*, 269-284.

De Brabander, M., Geuens, G., Nuydens, R., Willebrords, R., and De Mey, J. (1981). Taxol induces the assembly of free microtubules in living cells and blocks the organizing capacity of the centrosomes and kinetochores. Proceedings of the National Academy of Sciences of the United States of America *78*, 5608-5612.

De Brabander, M.J., Van de Veire, R.M., Aerts, F.E., Borgers, M., and Janssen, P.A. (1976). The effects of methyl (5-(2-thienylcarbonyl)-1H-benzimidazol-2-yl) carbamate, (R 17934; NSC 238159), a new synthetic antitumoral drug interfering with microtubules, on mammalian cells cultured in vitro. Cancer research *36*, 905-916.

de Carcer, G., Manning, G., and Malumbres, M. (2011). From Plk1 to Plk5: functional evolution of polo-like kinases. Cell Cycle *10*, 2255-2262.

De Souza, C.P., Hashmi, S.B., Osmani, A.H., and Osmani, S.A. (2014). Application of a new dual localization-affinity purification tag reveals novel aspects of protein kinase biology in Aspergillus nidulans. PloS one *9*, e90911.

DeLuca, J.G., Gall, W.E., Ciferri, C., Cimini, D., Musacchio, A., and Salmon, E.D. (2006). Kinetochore microtubule dynamics and attachment stability are regulated by Hec1. Cell *127*, 969-982.

Dewar, J.M., Budzowska, M., and Walter, J.C. (2015). The mechanism of DNA replication termination in vertebrates. Nature *525*, 345-350.

Ditchfield, C., Johnson, V.L., Tighe, A., Ellston, R., Haworth, C., Johnson, T., Mortlock, A., Keen, N., and Taylor, S.S. (2003). Aurora B couples chromosome alignment with anaphase by targeting BubR1, Mad2, and Cenp-E to kinetochores. The Journal of cell biology *161*, 267-280.

Doxsey, S.J., Stein, P., Evans, L., Calarco, P.D., and Kirschner, M. (1994). Pericentrin, a highly conserved centrosome protein involved in microtubule organization. Cell *76*, 639-650.

Duderstadt, K.E., Reyes-Lamothe, R., van Oijen, A.M., and Sherratt, D.J. (2014). Replication-fork dynamics. Cold Spring Harbor perspectives in biology *6*.

Emanuele, M.J., Lan, W., Jwa, M., Miller, S.A., Chan, C.S., and Stukenberg, P.T. (2008). Aurora B kinase and protein phosphatase 1 have opposing roles in modulating kinetochore assembly. The Journal of cell biology *181*, 241-254.

Eot-Houllier, G., Venoux, M., Vidal-Eychenie, S., Hoang, M.T., Giorgi, D., and Rouquier, S. (2010). Plk1 regulates both ASAP localization and its role in spindle pole integrity. The Journal of biological chemistry *285*, 29556-29568.

Espert, A., Uluocak, P., Bastos, R.N., Mangat, D., Graab, P., and Gruneberg, U. (2014). PP2A-B56 opposes Mps1 phosphorylation of Knl1 and thereby promotes spindle assembly checkpoint silencing. The Journal of cell biology *206*, 833-842.

Espeut, J., Lara-Gonzalez, P., Sassine, M., Shiau, A.K., Desai, A., and Abrieu, A. (2015). Natural Loss of Mps1 Kinase in Nematodes Uncovers a Role for Polo-like Kinase 1 in Spindle Checkpoint Initiation. Cell reports *12*, 58-65.

Fang, G. (2002). Checkpoint protein BubR1 acts synergistically with Mad2 to inhibit anaphase-promoting complex. Molecular biology of the cell *13*, 755-766.

Ferguson, R.L., Pascreau, G., and Maller, J.L. (2010). The cyclin A centrosomal localization sequence recruits MCM5 and Orc1 to regulate centrosome reduplication. Journal of cell science *123*, 2743-2749.

Ferreira, M.F., Santocanale, C., Drury, L.S., and Diffley, J.F. (2000). Dbf4p, an essential S phase-promoting factor, is targeted for degradation by the anaphase-promoting complex. Molecular and cellular biology *20*, 242-248.

Foley, E.A., Maldonado, M., and Kapoor, T.M. (2011). Formation of stable attachments between kinetochores and microtubules depends on the B56-PP2A phosphatase. Nature cell biology *13*, 1265-1271.

Fragkos, M., Ganier, O., Coulombe, P., and Mechali, M. (2015). DNA replication origin activation in space and time. Nature reviews Molecular cell biology *16*, 360-374.

Francisco, L., Wang, W., and Chan, C.S. (1994). Type 1 protein phosphatase acts in opposition to IpL1 protein kinase in regulating yeast chromosome segregation. Molecular and cellular biology *14*, 4731-4740.

Gadea, B.B., and Ruderman, J.V. (2005). Aurora kinase inhibitor ZM447439 blocks chromosome-induced spindle assembly, the completion of chromosome condensation, and the establishment of the spindle integrity checkpoint in Xenopus egg extracts. Molecular biology of the cell *16*, 1305-1318.

Garg, P., and Burgers, P.M. (2005). How the cell deals with DNA nicks. Cell Cycle *4*, 221-224.

Gargiulo, D., Kumar, G.S., Musser, S.S., and Tomasz, M. (1995). Structural and function modification of DNA by mitomycin C. Mechanism of the DNA sequence specificity of mitomycins. Nucleic acids symposium series, 169-170.

Gascoigne, K.E., and Taylor, S.S. (2008). Cancer cells display profound intra- and interline variation following prolonged exposure to antimitotic drugs. Cancer cell *14*, 111-122.

Ghenoiu, C., Wheelock, M.S., and Funabiki, H. (2013). Autoinhibition and Polo-dependent multisite phosphorylation restrict activity of the histone H3 kinase Haspin to mitosis. Molecular cell *52*, 734-745.

Giam, M., and Rancati, G. (2015). Aneuploidy and chromosomal instability in cancer: a jackpot to chaos. Cell division *10*, 3.

Glotzer, M. (2001). Animal cell cytokinesis. Annual review of cell and developmental biology *17*, 351-386.

Glotzer, M., Murray, A.W., and Kirschner, M.W. (1991). Cyclin is degraded by the ubiquitin pathway. Nature *349*, 132-138.

Gonzalez Besteiro, M.A., and Gottifredi, V. (2015). The fork and the kinase: a DNA replication tale from a CHK1 perspective. Mutation research Reviews in mutation research *763*, 168-180.

Gonzalez, R.E., Lim, C.U., Cole, K., Bianchini, C.H., Schools, G.P., Davis, B.E., Wada, I., Roninson, I.B., and Broude, E.V. (2011). Effects of conditional depletion of topoisomerase II on cell cycle progression in mammalian cells. Cell Cycle *10*, 3505-3514.

Gregan, J., Polakova, S., Zhang, L., Tolic-Norrelykke, I.M., and Cimini, D. (2011). Merotelic kinetochore attachment: causes and effects. Trends in cell biology *21*, 374-381.
Guan, R., Tapang, P., Leverson, J.D., Albert, D., Giranda, V.L., and Luo, Y. (2005). Small interfering RNA-mediated Polo-like kinase 1 depletion preferentially reduces the survival of p53-defective, oncogenic transformed cells and inhibits tumor growth in animals. Cancer research *65*, 2698-2704.

Hanahan, D., and Weinberg, R.A. (2000). The hallmarks of cancer. Cell *100*, 57-70.
Hanahan, D., and Weinberg, R.A. (2011). Hallmarks of cancer: the next generation. Cell *144*, 646-674.

Hansen, D.V., Loktev, A.V., Ban, K.H., and Jackson, P.K. (2004). Plk1 regulates activation of the anaphase promoting complex by phosphorylating and triggering SCFbetaTrCP-dependent destruction of the APC Inhibitor Emi1. Molecular biology of the cell *15*, 5623-5634.

Hardy, C.F., Dryga, O., Seematter, S., Pahl, P.M., and Sclafani, R.A. (1997). mcm5/cdc46-bob1 bypasses the requirement for the S phase activator Cdc7p. Proceedings of the National Academy of Sciences of the United States of America *94*, 3151-3155.

Hartwell, L.H. (1973). Three additional genes required for deoxyribonucleic acid synthesis in Saccharomyces cerevisiae. Journal of bacteriology *115*, 966-974.

Hauf, S., Cole, R.W., LaTerra, S., Zimmer, C., Schnapp, G., Walter, R., Heckel, A., van Meel, J., Rieder, C.L., and Peters, J.M. (2003). The small molecule Hesperadin reveals a role for Aurora B in correcting kinetochore-microtubule attachment and in maintaining the spindle assembly checkpoint. The Journal of cell biology *161*, 281-294.

Hegarat, N., Rata, S., and Hochegger, H. (2016). Bistability of mitotic entry and exit switches during open mitosis in mammalian cells. BioEssays : news and reviews in molecular, cellular and developmental biology *38*, 627-643.

Hehlmann, R., Heimpel, H., Hasford, J., Kolb, H.J., Pralle, H., Hossfeld, D.K., Queisser, W., Loffler, H., Heinze, B., Georgii, A., *et al.* (1993). Randomized comparison of busulfan and hydroxyurea in chronic myelogenous leukemia: prolongation of survival by hydroxyurea. The German CML Study Group. Blood *82*, 398-407.

Helleday, T., Eshtad, S., and Nik-Zainal, S. (2014). Mechanisms underlying mutational signatures in human cancers. Nature reviews Genetics *15*, 585-598.

Helmke, C., Becker, S., and Strebhardt, K. (2016). The role of Plk3 in oncogenesis. Oncogene *35*, 135-147.

Hendrickx, A., Beullens, M., Ceulemans, H., Den Abt, T., Van Eynde, A., Nicolaescu, E., Lesage, B., and Bollen, M. (2009). Docking motif-guided mapping of the interactome of protein phosphatase-1. Chemistry & biology *16*, 365-371.

Hickson, I., Zhao, Y., Richardson, C.J., Green, S.J., Martin, N.M., Orr, A.I., Reaper, P.M., Jackson, S.P., Curtin, N.J., and Smith, G.C. (2004). Identification and characterization of a novel and specific inhibitor of the ataxia-telangiectasia mutated kinase ATM. Cancer research *64*, 9152-9159.

Hirota, T., Lipp, J.J., Toh, B.H., and Peters, J.M. (2005). Histone H3 serine 10 phosphorylation by Aurora B causes HP1 dissociation from heterochromatin. Nature *438*, 1176-1180.

Hiruma, Y., Sacristan, C., Pachis, S.T., Adamopoulos, A., Kuijt, T., Ubbink, M., von Castelmur, E., Perrakis, A., and Kops, G.J. (2015). CELL DIVISION CYCLE. Competition between MPS1 and microtubules at kinetochores regulates spindle checkpoint signaling. Science *348*, 1264-1267.

Hoeijmakers, J.H. (2009). DNA damage, aging, and cancer. The New England journal of medicine *361*, 1475-1485.

Howell, B.J., McEwen, B.F., Canman, J.C., Hoffman, D.B., Farrar, E.M., Rieder, C.L., and Salmon, E.D. (2001). Cytoplasmic dynein/dynactin drives kinetochore protein transport to the spindle poles and has a role in mitotic spindle checkpoint inactivation. The Journal of cell biology *155*, 1159-1172.

Hsiang, Y.H., Hertzberg, R., Hecht, S., and Liu, L.F. (1985). Camptothecin induces protein-linked DNA breaks via mammalian DNA topoisomerase I. The Journal of biological chemistry *260*, 14873-14878.

Huberman, J.A. (1981). New views of the biochemistry of eucaryotic DNA replication revealed by aphidicolin, an unusual inhibitor of DNA polymerase alpha. Cell *23*, 647-648.

Huggett, M.T., Tudzarova, S., Proctor, I., Loddo, M., Keane, M.G., Stoeber, K., Williams, G.H., and Pereira, S.P. (2016). Cdc7 is a potent anti-cancer target in pancreatic cancer due to abrogation of the DNA origin activation checkpoint. Oncotarget *7*, 18495-18507.

Hughes, S., Elustondo, F., Di Fonzo, A., Leroux, F.G., Wong, A.C., Snijders, A.P., Matthews, S.J., and Cherepanov, P. (2012). Crystal structure of human CDC7 kinase in complex with its activator DBF4. Nature structural & molecular biology *19*, 1101-1107.

Ikegami, S., Taguchi, T., Ohashi, M., Oguro, M., Nagano, H., and Mano, Y. (1978). Aphidicolin prevents mitotic cell division by interfering with the activity of DNA polymerase-alpha. Nature *275*, 458-460.

Ito, S., Ishii, A., Kakusho, N., Taniyama, C., Yamazaki, S., Fukatsu, R., Sakaue-Sawano, A., Miyawaki, A., and Masai, H. (2012). Mechanism of cancer cell death induced by depletion of an essential replication regulator. PloS one *7*, e36372.

Jackson, A.L., Pahl, P.M., Harrison, K., Rosamond, J., and Sclafani, R.A. (1993). Cell cycle regulation of the yeast Cdc7 protein kinase by association with the Dbf4 protein. Molecular and cellular biology *13*, 2899-2908.

Jelluma, N., Brenkman, A.B., van den Broek, N.J., Cruijsen, C.W., van Osch, M.H., Lens, S.M., Medema, R.H., and Kops, G.J. (2008). Mps1 phosphorylates Borealin to control Aurora B activity and chromosome alignment. Cell *132*, 233-246.

Jelluma, N., Dansen, T.B., Sliedrecht, T., Kwiatkowski, N.P., and Kops, G.J. (2010). Release of Mps1 from kinetochores is crucial for timely anaphase onset. The Journal of cell biology *191*, 281-290.

Jemaa, M., Galluzzi, L., Kepp, O., Senovilla, L., Brands, M., Boemer, U., Koppitz, M., Lienau, P., Prechtl, S., Schulze, V., *et al.* (2013). Characterization of novel MPS1 inhibitors with preclinical anticancer activity. Cell death and differentiation *20*, 1532-1545.

Jia, L., Kim, S., and Yu, H. (2013). Tracking spindle checkpoint signals from kinetochores to APC/C. Trends in biochemical sciences *38*, 302-311.

Jiang, W., and Hunter, T. (1997). Identification and characterization of a human protein kinase related to budding yeast Cdc7p. Proceedings of the National Academy of Sciences of the United States of America *94*, 14320-14325.

Jiang, W., McDonald, D., Hope, T.J., and Hunter, T. (1999). Mammalian Cdc7-Dbf4 protein kinase complex is essential for initiation of DNA replication. The EMBO journal *18*, 5703-5713.

Johnson, V.L., Scott, M.I., Holt, S.V., Hussein, D., and Taylor, S.S. (2004). Bub1 is required for kinetochore localization of BubR1, Cenp-E, Cenp-F and Mad2, and chromosome congression. Journal of cell science *117*, 1577-1589.

Johnston, L.H., and Thomas, A.P. (1982). A further two mutants defective in initiation of the S phase in the yeast Saccharomyces cerevisiae. Molecular & general genetics : MGG *186*, 445-448.

Kang, Y.H., Park, J.E., Yu, L.R., Soung, N.K., Yun, S.M., Bang, J.K., Seong, Y.S., Yu, H., Garfield, S., Veenstra, T.D., *et al.* (2006). Self-regulated Plk1 recruitment to kinetochores by the Plk1-PBIP1 interaction is critical for proper chromosome segregation. Molecular cell *24*, 409-422.

Kasuboski, J.M., Bader, J.R., Vaughan, P.S., Tauhata, S.B., Winding, M., Morrissey, M.A., Joyce, M.V., Boggess, W., Vos, L., Chan, G.K., *et al.* (2011). Zwint-1 is a novel Aurora B substrate required for the assembly of a dynein-binding platform on kinetochores. Molecular biology of the cell *22*, 3318-3330.

Kawashima, S.A., Yamagishi, Y., Honda, T., Ishiguro, K., and Watanabe, Y. (2010). Phosphorylation of H2A by Bub1 prevents chromosomal instability through localizing shugoshin. Science *327*, 172-177.

Kim, J.M., Kakusho, N., Yamada, M., Kanoh, Y., Takemoto, N., and Masai, H. (2008). Cdc7 kinase mediates Claspin phosphorylation in DNA replication checkpoint. Oncogene *27*, 3475-3482.

Knockleby, J., and Lee, H. (2010). Same partners, different dance: involvement of DNA replication proteins in centrosome regulation. Cell Cycle *9*, 4487-4491.

Kollareddy, M., Zheleva, D., Dzubak, P., Brahmkshatriya, P.S., Lepsik, M., and Hajduch, M. (2012). Aurora kinase inhibitors: progress towards the clinic. Investigational new drugs *30*, 2411-2432.

Koltun, E.S., Tsuhako, A.L., Brown, D.S., Aay, N., Arcalas, A., Chan, V., Du, H., Engst, S., Ferguson, K., Franzini, M., *et al.* (2012). Discovery of XL413, a potent and selective CDC7 inhibitor. Bioorganic & medicinal chemistry letters *22*, 3727-3731.

Krenn, V., Overlack, K., Primorac, I., van Gerwen, S., and Musacchio, A. (2014). KI motifs of human Knl1 enhance assembly of comprehensive spindle checkpoint complexes around MELT repeats. Current biology : CB *24*, 29-39.

Kulkarni, A.A., Kingsbury, S.R., Tudzarova, S., Hong, H.K., Loddo, M., Rashid, M., Rodriguez-Acebes, S., Prevost, A.T., Ledermann, J.A., Stoeber, K., *et al.* (2009). Cdc7 kinase is a predictor of survival and a novel therapeutic target in epithelial ovarian carcinoma. Clin Cancer Res *15*, 2417-2425.

Kumagai, H., Sato, N., Yamada, M., Mahony, D., Seghezzi, W., Lees, E., Arai, K., and Masai, H. (1999). A novel growth- and cell cycle-regulated protein, ASK, activates human Cdc7-related kinase and is essential for G1/S transition in mammalian cells. Molecular and cellular biology *19*, 5083-5095.

Kurai, M., Shiozawa, T., Shih, H.C., Miyamoto, T., Feng, Y.Z., Kashima, H., Suzuki, A., and Konishi, I. (2005). Expression of Aurora kinases A and B in normal, hyperplastic, and malignant human endometrium: Aurora B as a predictor for poor prognosis in endometrial carcinoma. Human pathology *36*, 1281-1288.

Labib, K. (2010). How do Cdc7 and cyclin-dependent kinases trigger the initiation of chromosome replication in eukaryotic cells? Genes & development *24*, 1208-1219.

Laemmli, U.K. (1970). Cleavage of structural proteins during the assembly of the head of bacteriophage T4. Nature *227*, 680-685.

Lan, W., Zhang, X., Kline-Smith, S.L., Rosasco, S.E., Barrett-Wilt, G.A., Shabanowitz, J., Hunt, D.F., Walczak, C.E., and Stukenberg, P.T. (2004). Aurora B phosphorylates centromeric MCAK and regulates its localization and microtubule depolymerization activity. Current biology : CB *14*, 273-286.

Lansing, T.J., McConnell, R.T., Duckett, D.R., Spehar, G.M., Knick, V.B., Hassler, D.F., Noro, N., Furuta, M., Emmitte, K.A., Gilmer, T.M., *et al.* (2007). In vitro biological activity of a novel small-molecule inhibitor of polo-like kinase 1. Molecular cancer therapeutics *6*, 450-459.

Lara-Gonzalez, P., Westhorpe, F.G., and Taylor, S.S. (2012). The spindle assembly checkpoint. Current biology : CB *22*, R966-980.

Lee, A.Y., Chiba, T., Truong, L.N., Cheng, A.N., Do, J., Cho, M.J., Chen, L., and Wu, X. (2012). Dbf4 is direct downstream target of ataxia telangiectasia mutated (ATM) and ataxia telangiectasia and Rad3-related (ATR) protein to regulate intra-S-phase checkpoint. The Journal of biological chemistry *287*, 2531-2543.

Lee, H.O., Davidson, J.M., and Duronio, R.J. (2009). Endoreplication: polyploidy with purpose. Genes & development *23*, 2461-2477.

Lei, M., Kawasaki, Y., Young, M.R., Kihara, M., Sugino, A., and Tye, B.K. (1997). Mcm2 is a target of regulation by Cdc7-Dbf4 during the initiation of DNA synthesis. Genes & development *11*, 3365-3374.

Li, H., and Stillman, B. (2012). The origin recognition complex: a biochemical and structural view. Sub-cellular biochemistry *62*, 37-58.

Li, J., Hong, M.J., Chow, J.P., Man, W.Y., Mak, J.P., Ma, H.T., and Poon, R.Y. (2015). Co-inhibition of polo-like kinase 1 and Aurora kinases promotes mitotic catastrophe. Oncotarget *6*, 9327-9340.

Lindon, C., and Pines, J. (2004). Ordered proteolysis in anaphase inactivates Plk1 to contribute to proper mitotic exit in human cells. The Journal of cell biology *164*, 233-241.

Lindqvist, A., Rodriguez-Bravo, V., and Medema, R.H. (2009). The decision to enter mitosis: feedback and redundancy in the mitotic entry network. The Journal of cell biology *185*, 193-202.

Ling, Y., Zhang, X., Bai, Y., Li, P., Wei, C., Song, T., Zheng, Z., Guan, K., Zhang, Y., Zhang, B., *et al.* (2014). Overexpression of Mps1 in colon cancer cells attenuates the spindle assembly checkpoint and increases aneuploidy. Biochemical and biophysical research communications *450*, 1690-1695.

Liu, D., Davydenko, O., and Lampson, M.A. (2012). Polo-like kinase-1 regulates kinetochore-microtubule dynamics and spindle checkpoint silencing. The Journal of cell biology *198*, 491-499.

Liu, D., Vleugel, M., Backer, C.B., Hori, T., Fukagawa, T., Cheeseman, I.M., and Lampson, M.A. (2010). Regulated targeting of protein phosphatase 1 to the outer kinetochore by KNL1 opposes Aurora B kinase. The Journal of cell biology *188*, 809-820.

Liu, Q., Guntuku, S., Cui, X.S., Matsuoka, S., Cortez, D., Tamai, K., Luo, G., Carattini-Rivera, S., DeMayo, F., Bradley, A., *et al.* (2000). Chk1 is an essential kinase that is regulated by Atr and required for the G(2)/M DNA damage checkpoint. Genes & development *14*, 1448-1459.

Loehrer, P.J., and Einhorn, L.H. (1984). Drugs five years later. Cisplatin. Annals of internal medicine *100*, 704-713.

London, N., and Biggins, S. (2014). Mad1 kinetochore recruitment by Mps1-mediated phosphorylation of Bub1 signals the spindle checkpoint. Genes & development *28*, 140-152.

Longley, D.B., and Johnston, P.G. (2005). Molecular mechanisms of drug resistance. The Journal of pathology *205*, 275-292.

Lopes, C.S., and Sunkel, C.E. (2003). The spindle checkpoint: from normal cell division to tumorigenesis. Archives of medical research *34*, 155-165.

Lu, F., Lan, R., Zhang, H., Jiang, Q., and Zhang, C. (2009). Geminin is partially localized to the centrosome and plays a role in proper centrosome duplication. Biology of the cell / under the auspices of the European Cell Biology Organization *101*, 273-285.

Luo, X., Tang, Z., Rizo, J., and Yu, H. (2002). The Mad2 spindle checkpoint protein undergoes similar major conformational changes upon binding to either Mad1 or Cdc20. Molecular cell *9*, 59-71.

Maldonado, M., and Kapoor, T.M. (2011). Constitutive Mad1 targeting to kinetochores uncouples checkpoint signalling from chromosome biorientation. Nature cell biology *13*, 475-482.

Malumbres, M., and Barbacid, M. (2005). Mammalian cyclin-dependent kinases. Trends in biochemical sciences *30*, 630-641.

Marechal, A., and Zou, L. (2013). DNA damage sensing by the ATM and ATR kinases. Cold Spring Harbor perspectives in biology *5*.

Maric, M., Maculins, T., De Piccoli, G., and Labib, K. (2014). Cdc48 and a ubiquitin ligase drive disassembly of the CMG helicase at the end of DNA replication. Science *346*, 1253596.

Masai, H., Taniyama, C., Ogino, K., Matsui, E., Kakusho, N., Matsumoto, S., Kim, J.M., Ishii, A., Tanaka, T., Kobayashi, T., *et al.* (2006). Phosphorylation of MCM4 by Cdc7 kinase facilitates its interaction with Cdc45 on the chromatin. The Journal of biological chemistry *281*, 39249-39261.

McGarry, E., Gaboriau, D., Rainey, M.D., Restuccia, U., Bachi, A., and Santocanale, C. (2016). The Deubiquitinase USP9X Maintains DNA Replication Fork Stability and DNA Damage Checkpoint Responses by Regulating CLASPIN during S-Phase. Cancer research *76*, 2384-2393.

Mechali, M. (2010). Eukaryotic DNA replication origins: many choices for appropriate answers. Nature reviews Molecular cell biology *11*, 728-738.

Melixetian, M., Ballabeni, A., Masiero, L., Gasparini, P., Zamponi, R., Bartek, J., Lukas, J., and Helin, K. (2004). Loss of Geminin induces rereplication in the presence of functional p53. The Journal of cell biology *165*, 473-482.

Mendez, J., and Stillman, B. (2000). Chromatin association of human origin recognition complex, cdc6, and minichromosome maintenance proteins during the cell cycle: assembly of prereplication complexes in late mitosis. Molecular and cellular biology *20*, 8602-8612.

Meppelink, A., Kabeche, L., Vromans, M.J., Compton, D.A., and Lens, S.M. (2015). Shugoshin-1 balances Aurora B kinase activity via PP2A to promote chromosome bi-orientation. Cell reports *11*, 508-515.

Miller, C.T., Gabrielse, C., Chen, Y.C., and Weinreich, M. (2009). Cdc7p-Dbf4p regulates mitotic exit by inhibiting Polo kinase. PLoS genetics *5*, e1000498.

Montagnoli, A., Bosotti, R., Villa, F., Rialland, M., Brotherton, D., Mercurio, C., Berthelsen, J., and Santocanale, C. (2002). Drf1, a novel regulatory subunit for human Cdc7 kinase. The EMBO journal *21*, 3171-3181.

Montagnoli, A., Tenca, P., Sola, F., Carpani, D., Brotherton, D., Albanese, C., and Santocanale, C. (2004). Cdc7 inhibition reveals a p53-dependent replication checkpoint that is defective in cancer cells. Cancer research *64*, 7110-7116.

Montagnoli, A., Valsasina, B., Brotherton, D., Troiani, S., Rainoldi, S., Tenca, P., Molinari, A., and Santocanale, C. (2006). Identification of Mcm2 phosphorylation sites by S-phase-regulating kinases. The Journal of biological chemistry *281*, 10281-10290.

Montagnoli, A., Valsasina, B., Croci, V., Menichincheri, M., Rainoldi, S., Marchesi, V., Tibolla, M., Tenca, P., Brotherton, D., Albanese, C., *et al.* (2008). A Cdc7 kinase inhibitor restricts initiation of DNA replication and has antitumor activity. Nature chemical biology *4*, 357-365.

Mross, K., Frost, A., Steinbild, S., Hedbom, S., Rentschler, J., Kaiser, R., Rouyrre, N., Trommeshauser, D., Hoesl, C.E., and Munzert, G. (2008). Phase I dose escalation and pharmacokinetic study of BI 2536, a novel Polo-like kinase 1 inhibitor, in patients with advanced solid tumors. Journal of clinical oncology : official journal of the American Society of Clinical Oncology *26*, 5511-5517.

Musacchio, A. (2011). Spindle assembly checkpoint: the third decade. Philosophical transactions of the Royal Society of London Series B, Biological sciences *366*, 3595-3604.

Musacchio, A. (2015). The Molecular Biology of Spindle Assembly Checkpoint Signaling Dynamics. Current biology : CB *25*, R1002-1018.

Musacchio, A., and Salmon, E.D. (2007). The spindle-assembly checkpoint in space and time. Nature reviews Molecular cell biology *8*, 379-393.

Nakajima, H., Toyoshima-Morimoto, F., Taniguchi, E., and Nishida, E. (2003). Identification of a consensus motif for Plk (Polo-like kinase) phosphorylation reveals Myt1 as a Plk1 substrate. The Journal of biological chemistry *278*, 25277-25280.

Natoni, A., Coyne, M.R., Jacobsen, A., Rainey, M.D., O'Brien, G., Healy, S., Montagnoli, A., Moll, J., O'Dwyer, M., and Santocanale, C. (2013). Characterization of a Dual CDC7/CDK9 Inhibitor in Multiple Myeloma Cellular Models. Cancers *5*, 901-918.

Natsume, T., Muller, C.A., Katou, Y., Retkute, R., Gierlinski, M., Araki, H., Blow, J.J., Shirahige, K., Nieduszynski, C.A., and Tanaka, T.U. (2013). Kinetochores coordinate pericentromeric cohesion and early DNA replication by Cdc7-Dbf4 kinase recruitment. Molecular cell *50*, 661-674.

Neef, R., Preisinger, C., Sutcliffe, J., Kopajtich, R., Nigg, E.A., Mayer, T.U., and Barr, F.A. (2003). Phosphorylation of mitotic kinesin-like protein 2 by polo-like kinase 1 is required for cytokinesis. The Journal of cell biology *162*, 863-875.

Nigg, E.A. (2001). Mitotic kinases as regulators of cell division and its checkpoints. Nature reviews Molecular cell biology *2*, 21-32.

Nijenhuis, W., Vallardi, G., Teixeira, A., Kops, G.J., and Saurin, A.T. (2014). Negative feedback at kinetochores underlies a responsive spindle checkpoint signal. Nature cell biology *16*, 1257-1264.

Nishitani, H., Taraviras, S., Lygerou, Z., and Nishimoto, T. (2001). The human licensing factor for DNA replication Cdt1 accumulates in G1 and is destabilized after initiation of S-phase. The Journal of biological chemistry *276*, 44905-44911.

Nitiss, J.L. (2009). Targeting DNA topoisomerase II in cancer chemotherapy. Nature reviews Cancer *9*, 338-350.

Nomoto, S., Haruki, N., Takahashi, T., Masuda, A., Koshikawa, T., Fujii, Y., and Osada, H. (1999). Search for in vivo somatic mutations in the mitotic checkpoint gene, hMAD1, in human lung cancers. Oncogene *18*, 7180-7183.

Nurse, P. (2000). A long twentieth century of the cell cycle and beyond. Cell *100*, 71-78.

O'Connor, A., Maffini, S., Rainey, M.D., Kaczmarczyk, A., Gaboriau, D., Musacchio, A., and Santocanale, C. (2015). Requirement for PLK1 kinase activity in the maintenance of a robust spindle assembly checkpoint. Biology open *5*, 11-19.

Ogino, K., Takeda, T., Matsui, E., Iiyama, H., Taniyama, C., Arai, K., and Masai, H. (2001). Bipartite binding of a kinase activator activates Cdc7-related kinase essential for S phase. The Journal of biological chemistry *276*, 31376-31387.

Ohshima, K., Haraoka, S., Yoshioka, S., Hamasaki, M., Fujiki, T., Suzumiya, J., Kawasaki, C., Kanda, M., and Kikuchi, M. (2000). Mutation analysis of mitotic checkpoint genes (hBUB1 and hBUBR1) and microsatellite instability in adult T-cell leukemia/lymphoma. Cancer letters *158*, 141-150.

Overlack, K., Primorac, I., Vleugel, M., Krenn, V., Maffini, S., Hoffmann, I., Kops, G.J., and Musacchio, A. (2015). A molecular basis for the differential roles of Bub1 and BubR1 in the spindle assembly checkpoint. eLife *4*, e05269.

Parker, L.L., and Piwnica-Worms, H. (1992). Inactivation of the p34cdc2-cyclin B complex by the human WEE1 tyrosine kinase. Science *257*, 1955-1957.

Perez de Castro, I., de Carcer, G., Montoya, G., and Malumbres, M. (2008). Emerging cancer therapeutic opportunities by inhibiting mitotic kinases. Current opinion in pharmacology *8*, 375-383.

Pines, J., and Hunter, T. (1991). Human cyclins A and B1 are differentially located in the cell and undergo cell cycle-dependent nuclear transport. The Journal of cell biology *115*, 1-17.

Polo, S.E., and Jackson, S.P. (2011). Dynamics of DNA damage response proteins at DNA breaks: a focus on protein modifications. Genes & development *25*, 409-433.

Potenski, C.J., and Klein, H.L. (2014). How the misincorporation of ribonucleotides into genomic DNA can be both harmful and helpful to cells. Nucleic acids research *42*, 10226-10234.

Prakash, S., Johnson, R.E., and Prakash, L. (2005). Eukaryotic translesion synthesis DNA polymerases: specificity of structure and function. Annual review of biochemistry *74*, 317-353.

Prasanth, S.G., Prasanth, K.V., Siddiqui, K., Spector, D.L., and Stillman, B. (2004). Human Orc2 localizes to centrosomes, centromeres and heterochromatin during chromosome inheritance. The EMBO journal *23*, 2651-2663.

Pursell, Z.F., Isoz, I., Lundstrom, E.B., Johansson, E., and Kunkel, T.A. (2007). Yeast DNA polymerase epsilon participates in leading-strand DNA replication. Science *317*, 127-130.

Raab, M., Kramer, A., Hehlgans, S., Sanhaji, M., Kurunci-Csacsko, E., Dotsch, C., Bug, G., Ottmann, O., Becker, S., Pachl, F., *et al.* (2015). Mitotic arrest and slippage induced by pharmacological inhibition of Polo-like kinase 1. Molecular oncology *9*, 140-154.

Rainey, M.D., Harhen, B., Wang, G.N., Murphy, P.V., and Santocanale, C. (2013). Cdc7-dependent and -independent phosphorylation of Claspin in the induction of the DNA replication checkpoint. Cell Cycle *12*, 1560-1568.

Ramer, M.D., Suman, E.S., Richter, H., Stanger, K., Spranger, M., Bieberstein, N., and Duncker, B.P. (2013). Dbf4 and Cdc7 proteins promote DNA replication through interactions with distinct Mcm2-7 protein subunits. The Journal of biological chemistry *288*, 14926-14935.

Rodriguez-Acebes, S., Proctor, I., Loddo, M., Wollenschlaeger, A., Rashid, M., Falzon, M., Prevost, A.T., Sainsbury, R., Stoeber, K., and Williams, G.H. (2010). Targeting DNA replication before it starts: Cdc7 as a therapeutic target in p53-mutant breast cancers. The American journal of pathology *177*, 2034-2045.

Ru, H.Y., Chen, R.L., Lu, W.C., and Chen, J.H. (2002). hBUB1 defects in leukemia and lymphoma cells. Oncogene *21*, 4673-4679.

Rudolph, D., Steegmaier, M., Hoffmann, M., Grauert, M., Baum, A., Quant, J., Haslinger, C., Garin-Chesa, P., and Adolf, G.R. (2009). BI 6727, a Polo-like kinase inhibitor with improved pharmacokinetic profile and broad antitumor activity. Clin Cancer Res *15*, 3094-3102.

Sakaue-Sawano, A., Kurokawa, H., Morimura, T., Hanyu, A., Hama, H., Osawa, H., Kashiwagi, S., Fukami, K., Miyata, T., Miyoshi, H., *et al.* (2008). Visualizing spatiotemporal dynamics of multicellular cell-cycle progression. Cell *132*, 487-498.

Santaguida, S., Tighe, A., D'Alise, A.M., Taylor, S.S., and Musacchio, A. (2010). Dissecting the role of MPS1 in chromosome biorientation and the spindle checkpoint through the small molecule inhibitor reversine. The Journal of cell biology *190*, 73-87.

Santaguida, S., Vernieri, C., Villa, F., Ciliberto, A., and Musacchio, A. (2011). Evidence that Aurora B is implicated in spindle checkpoint signalling independently of error correction. The EMBO journal *30*, 1508-1519.

Santamaria, D., Viguera, E., Martinez-Robles, M.L., Hyrien, O., Hernandez, P., Krimer, D.B., and Schvartzman, J.B. (2000). Bi-directional replication and random termination. Nucleic acids research *28*, 2099-2107.

Sato, N., Sato, M., Nakayama, M., Saitoh, R., Arai, K., and Masai, H. (2003). Cell cycle regulation of chromatin binding and nuclear localization of human Cdc7-ASK kinase complex. Genes to cells : devoted to molecular & cellular mechanisms *8*, 451-463.

Saurin, A.T., van der Waal, M.S., Medema, R.H., Lens, S.M., and Kops, G.J. (2011). Aurora B potentiates Mps1 activation to ensure rapid checkpoint establishment at the onset of mitosis. Nat Commun *2*, 316.

Scaerou, F., Starr, D.A., Piano, F., Papoulas, O., Karess, R.E., and Goldberg, M.L. (2001). The ZW10 and Rough Deal checkpoint proteins function together in a large, evolutionarily conserved complex targeted to the kinetochore. Journal of cell science *114*, 3103-3114.

Schoffski, P. (2009). Polo-like kinase (PLK) inhibitors in preclinical and early clinical development in oncology. The oncologist *14*, 559-570.

Sclafani, R.A., and Holzen, T.M. (2007). Cell cycle regulation of DNA replication. Annual review of genetics *41*, 237-280.

Seki, A., Coppinger, J.A., Jang, C.Y., Yates, J.R., and Fang, G. (2008). Bora and the kinase Aurora a cooperatively activate the kinase Plk1 and control mitotic entry. Science *320*, 1655-1658.

Shen, Z. (2011). Genomic instability and cancer: an introduction. Journal of molecular cell biology *3*, 1-3.

Sheu, Y.J., and Stillman, B. (2010). The Dbf4-Cdc7 kinase promotes S phase by alleviating an inhibitory activity in Mcm4. Nature *463*, 113-117.

Silva, T., Bradley, R.H., Gao, Y., and Coue, M. (2006). Xenopus CDC7/DRF1 complex is required for the initiation of DNA replication. The Journal of biological chemistry *281*, 11569-11576.

Sironi, L., Mapelli, M., Knapp, S., De Antoni, A., Jeang, K.T., and Musacchio, A. (2002). Crystal structure of the tetrameric Mad1-Mad2 core complex: implications of a 'safety belt' binding mechanism for the spindle checkpoint. The EMBO journal *21*, 2496-2506.

Skoog, L., and Bjursell, G. (1974). Nuclear and cytoplasmic pools of deoxyribonucleoside triphosphates in Chinese hamster ovary cells. The Journal of biological chemistry *249*, 6434-6438.

Skoog, L., and Nordenskjold, B. (1971). Effects of hydroxyurea and 1-beta-D-arabinofuranosyl-cytosine on deoxyribonucleotide pools in mouse embryo cells. European journal of biochemistry / FEBS *19*, 81-89.

Smith, J., Tho, L.M., Xu, N., and Gillespie, D.A. (2010). The ATM-Chk2 and ATR-Chk1 pathways in DNA damage signaling and cancer. Advances in cancer research *108*, 73-112.

Song, B., Liu, X.S., Davis, K., and Liu, X. (2011). Plk1 phosphorylation of Orc2 promotes DNA replication under conditions of stress. Molecular and cellular biology *31*, 4844-4856.

Song, B., Liu, X.S., and Liu, X. (2012). Polo-like kinase 1 (Plk1): an Unexpected Player in DNA Replication. Cell division *7*, 3.

Strebhardt, K., and Ullrich, A. (2006). Targeting polo-like kinase 1 for cancer therapy. Nature reviews Cancer *6*, 321-330.

Sudakin, V., Chan, G.K., and Yen, T.J. (2001). Checkpoint inhibition of the APC/C in HeLa cells is mediated by a complex of BUBR1, BUB3, CDC20, and MAD2. The Journal of cell biology *154*, 925-936.

Suijkerbuijk, S.J., Vleugel, M., Teixeira, A., and Kops, G.J. (2012). Integration of kinase and phosphatase activities by BUBR1 ensures formation of stable kinetochore-microtubule attachments. Developmental cell *23*, 745-755.

Sumara, I., Gimenez-Abian, J.F., Gerlich, D., Hirota, T., Kraft, C., de la Torre, C., Ellenberg, J., and Peters, J.M. (2004). Roles of polo-like kinase 1 in the assembly of functional mitotic spindles. Current biology : CB *14*, 1712-1722.

Swords, R., Mahalingam, D., O'Dwyer, M., Santocanale, C., Kelly, K., Carew, J., and Giles, F. (2010). Cdc7 kinase - a new target for drug development. Eur J Cancer *46*, 33-40.

Takahashi, T.S., Basu, A., Bermudez, V., Hurwitz, J., and Walter, J.C. (2008). Cdc7-Drf1 kinase links chromosome cohesion to the initiation of DNA replication in Xenopus egg extracts. Genes & development *22*, 1894-1905.

Takai, N., Hamanaka, R., Yoshimatsu, J., and Miyakawa, I. (2005). Polo-like kinases (Plks) and cancer. Oncogene *24*, 287-291.

Tang, Z., Bharadwaj, R., Li, B., and Yu, H. (2001). Mad2-Independent inhibition of APCCdc20 by the mitotic checkpoint protein BubR1. Developmental cell *1*, 227-237.

Taylor, W.R., and Stark, G.R. (2001). Regulation of the G2/M transition by p53. Oncogene *20*, 1803-1815.

Tenca, P., Brotherton, D., Montagnoli, A., Rainoldi, S., Albanese, C., and Santocanale, C. (2007). Cdc7 is an active kinase in human cancer cells undergoing replication stress. The Journal of biological chemistry *282*, 208-215.

Topham, C.H., and Taylor, S.S. (2013). Mitosis and apoptosis: how is the balance set? Current opinion in cell biology *25*, 780-785.

Trenz, K., Errico, A., and Costanzo, V. (2008). Plx1 is required for chromosomal DNA replication under stressful conditions. The EMBO journal *27*, 876-885.

Tsuji, T., Ficarro, S.B., and Jiang, W. (2006). Essential role of phosphorylation of MCM2 by Cdc7/Dbf4 in the initiation of DNA replication in mammalian cells. Molecular biology of the cell *17*, 4459-4472.

Tsukahara, T., Tanno, Y., and Watanabe, Y. (2010). Phosphorylation of the CPC by Cdk1 promotes chromosome bi-orientation. Nature *467*, 719-723.

Tsvetkov, L., and Stern, D.F. (2005). Interaction of chromatin-associated Plk1 and Mcm7. The Journal of biological chemistry *280*, 11943-11947.

Tudzarova, S., Trotter, M.W., Wollenschlaeger, A., Mulvey, C., Godovac-Zimmermann, J., Williams, G.H., and Stoeber, K. (2010). Molecular architecture of the DNA replication origin activation checkpoint. The EMBO journal *29*, 3381-3394.

Uchida, K.S., Takagaki, K., Kumada, K., Hirayama, Y., Noda, T., and Hirota, T. (2009). Kinetochore stretching inactivates the spindle assembly checkpoint. The Journal of cell biology *184*, 383-390.

Uhlmann, F., Wernic, D., Poupart, M.A., Koonin, E.V., and Nasmyth, K. (2000). Cleavage of cohesin by the CD clan protease separin triggers anaphase in yeast. Cell *103*, 375-386.

van Vugt, M.A., and Medema, R.H. (2005). Getting in and out of mitosis with Polo-like kinase-1. Oncogene *24*, 2844-2859.

Vassilev, L.T., Tovar, C., Chen, S., Knezevic, D., Zhao, X., Sun, H., Heimbrook, D.C., and Chen, L. (2006). Selective small-molecule inhibitor reveals critical mitotic functions of human CDK1. Proceedings of the National Academy of Sciences of the United States of America *103*, 10660-10665.

Visintin, R., Prinz, S., and Amon, A. (1997). CDC20 and CDH1: a family of substrate-specific activators of APC-dependent proteolysis. Science *278*, 460-463.

Vitale, I., Galluzzi, L., Castedo, M., and Kroemer, G. (2011). Mitotic catastrophe: a mechanism for avoiding genomic instability. Nature reviews Molecular cell biology *12*, 385-392.

von Schubert, C., Cubizolles, F., Bracher, J.M., Sliedrecht, T., Kops, G.J., and Nigg, E.A. (2015). Plk1 and Mps1 Cooperatively Regulate the Spindle Assembly Checkpoint in Human Cells. Cell reports *12*, 66-78.

Walczak, C.E., Cai, S., and Khodjakov, A. (2010). Mechanisms of chromosome behaviour during mitosis. Nature reviews Molecular cell biology *11*, 91-102.

Wan, L., Zhang, C., Shokat, K.M., and Hollingsworth, N.M. (2006). Chemical inactivation of cdc7 kinase in budding yeast results in a reversible arrest that allows efficient cell synchronization prior to meiotic recombination. Genetics *174*, 1767-1774.

Wang, F., Dai, J., Daum, J.R., Niedzialkowska, E., Banerjee, B., Stukenberg, P.T., Gorbsky, G.J., and Higgins, J.M. (2010). Histone H3 Thr-3 phosphorylation by Haspin positions Aurora B at centromeres in mitosis. Science *330*, 231-235.

Wang, F., Ulyanova, N.P., van der Waal, M.S., Patnaik, D., Lens, S.M., and Higgins, J.M. (2011). A positive feedback loop involving Haspin and Aurora B promotes CPC accumulation at centromeres in mitosis. Current biology : CB *21*, 1061-1069.

Watanabe, N., Arai, H., Nishihara, Y., Taniguchi, M., Hunter, T., and Osada, H. (2004). M-phase kinases induce phospho-dependent ubiquitination of somatic Wee1 by SCFbeta-TrCP. Proceedings of the National Academy of Sciences of the United States of America *101*, 4419-4424.

Weaver, B.A., and Cleveland, D.W. (2005). Decoding the links between mitosis, cancer, and chemotherapy: The mitotic checkpoint, adaptation, and cell death. Cancer cell *8*, 7-12.

Wilkinson, R.W., Odedra, R., Heaton, S.P., Wedge, S.R., Keen, N.J., Crafter, C., Foster, J.R., Brady, M.C., Bigley, A., Brown, E., *et al.* (2007). AZD1152, a selective inhibitor of Aurora B kinase, inhibits human tumor xenograft growth by inducing apoptosis. Clin Cancer Res *13*, 3682-3688.

Williams, B.C., Li, Z., Liu, S., Williams, E.V., Leung, G., Yen, T.J., and Goldberg, M.L. (2003). Zwilch, a new component of the ZW10/ROD complex required for kinetochore functions. Molecular biology of the cell *14*, 1379-1391.

Wittmann, T., Boleti, H., Antony, C., Karsenti, E., and Vernos, I. (1998). Localization of the kinesin-like protein Xklp2 to spindle poles requires a leucine zipper, a microtubule-associated protein, and dynein. The Journal of cell biology *143*, 673-685.

Wu, K.Z., Wang, G.N., Fitzgerald, J., Quachthithu, H., Rainey, M.D., Cattaneo, A., Bachi, A., and Santocanale, C. (2016). DDK dependent regulation of TOP2A at centromeres revealed by a chemical genetics approach. Nucleic acids research.

Yamada, M., Sato, N., Taniyama, C., Ohtani, K., Arai, K., and Masai, H. (2002). A 63-base pair DNA segment containing an Sp1 site but not a canonical E2F site can confer growth-dependent and E2F-mediated transcriptional stimulation of the human ASK gene encoding the regulatory subunit for human Cdc7-related kinase. The Journal of biological chemistry *277*, 27668-27681.

Yamada, M., Watanabe, K., Mistrik, M., Vesela, E., Protivankova, I., Mailand, N., Lee, M., Masai, H., Lukas, J., and Bartek, J. (2013). ATR-Chk1-APC/CCdh1-dependent stabilization of Cdc7-ASK (Dbf4) kinase is required for DNA lesion bypass under replication stress. Genes & development *27*, 2459-2472.

Yamagishi, Y., Yang, C.H., Tanno, Y., and Watanabe, Y. (2012). MPS1/Mph1 phosphorylates the kinetochore protein KNL1/Spc7 to recruit SAC components. Nature cell biology *14*, 746-752.

Yamashita, N., Kim, J.M., Koiwai, O., Arai, K., and Masai, H. (2005). Functional analyses of mouse ASK, an activation subunit for Cdc7 kinase, using conditional ASK knockout ES cells. Genes to cells : devoted to molecular & cellular mechanisms *10*, 551-563.

Yang, M., Li, B., Tomchick, D.R., Machius, M., Rizo, J., Yu, H., and Luo, X. (2007). p31comet blocks Mad2 activation through structural mimicry. Cell *131*, 744-755.

Yarm, F.R. (2002). Plk phosphorylation regulates the microtubule-stabilizing protein TCTP. Molecular and cellular biology *22*, 6209-6221.

Yoshizawa-Sugata, N., Ishii, A., Taniyama, C., Matsui, E., Arai, K., and Masai, H. (2005). A second human Dbf4/ASK-related protein, Drf1/ASKL1, is required for efficient progression of S and M phases. The Journal of biological chemistry *280*, 13062-13070.

Zegerman, P., and Diffley, J.F. (2010). Checkpoint-dependent inhibition of DNA replication initiation by Sld3 and Dbf4 phosphorylation. Nature *467*, 474-478.

Zeitlin, S.G., Shelby, R.D., and Sullivan, K.F. (2001). CENP-A is phosphorylated by Aurora B kinase and plays an unexpected role in completion of cytokinesis. The Journal of cell biology *155*, 1147-1157.

Zeman, M.K., and Cimprich, K.A. (2014). Causes and consequences of replication stress. Nature cell biology *16*, 2-9.

Zhang, N., Panigrahi, A.K., Mao, Q., and Pati, D. (2011). Interaction of Sororin protein with polo-like kinase 1 mediates resolution of chromosomal arm cohesion. The Journal of biological chemistry *286*, 41826-41837.

Zhang, X., Lan, W., Ems-McClung, S.C., Stukenberg, P.T., and Walczak, C.E. (2007). Aurora B phosphorylates multiple sites on mitotic centromere-associated kinesin to spatially and temporally regulate its function. Molecular biology of the cell *18*, 3264-3276.

Zhao, H., and Piwnica-Worms, H. (2001). ATR-mediated checkpoint pathways regulate phosphorylation and activation of human Chk1. Molecular and cellular biology *21*, 4129-4139.

Zhou, L., Tian, X., Zhu, C., Wang, F., and Higgins, J.M. (2014). Polo-like kinase-1 triggers histone phosphorylation by Haspin in mitosis. EMBO reports *15*, 273-281.

Zhu, T., Dou, Z., Qin, B., Jin, C., Wang, X., Xu, L., Wang, Z., Zhu, L., Liu, F., Gao, X., *et al.* (2013). Phosphorylation of microtubule-binding protein Hec1 by mitotic kinase Aurora B specifies spindle checkpoint kinase Mps1 signaling at the kinetochore. The Journal of biological chemistry *288*, 36149-36159.

Zitouni, S., Nabais, C., Jana, S.C., Guerrero, A., and Bettencourt-Dias, M. (2014). Polo-like kinases: structural variations lead to multiple functions. Nature reviews Molecular cell biology *15*, 433-452.

Zou, L., and Elledge, S.J. (2003). Sensing DNA damage through ATRIP recognition of RPA-ssDNA complexes. Science *300*, 1542-1548.